Oklahoma Department of Transportation
200 NE 21st Street, Oklahoma City, OK 73105-3204

FINAL REPORT ~ FHWA-OK-14-17

# THE STUDY OF VEHICLE CLASSIFICATION EQUIPMENT WITH SOLUTIONS TO IMPROVE ACCURACY IN OKLAHOMA

**Hazem Refai, Ph.D.**
**Naim Bitar**
**Jesse Schettler**
**Omar Al Kalaa, M.Sc.**

**School of Electrical and Computer Engineering**
**College of Engineering**
**The University of Oklahoma**

**December 2014**

Oklahoma Department of Transportation

**DISCLAIMER**

The contents of this report reflect the views of the author(s) who is responsible for the facts and the accuracy of the data presented herein. The contents do not necessarily reflect the views of the Oklahoma Department of Transportation or the Federal Highway Administration. This report does not constitute a standard, specification, or regulation. While trade names may be used in this report, it is not intended as an endorsement of any machine, contractor, process, or product.

# THE STUDY OF VEHICLE CLASSIFICATION EQUIPMENT WITH SOLUTIONS TO IMPROVE ACCURACY IN OKLAHOMA

**FINAL REPORT ~ FHWA-OK-14-17**
ODOT SP&R ITEM NUMBER 2250

**Submitted to:**
John R. Bowman, P.E.
Director of Capital Programs
Oklahoma Department of Transportation

**Submitted by:**
Hazem Refai, Ph.D.
Naim Bitar, Graduate Student
Jesse Schettler, Graduate Student
Omar Al Kalaa, Graduate Student

School of Electrical and Computer Engineering (ECE)
The University of Oklahoma


December 2014

## TECHNICAL REPORT DOCUMENTATION PAGE

| 1. REPORT NO. | 2. GOVERNMENT ACCESSION NO. | 3. RECIPIENT'S CATALOG NO. |
|---|---|---|
| FHWA-OK-14-17 | | |

| 4. TITLE AND SUBTITLE | 5. REPORT DATE |
|---|---|
| The Study of Vehicle Classification Equipment with Solutions to Improve Accuracy in Oklahoma | Dec 2014 |
| | 6. PERFORMING ORGANIZATION CODE |

| 7. AUTHOR(S) | 8. PERFORMING ORGANIZATION REPORT |
|---|---|
| Hazem Refai, Ph.D., Naim Bitar, Jesse Schettler, Omar Al Kalaa. | |

| 9. PERFORMING ORGANIZATION NAME AND ADDRESS | 10. WORK UNIT NO. |
|---|---|
| School of Electrical and Computer Engineering<br>The University of Oklahoma<br>202 W. Boyd St., Room 104<br>Norman, OK. 73019-0631 | 11. CONTRACT OR GRANT NO.<br>ODOT SP&R Item Number 2250 |

| 12. SPONSORING AGENCY NAME AND ADDRESS | 13. TYPE OF REPORT AND PERIOD COVERED |
|---|---|
| Oklahoma Department of Transportation<br>Materials and Research Division<br>200 N.E. 21st Street, Room 3A7<br>Oklahoma City, OK 73105 | Final Report<br>Oct 2013 - Oct 2014 |
| | 14. SPONSORING AGENCY CODE |

15. SUPPLEMENTARY NOTES

Click here to enter text.

16. ABSTRACT

The accuracy of vehicle counting and classification data is vital for appropriate future highway and road design, including determining pavement characteristics, eliminating traffic jams, and improving safety. Organizations relying on vehicle classifiers for data collection should be aware that systems can be affected by hardware and sensor malfunction, as well as the equipment's implementation of classification scheme (i.e., algorithm). This report presents outcomes from an extensive statewide examination of vehicle misclassification at Oklahoma Department of Transportation (ODOT) AVC stations employing the PEEK Traffic 'FHWA-USA' classification algorithm. A ground truth system utilizing continuous video recordings was developed and utilized. Results from the rigorous investigation are reported herein. Also detailed in this report is a novel method for an improved classification algorithm designed to reduce the number of classification errors. Thirteen Gaussian distributions were employed to model axle spacing for each of the 13 FHWA vehicle types. Classifications obtained from video recordings and PEEK Traffic axle spacing measurements for a sample of 20,000 vehicles were recorded and analyzed to obtain 13 good-fit Gaussian distributions that correspond with each vehicle class. An optimization algorithm was then implemented to develop axle spacing thresholds for vehicles currently traveling Oklahoma's highways and to minimize vehicle misclassification. The new scheme was then implemented in the PEEK Traffic automatic data record equipment and experimentally evaluated for accuracy. Results demonstrated its effectiveness in improving vehicle classifications and reducing persistent overall system errors characteristic of the 'FHWA-USA' Scheme. Analysis methodology detailed in this report will benefit organizations interested in improving vehicle classification and overall system accuracy.

| 17. KEY WORDS | 18. DISTRIBUTION STATEMENT |
|---|---|
| Classification, ADR, AVC, WIM, Algorithm | No restrictions. This publication is available from the Materials and Research Div., Oklahoma DOT. |

| 19. SECURITY CLASSIF. (OF THIS REPORT) | 20. SECURITY CLASSIF. (OF THIS PAGE) | 21. NO. OF PAGES | 22. PRICE |
|---|---|---|---|
| Unclassified | Unclassified | 104 | N/A |

**SI* (MODERN METRIC) CONVERSION FACTORS**

| APPROXIMATE CONVERSIONS TO SI UNITS | | | | |
|---|---|---|---|---|
| **SYMBOL** | **WHEN YOU KNOW** | **MULTIPLY BY** | **TO FIND** | **SYMBOL** |
| **LENGTH** | | | | |
| **in** | inches | 25.4 | millimeters | mm |
| **ft** | feet | 0.305 | meters | m |
| **yd** | yards | 0.914 | meters | m |
| **mi** | miles | 1.61 | kilometers | km |
| **AREA** | | | | |
| **$in^2$** | square inches | 645.2 | square millimeters | $mm^2$ |
| **$ft^2$** | square feet | 0.093 | square meters | $m^2$ |
| **$yd^2$** | square yard | 0.836 | square meters | $m^2$ |
| **ac** | acres | 0.405 | hectares | ha |
| **$mi^2$** | square miles | 2.59 | square kilometers | $km^2$ |
| **VOLUME** | | | | |
| **fl oz** | fluid ounces | 29.57 | milliliters | mL |
| **gal** | gallons | 3.785 | liters | L |
| **$ft^3$** | cubic feet | 0.028 | cubic meters | $m^3$ |
| **$yd^3$** | cubic yards | 0.765 | cubic meters | $m^3$ |
| NOTE: volumes greater than 1000 L shall be shown in $m^3$ | | | | |
| **MASS** | | | | |
| **oz** | ounces | 28.35 | grams | g |
| **lb** | pounds | 0.454 | kilograms | kg |
| **T** | short tons (2000 lb) | 0.907 | megagrams (or "metric ton") | Mg (or "t") |
| **TEMPERATURE (exact degrees)** | | | | |
| **$^oF$** | Fahrenheit | 5 (F-32)/9<br>or (F-32)/1.8 | Celsius | $^oC$ |
| **ILLUMINATION** | | | | |
| **fc** | foot-candles | 10.76 | lux | lx |
| **fl** | foot-Lamberts | 3.426 | $candela/m^2$ | $cd/m^2$ |
| **FORCE and PRESSURE or STRESS** | | | | |
| **lbf** | poundforce | 4.45 | newtons | N |
| **$lbf/in^2$** | poundforce per square inch | 6.89 | kilopascals | kPa |

| APPROXIMATE CONVERSIONS FROM SI UNITS | | | | |
|---|---|---|---|---|
| **SYMBOL** | **WHEN YOU KNOW** | **MULTIPLY BY** | **TO FIND** | **SYMBOL** |
| **LENGTH** | | | | |
| **mm** | millimeters | 0.039 | inches | in |
| **m** | meters | 3.28 | feet | ft |
| **m** | meters | 1.09 | yards | yd |
| **km** | kilometers | 0.621 | miles | mi |
| **AREA** | | | | |
| **$mm^2$** | square millimeters | 0.0016 | square inches | $in^2$ |
| **$m^2$** | square meters | 10.764 | square feet | $ft^2$ |
| **$m^2$** | square meters | 1.195 | square yards | $yd^2$ |
| **ha** | hectares | 2.47 | acres | ac |
| **$km^2$** | square kilometers | 0.386 | square miles | $mi^2$ |
| **VOLUME** | | | | |
| **mL** | milliliters | 0.034 | fluid ounces | fl oz |
| **L** | liters | 0.264 | gallons | gal |
| **$m^3$** | cubic meters | 35.314 | cubic feet | $ft^3$ |
| **$m^3$** | cubic meters | 1.307 | cubic yards | $yd^3$ |
| **MASS** | | | | |
| **g** | grams | 0.035 | ounces | oz |
| **kg** | kilograms | 2.202 | pounds | lb |
| **Mg (or "t")** | megagrams (or "metric ton") | 1.103 | short tons (2000 lb) | T |
| TEMPERATURE (exact degrees) | | | | |
| **$^oC$** | Celsius | 1.8C+32 | Fahrenheit | $^oF$ |
| **ILLUMINATION** | | | | |
| **lx** | lux | 0.0929 | foot-candles | fc |
| **$cd/m^2$** | $candela/m^2$ | 0.2919 | foot-Lamberts | fl |
| **FORCE and PRESSURE or STRESS** | | | | |
| **N** | newtons | 0.225 | poundforce | lbf |
| **kPa** | kilopascals | 0.145 | poundforce per square inch | $lbf/in^2$ |

*SI is the symbol for the International System of Units. Appropriate rounding should be made to comply with Section 4 of ASTM E380.

## ACKNOWLEDGMENTS

PI Dr. Refai and his research team recognize Mr. Daryl Johnson, Aaron Fridrich, and Brian Thompson at the Oklahoma Department of Transportation for their support and for the insightful discussions that occurred throughout the duration of this project. The authors also acknowledge Peak Traffic for their technical support during the coding of the newly proposed algorithm on the ADR classification equipment.

## TABLE OF CONTENTS

## LIST OF FIGURES

## Executive Summary

Vehicle counting and classification data plays a vital role in designing roadways, determining pavement characteristics, eliminating traffic jams, and improving road safety. To realize the greatest benefit of such information, verifying data accuracy reported by statewide automatic vehicle classifier (AVC) is of the utmost importance. Currently, PEEK Traffic Automatic Data Recorders (ADR 2000) are used to count and classify traveling vehicles; however, this system is not completely accurate. Classification inaccuracies are the result of hardware and/or sensor malfunction, as well as classification schemes or algorithms implemented in the device. This study focuses on inaccuracies resulting from classification algorithm error—not hardware-related issues.

In general, vehicles are classified based on number of axles and wheelbase axle spacing. ODOT's ADR equipment is currently based on the 18-year-old 'FHWA-USA' classification algorithm. An updated classification scheme is necessary to accurately represent the design and wheelbase axle spacing of late-model vehicles currently traveling on Oklahoma highways. Adopting such a scheme will reduce vehicle misclassification.

Axle-spacing overlap among vehicle classes and vehicles pulling one-, two-, or three-axle trailers are cause for substantial errors in axle-based AVC classifiers, especially for particular vehicle classes, as summarized in Table 21. A novel method for an improved classification algorithm was developed during this study. A sample of roughly 20,000 vehicles was included in the analysis. Accurate vehicle classification was manually determined using a ground-truth system with continuous video recording equipment. Vehicle axle spacings were obtained from currently deployed PEEK Traffic ADR 2000 equipment using per vehicle recording (PVR) configuration. Reported axle spacing was compared with vehicle manufacturer blueprint spacing and proven within 1% accuracy. Given these results, axle spacings measured and reported by ADR were used throughout this study.

Data collection, including video recordings and ADR axle spacings, were performed at many ODOT AVC sites located on urban and rural roadways to capture various traffic characteristics. During the first project year, one-minute binned ADR data was collected and analyzed. During the second project year, PVR data was collected and analyzed after PEEK Traffic agreed to provide the OU team with programming software enabling ADR to collect per vehicle information. During data collection and analysis, the research team developed and continuously evaluated/improved a new "OU-FHWA13" classification scheme. Notably, the new scheme was evaluated in sequence with the original scheme and not in parallel to it, meaning the ADR was configured to collect one hour of data using the original scheme and then another hour of data collection (in the same or different day) using the newly developed OU scheme. Hence, the number, type, and class of vehicles collected during the first hour did not necessarily match data collected in a subsequent hour. Although this had no effect on classification accuracy, the matching number of vehicles required to conduct a normalized comparison was lacking. Simultaneous recording of traffic using both the original and the OU scheme requires an AVC

site with two sets of sensors and controllers, which ODOT does not have. Hence, the OU scheme evaluation was always in sequence.

Video recordings and measured axle spacing were processed to develop 13 good-fit Gaussian distributions—one for each FHWA class. Hence, 13 Gaussian distributions were used to model wheelbase axle spacing for 13 FHWA vehicle classes. An optimization algorithm was implemented to determine axle spacing thresholds to minimize vehicle misclassification and improve overall system accuracy. Axle spacing thresholds were subsequently implemented as OU-FHWA13 scheme in the ADR equipment, and then experimentally evaluated for accuracy. Axle-spacing distribution accuracy depends on the number of vehicles captured per class during data collection. The higher the vehicle-count in the sample pool, the better-fit the Gaussian distribution. Low vehicle counts were recorded for class 7 (42 vehicles), 11 (47 vehicles), and class 12 (64 vehicles). In spite of this, the research team developed new thresholds and decision tree entries with a demonstrated improvement during scheme evaluation.

In this study, two key performance indicators were employed: mis-detection and false–detection. Mis-detection occurs when ADR doesn't show a class vehicle recorded by ground-truth; false-detection occurs when ADR wrongly classifies a class vehicle. Test results from OU-FHWA13 demonstrated substantial classification improvement for all classes, especially those with significant error as classes 8, 5, 6, 3 and 2 as well as those with fewer errors such as 7 and 10. Results confirmed nearly 45% decrease in false-detection for class 8 vehicles; 21% and 13% decrease in false- and mis-detection, respectively, for class 5. Evaluation results are detailed in Table 65 and 66. Classification improvement for classes 7 and 10 were achieved by adding entries missing in ODOT's current FHWA-USA algorithm. A 4% reduction in consolidated errors grouped by type was recorded for Single-Unit Trucks (SUT) (classes 5 to 7). A 50% reduction in error was achieved for passenger vehicle (PV) (classes 1 to 4). A 15% reduction in consolidated system error was achieved for Multi-Unit Trucks (MUTs) (classes 8 to 13), primarily due to accuracy improvements for class 8.

In summary, this report details the following: 1) Comprehensive evaluation of system classification accuracy for ODOT AVC sites; 2) Newly designed tools for acquiring and processing ground truth data for accuracy studies; 3) Recording and analyzing per vehicle data; 4) Populating a database with vehicle axle-spacing ground truth data; 5) Minimizing system errors and optimizing classification accuracy using a class-based database of probability density functions (PDFs); and 6) Improved classification algorithm for ODOT AVC stations.

This Page Is Intentionally Blank

# 1 Chapter I: Introduction and Background

## 1.1 Introduction

The Federal Highway Administration (FHWA) and Oklahoma Department of Transportation (ODOT) must keep apprised of continual improvements in vehicle classification systems. Improved accuracy is essential for suitable roadway design and to ensure adequate capacity, surface durability, and commuter safety for motorists.

This report details a study of vehicle classification accuracy of 13 FHWA classes measured at existing ODOT weigh-in-motion (WIM), automatic vehicle classifier (AVC), and short-term classification sites. A ground truth system utilizing on-site raw video recordings was developed and utilized for this study. Project efforts resulted in an improved classification algorithm that reduces vehicle classification errors at statewide ODOT AVC sites.

## 1.2 Existing knowledge

The earliest attempt to investigate the accuracy of Automatic Vehicle Classification (AVC) devices was reported in 1993 in the state of Georgia [1]. Final results of the study were published in 1995 [2]. Two cameras (one to monitor vehicles changing lanes and the other to record the individual vehicles that passed the test site) were used. A Computer Vehicle Classification and Reduction System (CVCRS) was used to consolidate video data into tables of time-stamped vehicle records, excluding data for vehicles changing lanes. The CVCRS operated by manually running and pausing video stream. The system captured the time stamp and made a preliminary classification based on length measurements provided by the operator, who would later confirm or modify the classification decision before restarting the video and waiting for the next vehicle image.

In a 1998 study on classification and weigh-in-motion data from sites in New England [3], researchers used *cusum* (cumulative sum) from statistical quality control theory for data quality check; however, no effort was made to inspect individual WIM or classification records.

A Montana DOT study in 2003 [4] aimed at improving the quality and quantity of truck weight and classification data to aid in pavement design comparing ESAL (Equivalent Single Axel Load) factors calculated for WIM classification data and weigh station data. No attempt was made to validate classification accuracy.

Colorado DOT reported results from a study of 15-minute classification count taken approximately every hour for a continuous 24-hour period [5]. Vehicles were classified by an on-site technician who would record and count vehicles traveling in both directions. As a quality control measure 15-minute segments of classification data recorded by each technician was verified by CDOT personnel examining video recorded during the manual collection. Software used to extract vehicle data from the video [6] enabled the CDOT operator to manually play and pause the video, and then log passing vehicle classification.

In an Indiana DOT study [7], video cameras were used to capture traffic flow and verify WIM vehicle classification accuracy. Video recordings were imported into software that automatically classified vehicle information into four categories using digital image processing techniques. A precision rate of 94.2% was purported. The Indiana DOT method does not produce a ground-truth data set primarily because the system groups vehicles into only four categories instead of 13 FHWA categories. Error between classes is thus, acceptable. Researchers in this study proposed a Transportable Infra-Red Traffic Logger (TIRTL) to generate a vehicle classification data set for comparison.

Minnesota DOT used road tubes with a TimeMark Delta IIIL device to conduct vehicle classification studies and update vehicle classification distributions for counties to use when designing pavement structures [8]; however, the accuracy of existing vehicle counters was not investigated.

Researchers in [9] performed an accuracy study in Hawaii for several selected non-intrusive vehicle classification sensors, relying on synchronous field observations (direct or videotaped) to establish ground truth data. Continued work [10] detailed a similar method of manual classification using simultaneous video recordings as ground truth. The method of extracting useful data from video recording was not described.

# 2 Chapter II: Equipment and Study Procedure

## 2.1 Equipment:

The following section presents a brief description of the AVC and WIM site equipment under study.

### 2.1.1 Peek Traffic ADR®

Peek Traffic ADR-2000 operates as a traffic counter and classifier, recording traffic volume and vehicular classification data using a variety of sensor types. The system's internal sensor interfaces modules that monitor sensor inputs from magnetic loops, piezoelectric, or contact enclosures. See Figure 1.


**Figure 1 -** Peek Traffic ADR-2000 Plus

The ADR-2000 Plus is portable and expandable, equipped with four slots (one for memory, three for sensor modules), enabling a range of application options. When fitted with three SC-514P contact closure input cards, the portable ADR-2000 Plus monitors a maximum of 42 traffic lanes.

ADR 2000 technical specifications are presented in Table 1:

| Feature | Description |
|---|---|
| Housing | Rugged, weatherproof cast aluminum housing, with brass body lock and two keys |
| Weight & Size | Typically 8 Kg (17.6 lbs) with battery |
| Height: | 163.2 mm (6.44”) |
| Depth: | 342.3 mm (13.48”) |
| Width: | 242 mm (9.53”) |
| Environmental range | -40ºC to +70ºC. Up to 95% humidity, non-condensing |
| Display | Display 20-digit x 4-line liquid-crystal display |
| | Inputs for four tubes, plus three additional slots that can contain any combination of the sensor boards listed below |
| 8-input | piezo sensor board |
| 8-input | loop sensor board |
| 4-input | contact closure sensor board |
| 8-input | piezo WIM sensor board |
| Count rate | 200 counts per input per second |
| Recording Interval | Selectable period of 1, 2, 5, 6, 10, 15, 30, or 60 minutes; 2, 3, 6, 12, or 24 hours. One normal and up to four daily peak periods are available. |
| File size (duration) | File duration is selectable: 24, 48, or 72 hours, or 7 days of continuous files or midnight to midnight daily files; Programmable for a preset start and end time, as well as date |
| Memory | Memory 2MB (256KB standard, with 127KB available for data storage); up to 64MB available on a PCMCIA memory card |
| Autonomy | 16 weeks with internal battery for roadtube counting |
| Accuracy | One count per interval or better than 10% at 95% confidence on gross weight or better than ASTM standard 13-18 |
| Power | Internal rechargeable lead/acid battery (6V, 10AH), or 4 x 1.5V D cells |
| external | Recharging via AC charger or solar panel (optional) |
| Communications | Selectable RS232 port between 300 and 19,200 baud for connection to PC |
| Palm | Pilot or modem for remote telemetry |
| Classification | FHWA and EEC, and programmable classification options |

**Table 1 -** Technical Specifications for the ADR 2000

## 2.2 Deployment and data acquisition

Two digital video recorders mounted on two tripods were utilized to record video ground truth data. Figure 2 illustrates the positioning of both cameras.

1) Camera one was located on the right shoulder of the highway and captured traffic flow passing over the sensors.

2) Camera two was located on the opposite side of the road, enabling vehicle detection otherwise obstructed from camera one. Hazardous conditions in early testing required revised camera placement on only one roadside with front- and back-view placement at optimal distances.

**Figure 2 -** Video data acquisition

A 5-step deployment was executed.

Step 1: Install a weather-protective tent for study team members.
Step 2: Start power generator and make connection to tent to support long period of testing deployments.
Step 3: Manually synchronize the time between the video camera recorder and existing site equipment (PEEK ADR or IRD iSINC Lite) within a second by observing the clock display on the device screen and setting the camera's clock to match.
Step 4: Install cameras at an appropriate distance on roadside shoulders to capture images of vehicles crossing over roadway ground sensors.
Step 5: Commence video recording on both cameras.

After site testing, video files were downloaded from the camera's internal memory to the hard disk of a laptop for post processing. Equipment utilized in the testing setup included:

- Sony Handycam HDR-CX290 video cameras
- 2 camera tripods
- Power generator
- Weather-protective tent
- ThinkPad T-430 laptop
- Traffic cones, when necessary

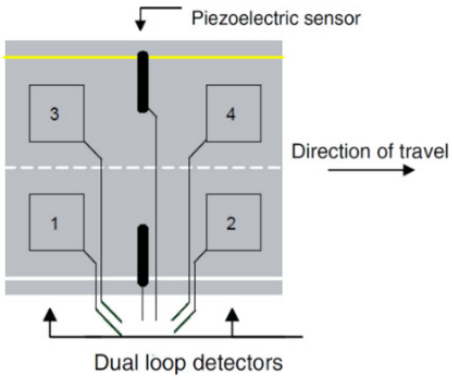


**Figure 3** - Schematic of typical AVC station

Classification stations utilized Loop-Axle-Loop Arrays, as depicted in Figure 3. Data collected included speed, class, (chassis) length, volume, headway, gap, direction by lane, or any combination thereof.

## 2.3 Analysis and Data Processing

After the video recording equipment and the recording classification unit recorded data, researchers performed post processing using custom-made Matlab tools. Initially, video data syncing was necessary to compensate for an offset between video camera timestamps and those from ADR unit output files. A no-cost online time code tool allowed simple conversion of ADR-recorded timestamp files into frames. Next, an empirical offset of 1 or 2 seconds was used to match video and ADR-recorded data. Matching was verified by cross correlating random streams of sample vehicle time-converted frames. Following synchronization, output files were input into custom-made tools for manual vehicle classification for vehicle images in the video footage. Ground truth databases were then constructed.

Because humans were employed to distinguish and classify vehicles, certain errors were inevitable. Most were attributed to restrictions imposed by the setup process and camera angle. Such errors might have a serious effect on the integrity and accuracy of the algorithm to be developed in this study. To compensate, video data collected by two cameras were analyzed separately. Initially, two engineers classified vehicles based on video captured from both sides of the road. Vehicle classification was then cross-correlated to determine human error in either of two separate classifications, which minimized the possibility of human detection error, especially errors due to camera positioning or camera angle. The results were verified and the accurate vehicle class data provided solid ground truth to be used in the study.

Human error was attributed to the following factors.

a) Difficulties differentiating classes, chiefly for classes 2 and 3, especially for certain types of SUVs.

   For example, the Honda CRV 2000 SUV has two axels spaced 2620mm (or 8.595801 feet) apart, which is within the range of a class 2 vehicle according to the algorithm currently employed by existing ADR equipment. A Suburban 2007 SUV with two axels spaced 3302mm (or 10.83333 feet) should be classified as a class 3 vehicle. Classification error when compared with the ADR output is evident in site summary results to be shown below.

b) Difficulties identifying the number of rear wheels, due to obscured camera view, regardless of camera angle.

## 2.4 Video Processing Tools

Two video processing tools developed during this implementation of this project to expedite the processing of highway video recordings (ground-truth).

### 2.4.1 Video processing Tool #1

#### 2.4.1.1 Introduction:

A semi-automated method to classify vehicles required someone to watch a video and manually record the class number, lane number, and the time at which each vehicle drove over the AVC device loops and sensors. Recorded data would be compared with AVC device data to determine device accuracy of the later.

Originally, a simple Matlab program was developed to detect motion in the highway videos and to prompt the user to input classification data for each vehicle image. Although this method significantly decreased the amount of time required to process each video, the process still required eight hours for each video. Because the purpose was to improve automated classification for a large number vehicles and effectively reduce video processing time, the program was written to automatically classify the majority of isolated class 2 compact passenger vehicles, which represents the bulk of traffic.

Figure 4 shows a map of AVC sites in Oklahoma, some of which were tested using the Matlab program.

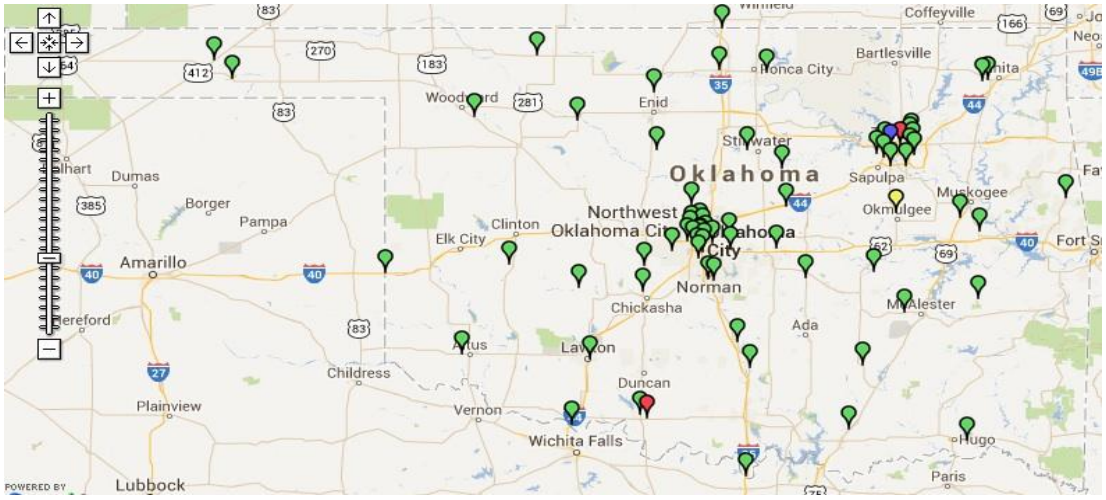


**Figure 4 -** Map of AVC Sites in Oklahoma

#### 2.4.1.2 Applicable Standards:

To determine program functionality for classifying each vehicle type, it was important to clearly define each class and its features. The Federal Highway Administration (FHWA) 13-class standard [11] was utilized. These are shown in Figure 5.

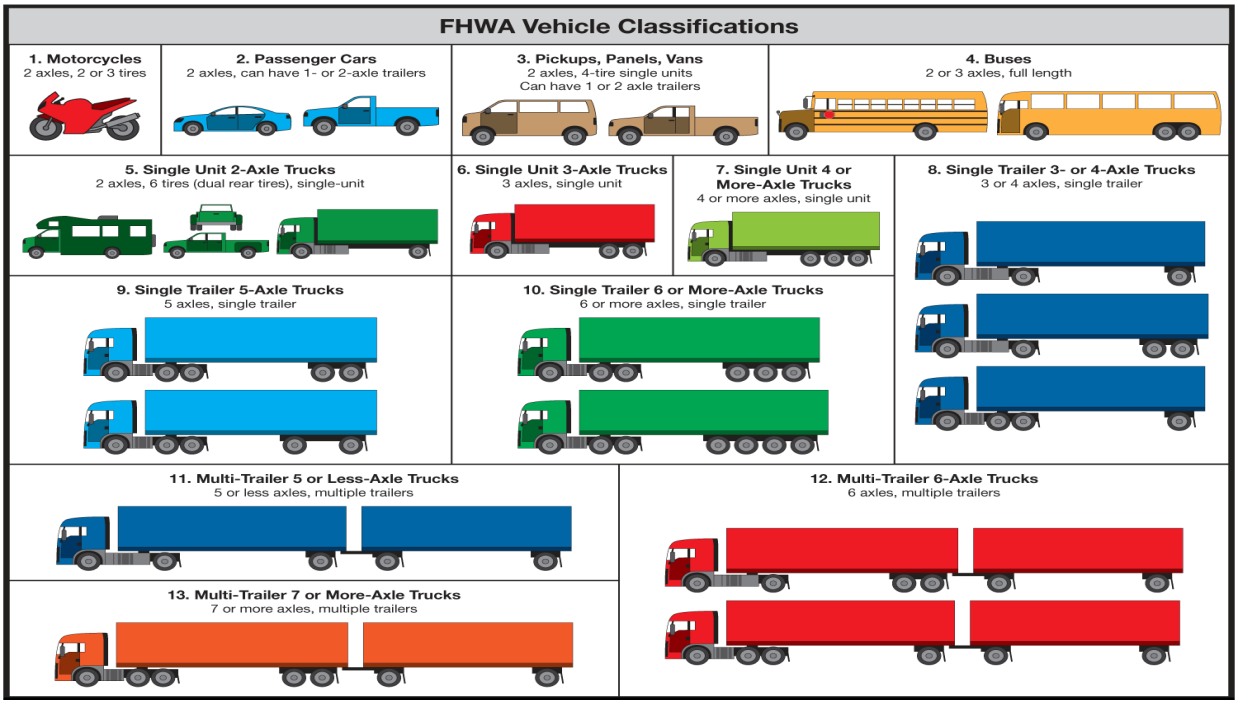


**Figure 5** - FHWA Vehicle Classifications

### 2.4.1.3 Research:

As previously mentioned, video footage was captured at a particular AVC site to test device accuracy. Two cameras were used to achieve images from two angles: one nearly perpendicular to the highway for a side view; the other for a frontal view to aid in distinguishing between lanes when analyzing video footage. Both cameras were mounted on tripods. Although filming specifications made camera angles relatively constant, tripod distance from the roadway were not identical from site to site. Differences in the number of lanes and curvature required customized camera setup. Camera views must include filming all roadway lanes, as well as devices under test (e.g., the AVC device or an alternative sensor device). Such efforts ensure that the timing recorded by the devices matches the timing of the video. Before filming commences, camera clocks must be synched to the AVC device clock and those of other devices under test. Filming typically lasted one to two hours, during which the ADR is configured to bin data every one minute instead of the typical fifteen-minute intervals. Information from the AVC device and any other devices are recorded. Figure 6 illustrates camera type used for the project.


**Figure 6** - Video Camera

Filming ceases following pre-determined data collection time. Video recordings are stored as MP4 files in the video cameras, and then transferred to a laptop computer. Matlab's built-in video reader function reads MP4 files without altering format; however, the user can alter video resolution to decrease computation time. Video footage is used to classify vehicles, and results are then compiled into an Excel spreadsheet. Vehicle class, lane number, frame number, time, and image are saved. Results are compared with those obtained from the AVC device and other devices to determine accuracy.

Because manually analyzing video footage is extremely time consuming, the research team initially developed the aforementioned Matlab program to semi-automate the process. The new program reads in each video files frame and detects the point at which motion is detected in a user-defined area. Subsequently, the program displays the image and prompts the user to classify the vehicle. Data is imported into a spreadsheet along with side and front images of the vehicle. The process continues for each video frame.

To develop Matlab's semi-automated vehicle classification program, a basic understanding of digital image processing was necessary. [12] provided Matlab functions for performing various tasks. For example, a color image can be converted to a gray-scale image, converted to a binary image by thresholding pixel values, filtered through dilation to reduce noise, and then scanned to detect circles representing tires. This combination of functions detects, extracts, and labels certain image objects. [12] contains examples for various functions used in image processing. Although the information is foundational and helpful, it is not sufficient specific problem solving. Methods detailed in [12] must be combined with additional customized methods for writing a program that successfully classifies vehicles.

Digital image processing and object detection in video footage were comprehensively researched and investigated (e.g., a function to track moving objects captured by a surveillance camera). [13] employs a motion flow field to foreground object validation and tracking from frame to frame. Following detection, object features (e.g., orientation, acceleration, and predicted trajectory) are calculated to help determine whether it is person, vehicle, or other type of object. By comparing object positioning in neighboring frames, a motion flow field is computed, which aids filtering non-moving foreground objects. Motion flow from frame to frame is "needed for real time surveillance applications" [13]. Even though it is not necessary to track vehicles in the

project from frame to frame using a motion flow field, key features of an object can be calculated and leveraged to distinguish one object from another object. Information from neighboring frames, as opposed to that from a single frame filters unwanted objects and noise.

A method to detect and classify vehicles [14] employs a virtual detection line (VDL) for producing a time-spatial image (TSI). VDL is a line placed perpendicular to the road in the video frames. As video advances from frame to frame, pixels contained in the VDL are saved and pieced together to form a TSI. Using multiple VDLs produces multiple TSIs that aid in identifying merged vehicles. Two vehicles appearing merged in one TSI might appear as two separate vehicles in another. Thus, multiple TSIs prevent error caused by merging. After a TSI has been produced for a video and each object has been identified as a separate vehicle, a cropped image of each is generated. Binary images of the TSIs and cropped images use image processing techniques, such as thresholding, edge detection, and dilation. Using binary images, width, area, compactness, length-width ratio, major-axis to minor-axis ratio, and rectangularity, identifying features for each vehicle are calculated and used to classify it into general categories (e.g., two-wheeler vehicle). Next, "three shape-invariant and four texture-based features are used to find the exact type of vehicle belonging to a certain broad class of vehicles" [14]. Successful test results reveal that using multiple TSIs decreases counting and classification errors and that using the two-step classification system increases classification accuracy.

Previously, [15] classified vehicles with an accuracy of 94% into eight different classes, some of which were FWHA defined. The work also determined in which lane on two-way roads a vehicle was traveling. Blob detection, principle component analysis (PCA), and linear discriminant analysis (LDA) were used for classification. Later, [16] improved this classification technique by drawing on facial recognition [17].

Most work in video-based AVC uses LDA and PCA classification for determining vehicle class (e.g. [18], which used the techniques on images processed with edge detection). In these, the algorithm detects the image's most differentiating features(the "principle components") and uses a function of these to place it in a multiple dimensional space. With any luck, the data points lie in linearly separable regions of the space for accurate LDA. Weighted-k nearest neighbor (wkNN) techniques are also used to determine the distance of an image from each cluster. As the vehicle advances along the road, multiple analyses are performed increase accuracy and confidence in the classification. Tracking specific objects is often accomplished using techniques presented in [19].

As mentioned briefly before, [17] developed a technique for improving methodology for facial recognition. "Fisherfaces" uses Fisher's Linear Discriminant to improve group classification and transform images from high to low dimensional image space improved and expedited classification. Further research is required to determine how to apply the technique to the work presented in this report. Fisherfaces are known to reduce the effects of lighting on recognition and work well for systems with predetermined classes.

Research detailed herein utilized a combination of principal component analysis and linear discriminant analysis to classify vehicles. Forty-four descriptors were defined, and Fisher's Linear Discriminant was used with a database of vehicle images to project the 44-dimensional

vectors into a two-dimensional vector space. Doing so maximized spacing between classes and minimized in-class scatter. To further improve rate of detection, efforts were focused on developing an algorithm entirely based on the target class 2 vehicles. Although data to classifying 12 other FWHA classes was ignored, the reduced amount of data enable improved separation for class 2 vehicles.

#### 2.4.1.4 System Overview:

Another tool was executed in three stages: setup, processing, and user classification. Setup determines video-specific parameters needed to process the video and obtain images and binary masks of vehicles. The bulk of this work is completed during the processing phase, wherein the program detects vehicles, determines lane, and attempts to automatically classify isolated vehicles. During classification the user is presented images of each unclassified vehicle and prompted to classify the vehicle. Upon completion, all necessary data required from the video has been extracted.

Vehicles are classified according to calculated values of their descriptors (measurements taken on its properties). For data in this report, properties included vehicle shape and image. Vehicle lane is also required. As such, the location of vehicles in each frame must be determined.

As a project constraint, video footage must contain only relatively stationary background objects, and vehicles. By defining the setup accordingly, vehicles can be detected relative to foreground objects (i.e., background subtraction), which first requires a background image without such objects. Since such an image is not always available, an adaptive solution to determine the true background is necessary, even in the presence of foreground objects. Moreover, given a quiet background, variations in lighting and cloud movements change background appearance over time. A single algorithm was created to robustly adapt changes without disrupting foreground object detection. Over time, the learned background converged to a true background notwithstanding a poor initial image. To do so, a sufficient amount of frames (e.g., 2000 frames) were processed by the algorithm in reverse order to reach the video start. The resulting background proved to be the original background, even in cases of high traffic. Figures 7 and 8 depict a frame and its resulting background.

**Figure 7 -** Example Frame

**Figure 8 -** Calculated Background Image

The second step of the setup process was determining lane position on the roadway to assign a lane number to vehicles and to filter out vehicles traveling the opposite direction. Lane lines are not required to be in perfect line with actual lanes. Rather, determining vehicle paths was of utmost importance. Each path corresponded to a lane and specifically identified where vehicles were traveling within the lane. Furthermore, the overlap of multiple vehicles was detected when the object appeared to follow two or more lanes lines.

The final step of the setup process was measuring vehicle velocities in each lane at different points in the frame. After collecting ample data points, polynomial fits were generated to describe average velocities of vehicles in each lane at each point [20]. Thus, vehicle tracking could predict vehicle movement after a vehicle became obscured so that basic properties relating pixels to real distance could be determined.

During this phase, the program reads one frame at a time, updating its learned background. Background image is used for each frame to determine which pixels are in the foreground. Morphological processing suppresses noise and converts pixels into blobs representing objects. Figures 9 and 10 show foreground objects before and after morphological processing.

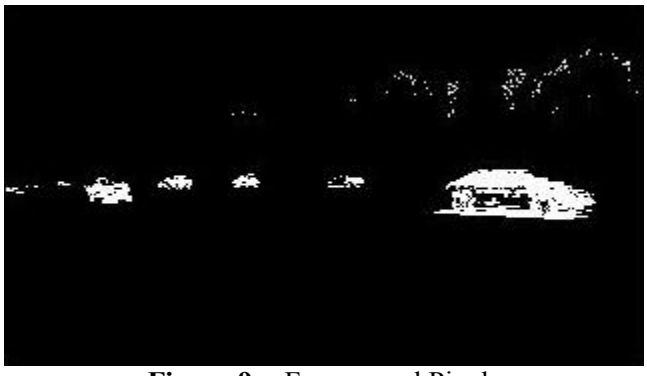

**Figure 9 -** Foreground Pixels

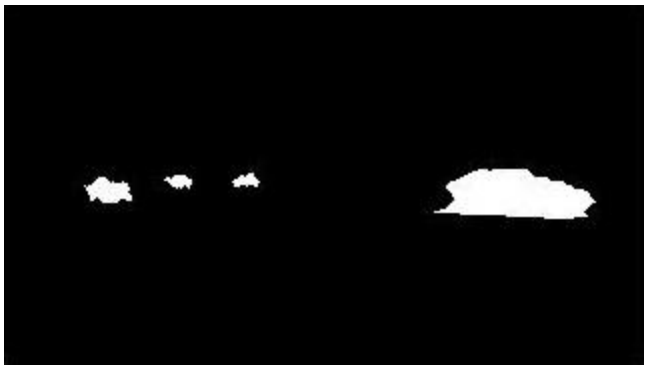

**Figure 10 -** Processed Foreground Image

The vehicle-tracking algorithm analyzes blobs each frame to determine vehicle lane. Information is tracked over time and images of the blob and the vehicle when not obstructed is saved. Once the vehicle reaches the edge of the frame, the algorithm measures vehicle properties and attempts vehicle classification. If successful, the classification and lane are input in the log file. If unsuccessful, class must be determined by the user.

A simple graphical user interface is displayed to aid the user in quickly and efficiently classifying vehicles. Lanes are predetermined and only the frames with unclassified vehicles are displayed. Manual classification can be completed while the program runs in the background, which speeds up the process. This GUI is displayed in Figure 11.

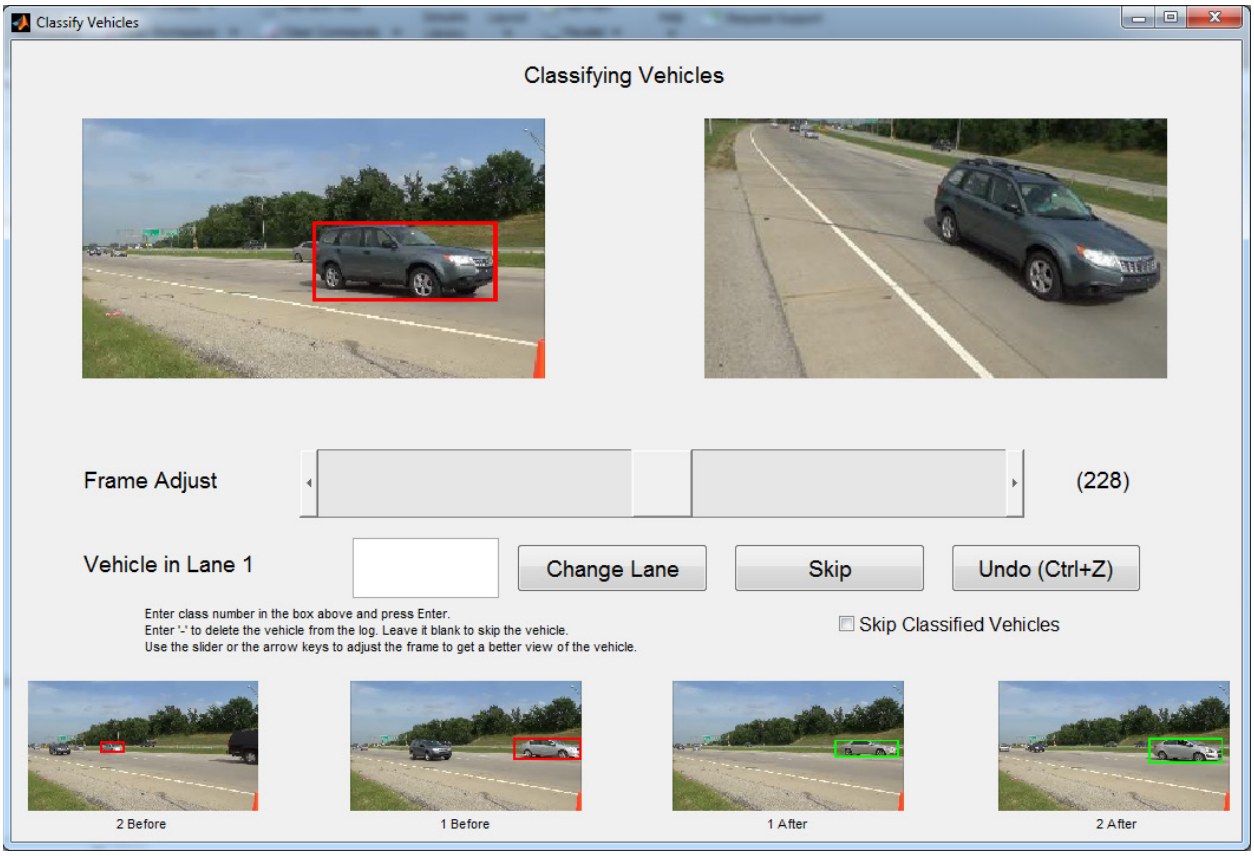


**Figure 11** - Classification User Interface

To decrease processing time, video resolution was reduced from the original 1280x720 to 320x180. This alteration did not decrease system accuracy or classification rate. Converting color to gray-scale footage was tested; however, color information proved necessary to preserve the integrity of blob shapes.

#### 2.4.1.5 Background Detection:

Background detection begins with program acceptance of the first frame as the background image. Foreground objects appearing in the background are replaced with true contents of the background determined over time via updates. To further explain, assume that the initial true background is known. Also consider the case of an empty road without foreground objects. Over time, the background will change as trees move with the wind and the clouds change. Variations in lighting will also affect scene brightness. To maintain the background, one could simply replace it with the current frame every time. Vehicles driving by are incorporated into the background and only difference from one frame to the next will appear as part of the foreground.

To combat this problem, a small percentage of the new frame could be added, based on observation that background objects move slowly. The background can then update quickly enough to follow clouds but slowly enough so foreground objects are not incorporated. Objects moving quickly influence the background. Although performance is vastly improved, an “echo

trail" of each passing vehicle remains, as a portion remains incorporated into the background as the vehicle passes the camera view. Further complicating the problem, vehicles generally have a relatively uniform color along the side panel. On a single pixel scale this factor appears as a stationary object. Clearly, this technique must be further improved.

Given that background objects move slowly, it can be assumed that individual pixel values of the background do not change significantly from frame to frame. Differences between current background and current frame allows individual weights to pixels such that similar pixels are increasingly incorporated and pixels vastly different are no longer updated into the background. This added layer of robustness again increases performance even though some problems remain.

The original algorithm adds yet another filtering layer. Instead of taking into account only a difference in current frame and background, the program tracks recent changes in each pixel over time, using a method similar to the original weighted learning method, although it is applied to learning pixels changes. Such variation values are then applied to the original learning weights and provide a customized coefficient for each color channel in each pixel. In this way the background updates quickly given small changes but slowly for large changes. The method adequately determines background over time, even in the presence of high traffic.

Since the goal is to determine which pixels are in the foreground, this method is still lacking. Although a reliable background image is achieved, using simple image subtraction does not take full advantage of color information contained in the video. Since changes in color channel is combined to determine a "color distance," the amount of change in a pixel results in too much weight for gray-scale color. Distance between completely green and completely red is the same as the distance between a light and dark gray. Given that roadways are typically grey and that passing clouds easily change its tone, the image subtraction technique washes out more pertinent changes in hue information with brightness changes.

To combat this, both background and foreground images are converted from RGB color space to HSV color space, thus allowing the distance between the hue of one pixel and another to be determined by scaling according to saturation. Low-saturation hue changes are visibly similar, whereas the change in high saturation is more significant. A weighted combination of differences between hue-saturation and values (brightness) of pixels is then used to determine true color distance between the pixels. These differences are then used to calculate background-updating weights and apply these to a threshold to determine which pixels are in the foreground.

#### 2.4.1.6 Morphological Processing:

After foreground pixels are obtained, a significant amount of noise remains in the image. This is due to a number of factors, primarily wind and color similarity. Wind moves trees back and forth at an appreciable speed, producing apparent foreground objects in what should be the background. Conversely, vehicles with color similar to a background object could appear to have holes, since the region of similar color appears as the same background. To mitigate such noise, morphological processing on the detected foreground image is performed.

Morphological processing operates primarily on binary images for reducing noise and improving

object shapes. Following significant experimentation and improvement in the background subtraction process, the developed program used three steps to process the binary mask of the foreground, decreasing computational time. The first operation was an area open operation, which removed connected blobs of pixels containing no more than a specified number of pixels. Individual pixels are removed, as are string-like pixel regions that appear along moving tree lines. Next, morphological closing using a diamond-shaped structuring element is executed with the intent to fill spaces with missing pieces of the blobs and to restore vehicle shape. The final step is another area opening—this time performed inversely so small regions of connected black pixels are filled in, eliminating holes that remain in a vehicle's blob of pixels. See Figures 8-11 above for illustrations of this morphological process in its entirety.

#### 2.4.1.7 Lane Detection:

Once foreground is distinguished from the background and the scene is undated accordingly, roadway lanes can be determined. Cars (ground-based vehicles) typically make contact with the road. Given accurate foreground detection, it is safe to assume that the bottom-most pixels of each blob correspond to the contact points between the car and the road. Although shadows can invalidate this assumption, constraints can be applied so that video filmed when shadows cast by vehicles are either on the far side or beneath the vehicles. In such cases, shadows are close enough to the vehicle that they are detected as part of it. Later it is shown that when operating in the border between acceptable and unacceptable shadows, some errors are introduced into the vehicle tracking process. The errors are minor, however, and found not significantly interfere with system operation.

Assuming that the bottommost pixels in each column of the blob correspond to the contact points of the road, other pixels were deleted from the image during the lane detection stage. Figure12 illustrates the blob before and after this process.

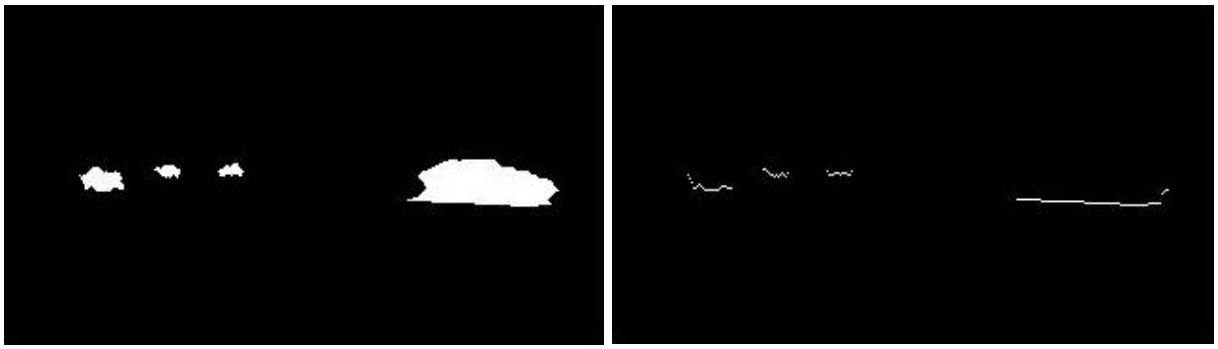

**Figure 12 -** Vehicle Blobs and Remaining Portions for Lane Detection

Most pixels in the resulting image correspond to points along the lanes in the roadway. This operation was completed for each frame, summing the resulting images. At the end of the process, the image was normalized, creating an intensity map of the most traveled paths in the frame. This intensity map is illustrated in Figure 13.

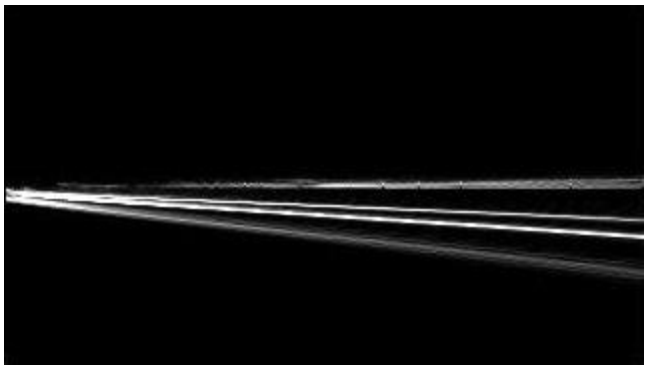

**Figure 13 -** Intensity Map of Most Traveled Paths

After obtaining the intensity map, the number and locations roadway lanes can be determined. For each column in the rightmost third of the image, peaks in the intensity were found, denoting them as points along a lane. Once complete, the process indicates the most common number of peaks for each column, revealing the number of lanes. Noise was filtered from columns appearing to have an incorrect number of lanes. Ignoring the columns revealed a set of points along each lane and created a linear fit to describe the lane. For added robustness, intersect points of each lane were checked, and an attempt was made to differentiate lanes that appeared to intersect in an incorrect location. Ideally, lane lines should only intersect at the vanishing point of the scene. However, camera resolution is not ample, and some error is to be expected near the vanishing point. As a result, the leftmost third of the frame is ignored for the purpose of vehicle tracking. The following figures demonstrate the linear fit process and accuracy of detected lanes matching vehicle location. Note that in most cases, only one lane was detected for vehicles traveling in the opposite direction due to camera distance. This was advantageous, since traffic traveling in the opposite interferes with classification on the intended side of the roadway. Figures 14 and 15 illustrate the lane detection process.

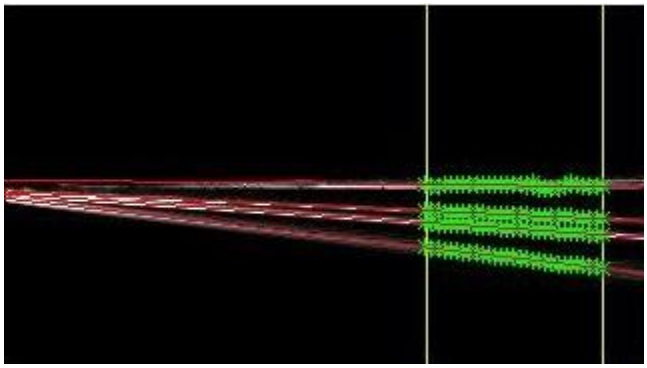

**Figure 14 -** Linear Fits for Lanes

**Figure 15** - Detected Lanes

#### 2.4.1.8 Vehicle Tracking:

The process of tracking vehicles from frame to frame on a lane-by-lane basis assumes vehicles do not change lanes during their video capture. Given that a vehicle changes lanes, it's image will be captured twice and the user must delete one. Doing so in accordance with the research team's design decision that it is better for the user to eliminate duplicates rather than manually locating a missing vehicle. This process is simplified due to the way in which the classification interface was designed for easy scenario identification.

For each frame, the vehicle-tracking algorithm detects blobs in the frame and computes its corresponding lane. Each pixel along the bottom edge of the blobs is examined, and the lane is calculated on a continuous scale. For example, a pixel between lanes 2 and 3 might have a value of 2.2. Such a figure results in a lane plot vs. x-coordinate for each blob in the image. The flat edges of vehicles cause stabilized plot in one lane. Analyzing smoothed curves of the lane plot derivative allows the program to reliably determine vehicle lane. Additionally, if the left portion of a blob appears to settle in one lane and the right potion settles in another, the algorithm detects this is possible only if the blob in question actually corresponds to multiple vehicles. The point at which the lane change is present is identified and interim edges of the vehicle are tracked.

The algorithm only tracks in which lane a vehicle is traveling, as well as the front and back coordinates along the lane. When either the front or back of the vehicle is obscured, the algorithm utilizes velocity curves from the setup phase to interpolate its position. Each endpoint in interpolated separately to account for apparent growth of the vehicle as it approaches the camera's location. For vehicles that are not obscured, the algorithm uses the same interpolation to step forward vehicles in the previous frame and match them with detected blobs in the current frame. Figure 16 depicts the process and steps performed to segment out vehicles and roadway lanes.

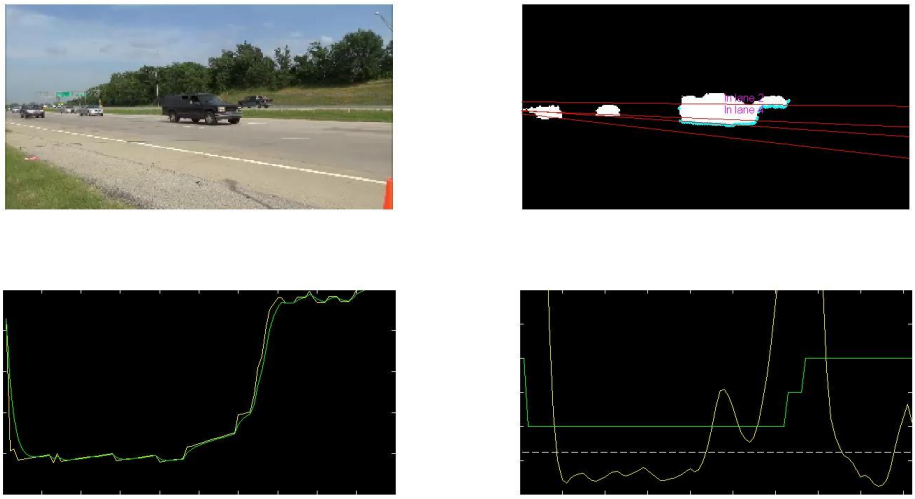

**Figure 16 -** Determining Vehicle Lanes

Clockwise from Top Left: a) Current Frame. b) Intersecting Multi-Vehicle Blob. c) Lane Plot for Blob. d) Lane Instability (Yellow), Stability Threshold (White), Discretized Lane (Green).

Once a vehicle image reaches the right edge of the frame, the vehicle-tracking algorithm attempts to use the previously saved image and blob for classification. If the program detects that the bounds of the vehicle are overlapping with another or that the vehicle was detected in the previous frame as a multiple-vehicle blob, classification is aborted since the shape is distorted. This occurrence is outside the scope of the project, as the objective was to classify isolated high number of traveling class 2 compact cars.

One drawback with this method of tracking is that if the camera set too low and aimed too perpendicular to the road, shadows cast by vehicles, especially pickup trucks, occasionally fall along another lane's linear fit. If the shadow extends past the vehicle, the algorithm will believe it to be two vehicles and will miss the opportunity to classify one. This scenario presents the user with a duplicate classification phase. To mitigate this problem, the research team incorporated a second camera angle to avoid a similar geometrical problem. However, careful setup is required so that the point at the right edge of the first camera's frame is within view of the second camera. Although a technique was developed to translate corresponding points on lanes from one video to another by analyzing traffic flow, not all videos assigned frames lined up correctly. During the project, a single camera was used for simplicity and efficient processing time. Future work could employ added care in setting up camera. Incorporating a second view might eliminate the shadow problem so that additional information about vehicle shape and size in three-dimension is possible.

#### 2.4.1.9 Automatic Classification:

Given an input video, the algorithm used in this study enabled image extraction, shape, and lanes

of vehicles traveling along the road. The automatic classification portion of the project takes these images and blobs and attempts to characterize the various classes of vehicles according to measurements of the images and blobs. The first step along this process generating numerical values of the image that describe its properties. A complete list of properties can be found in the source code under the function avcprops in AVCClassifier.m. These include axis ratio, area, centroid, pyramid histogram of oriented gradients, intensity, gradient distribution, and other properties of the blob and image [21]. Image scale was based on its lane number to improve class coherency. Descriptors form a 44-dimensional feature vector that describes the vehicle.

Vectors classification required generation of a database of vehicle blobs and images sorted by class. Vector values were calculated for each vehicle and stored in a large matrix of vectors and class labels. Using Fisher's Linear Discriminant, a matrix to optimally projects the 44-dimensional space onto two dimensions was created, maximizing distance between classes and minimizing between-class scatter [22]. Superior results were obtained experimentally after considering just four classes: class 3, class 2, class 2 compact cars only, and everything else. By lumping less common vehicles into one class, spacing of more populated classes improved. Splitting class 2 into two subclasses ensured adequate spacing between class 3 and compact cars. Failing to do so would have prevented the number of classified vehicles at 100% certainty, primarily because some class 2 vehicles, such as SUVs, are quite similar to class 3 pickup trucks. However, compact cars resemble neither of these and are best considered separate in this scenario. Attempting to only separate compact cars from everything else resulted in poorly conditioned matrices for projection that were somewhat over-tuned and unstable. Figure 17 illustrates the distribution of data points in two dimensions.

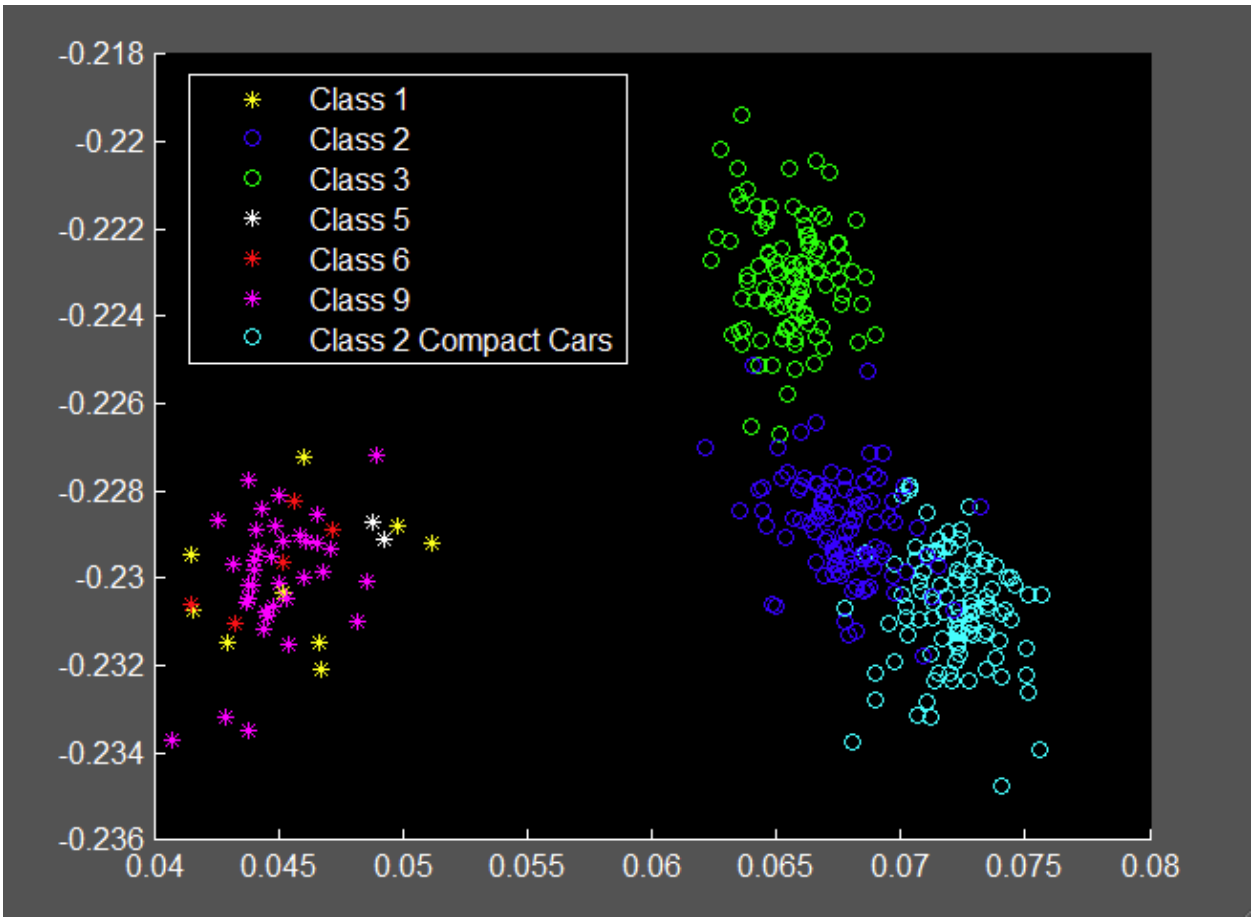


**Figure 17** - Distribution of Data Points of Classified Vehicles

Figure 17 demonstrates there is still a significant amount of overlap between compact cars and the rest of class 2. Fortunately, these types of vehicles are in same class, which is advantageous for this project. Clearly, no attempt was made to distinguish individual classes from the "everything else" category. This enables clear spacing between compact cars and class 3 vehicles.

To classify vehicles, a method similar to linear discriminant analysis was employed. Instead of defining a linear boundary, a polygon was drawn around points corresponding to compact cars, enveloping other class 2 vehicles, as well. When a vehicle is detected, measured properties utilize the fisher matrix to project vector to two dimensions, and verify that it lies within the class 2 specifications. Given affirmation, classification is made with certainty. A number of class 3 vehicles could also be classified given the unfortunate circumstance that pickup trucks with 4 tires are class 3, while pickup trucks with 6 tires are class 5. Thus, class 3 and class 5 pickup trucks cannot be distinguished from one another. Since the program is used for validation, such an error is unacceptable.

#### 2.4.1.10 User Interface:

To aid in ease of use, a graphical user interface was designed to augment the manual classification process. A single function call AVC.run(), starts the program and launches the screen shown in Figure 18.

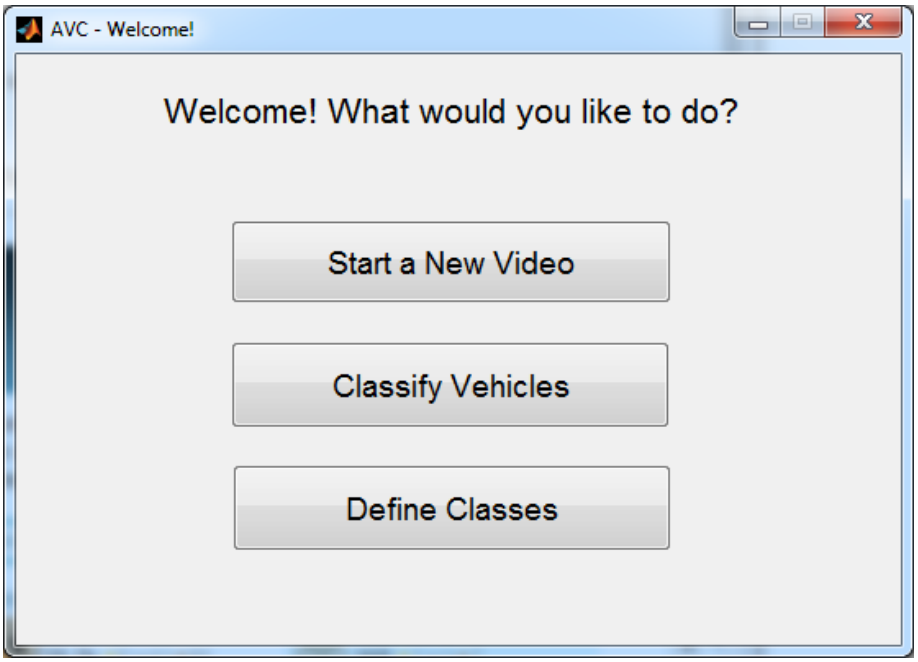


**Figure 18** - AVC Welcome Screen

A user is given the option to set up a new video for classification, to begin classifying a completed or in-progress video, or to define new classes using a custom database of vehicle images. The latter option extends program usefulness by permitting application in similar situations. Figure 19 shows the interface associated with starting a new video.

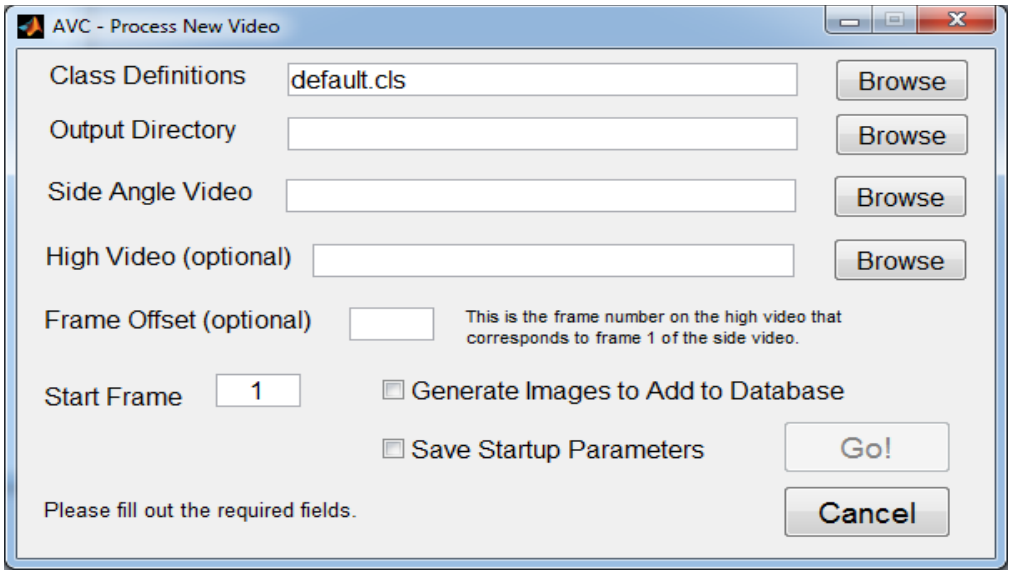


**Figure 19** - New Video Setup Screen

The program interface permits the user to select a class definition and guides them in selecting input files and parameters. Also, the interface offers the option to save parameters generated during setup (e.g., background, velocity curves, and lane lines). These can later be reloaded for debugging and/or analysis purposes. An option is also provided to generate database files that extend the current vehicle database and improve classification.

The setup and processing phase run for an extended period of time, depending on the length of input video. A user could begin the process, go onto another task, and then return later to classify vehicles. Of note is that the system is designed so that classification can occur during while processing is running in the background. It is important to keep in mind, however, that Matlab is not designed to support multithreading in its standard installation. Thus, a user must open another version of Matlab. Given that a user commences the program with AVC.runAndClassify() instead of AVC.run(),once the setup phase is complete, the program will automatically start a new instance of Matlab and open the classification interface. If not, the user must use the following procedure, whether or not processing is complete.

To classify vehicles detected by the system, a user should call AVC.run() and select the begin classification option. The user will then be prompted to select the file ending in "-config.mat" in the output folder notifying the program to locate needed files for the classification interface. A classification interface like the one shown in Figure 20 will open. Options are made available to change the automatically detected lane, to display the frames before and after the vehicle, to skip auto-classified vehicles, or to undo the last action taken. The vehicle in question is highlighted with a box. The previous and following two vehicles are also shown to aid in detecting duplicates. By using this interface in conjunction with the developed system, the time required to process a video is reduced to 12.5% of the initial time without sacrificing accuracy.

#### 2.4.1.11 Design Constraints:

Another tool must be similarly flexible to work with new videos. The camera should be located on the right side of the roadway, far enough from the roadway so that vehicles in each lane are in

full view. The camera should face oncoming traffic, making an approximate 45-degree angle with the road. Video must be filmed with sufficient ambient light and a stationary background. Shadows cast by vehicles must lie mostly beneath or on the opposite of the camera side of the vehicles. The camera cannot be moved during video recording. System behavior is undefined when non-vehicle objects are present (e.g. pedestrians, road workers).

Since the program is used to validate sensor data, the primary focus is accuracy. Although missing vehicles obscured by larger vehicles is unavoidable, other instances should be accounted for correctly. The goal of the project reported herein was to automatically classify over 65% of isolated compact cars with 97% accuracy. Vehicles not automatically classified should be manually classified by a user utilizing the method detailed above.

#### 2.4.1.12 Tool Validation:

The developed validation tool was tested against existing manually classified videos filmed at two separate AVC sites. Due to the limited number of videos available, one (identified as B in Table 2) was previously used to generate the classification database. For this reason, data from manually classified vehicles was effectively used to automatically classify some of the same vehicles. In spite of this, the validation tool provided a good measure of the number of vehicle models matched in the video. The other video (A in Table 2) was not used in generating the classification model, thus, performance was tested independently. Results from the second video were comparable to the first, showing that the system is not limited to videos from which it was trained.

To validate vehicle tracking, the number of vehicles detected automatically was compared to the number of vehicles shown in the high traffic video. Extracted images were examined to ensure consistent differentiation between multi-vehicle blobs. Automatically classified vehicles were also visually validated to ensure inexplicitly they were class 2. Finally, the number of classified vehicles was compared to the number of isolated compact cars to determine classification rate.

To validate the program interface, all team members were required to use the system to classify vehicles. The program was also demonstrated to research tem advisors.

#### 2.4.1.13 Results:

Results from testing the newly developed classification system are shown in the Table 3. Classification criteria were drawn conservatively, yielding 100% accuracy and exceeding an initial goal of 97% accuracy. Every automatic vehicle classification was correct. Notably, not every classified vehicle was one the research team intended to classify. Classification rate (i.e., percentage of isolated compact cars classified) was over 80%, again exceeding an initial goal of 65%. Overall processing time for each video was reduced to approximately 12.5% of the original time devoted to video classification. Table 2 details classification results for each video.

| Video | Accuracy | Classification Rate |
|---|---|---|
| A | 100% | 81.58% |
| B | 100% | 85.55% |

**Table 2 -** Results (Video B used to generate the classification model only)

### 2.4.2 Video Processing Tool #2

A second video-processing tool was developed and used when per vehicle data was available. Typically, an AVC device collects vehicle data and files the data in one-minute bins, meaning that the exact order of each vehicle passing over the AVC device is unknown. Given that specific order and timing of each vehicle is required, the AVC device must be configured to record per vehicle data. Such configuration was used in this project to identify errors and improve the AVC device classification algorithm.

Since the exact time each vehicle passes over the AVC device is gathered when the system is set for per vehicle data collection, time can be converted to frame numbers that correspond with when the vehicle appears video. This second video-processing tool uses frame numbers to show a user each vehicle counted by the AVC device. Instead processing each video frame and classifying vehicles when they are detected, the tool inspects only frames containing vehicles. When an image with a vehicle is displayed, the tool also displays AVC device-assigned class and lane, allowing the user to correct either value when necessary. This process enables quick validation and identification of errors in AVC device data and identify errors.

The validation tool is relatively simple when compared to the first tool, due to the fact that more specific information about each vehicle is available. The added information reduces user interaction to merely answering yes or no to the assigned classification rather than requiring him or her to independently classify each vehicle. Video processing time is reduced significantly.

#### 2.4.2.1 Preparing the Data

As mentioned earlier, the AVC device was configured to record per vehicle data. Once data is collected and organized into an Excel file, the frame number for each record is calculated. The easiest process for performing this task is to first open the video file and find the frame number that corresponds to the first vehicle. Then, using an Excel time code, each time stamp in the Excel file is converted to a frame number based on a frame rate of 30 frames per second. Time begins at zero, meaning that calculated frame number for the first vehicle will not match the frame number found in the video. By subtracting the difference between the two values from among the calculated frame numbers, accurate frame numbers can be obtained for each vehicle. Once these are calculated, the Excel file can be validated.

#### 2.4.2.2 Using the Data

Matlab's validator.m can be used once the data is prepared. The program begins by asking the user for the number of videos used for validation. Given that the user selects one, the program prompts the user to select a single video file. Given that the user selects two, the program prompts the user to select a primary and secondary video file, along with a frame offset corresponding to the offset between the two videos. After the videos are selected, the user is required to choose the data file under validation from a Excel file with the calculated frame numbers. Once a file is chosen, the program reads ithe data and runs the Validate.m program with video and data file inputs.

The next section demonstrates how Validate.m utilizes frame numbers from the data file to display vehicle images from the videos. The program also displays lane and frame numbers for easy manual validation. Since each row in the data file represents a single vehicle, Validate.m continues displaying data one row at a time until all data has been verified. Instead of attempting to automatically classify vehicles using a method similar to that employed by the first video-processing tool, the second tool assumes that the AVC device correctly classified most vehicles, meaning that all vehicles have been classified and a user is merely correcting errors.

#### 2.4.2.3 The Graphical User Interface (GUI)

Once Validate.m has loaded the data file, a graphical user interface (GUI) is initiated and data is displayed one record at a time, as shown in Figure 20.

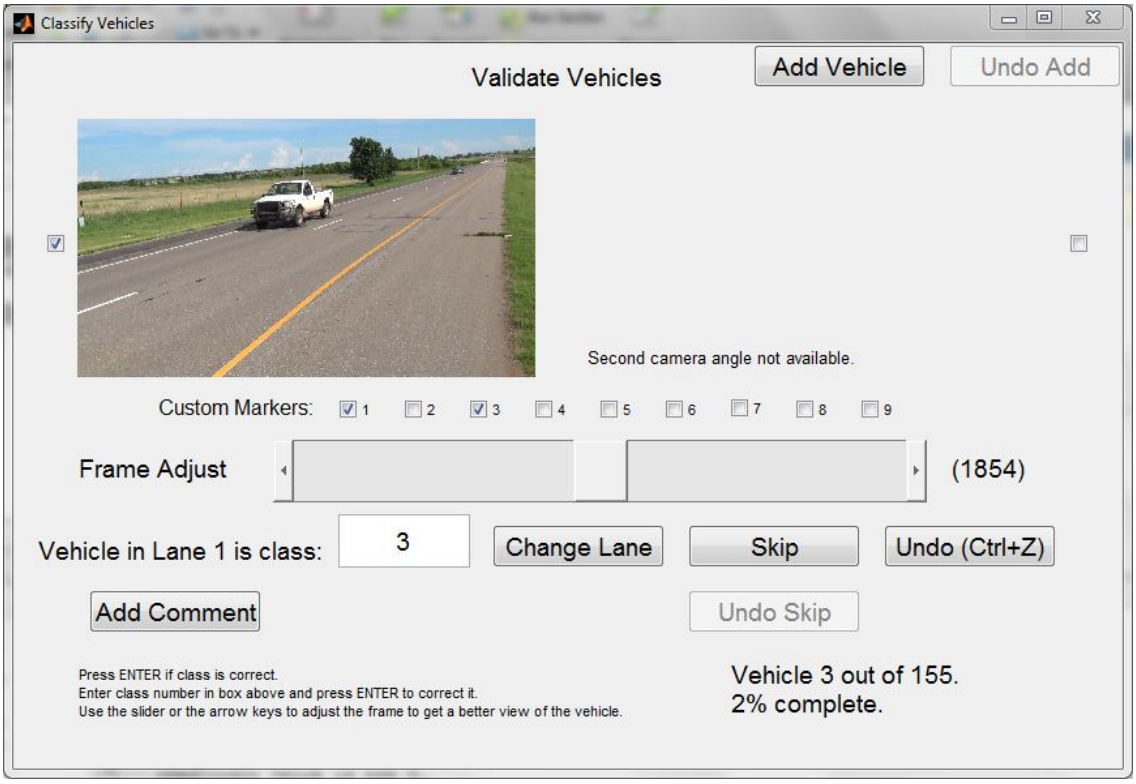


**Figure 20 -** GUI for Per Vehicle Data Validation

The program GUI displays a frame of the primary video in one area and a frame from the secondary video in another. Given that there a secondary video is not available, the text "second camera angle not available" is displayed in lieu of the frame. Boxes next to each frame can be checked to indicate in which video the vehicle appears. In some instances, a vehicle is visible in only one video (e.g. when a larger vehicle blocks a smaller vehicle from view). A slider below the image can be adjusted to indicate which frame is under review in case the vehicle is either difficult to see or out of view due to an error in frame number. Notably, frame number calculations are not always accurate since the AVC timing resolution is one second and each second is populated with 30 frames. The lane and class of the vehicle are displayed under the slider, along with options to change either value when an error is identified. If for some reason a

vehicle appears twice, an option to skip the second occurrence is provided. Likewise, if a vehicle is observed in the frame but was not counted by the AVC device, an option to add the vehicle to the records is provided. The latter instance commonly occurs when two vehicles are counted as one due to proximity. In the event that the user makes a mistake, the undo button allows previous actions to be corrected. Instructions for use are printed at the bottom of the GUI. User progress is displayed in the bottom right corner of the window, informing the user of how many records must be validated.

Additional GUI features permit user comments or tags with custom markers. This option useful when studying common types of errors or discovering rare occurrence. The comment button enables a user to note details about a record; the custom markers enables the user to group types of errors. For example, a user can tag all class 3 vehicles misclassified as class 5 with a "1" for easier identification at a later time.

As the user continues validating one record at a time, two values are printed to the Matlab command line, namely readCursor and printCursor. The readCursor value specifies the row in the data file from which the program is reading; the printCursor represents the row in which the program is printing in the output file. These values allow the user to quit the program and resume at the same point at a later time. When Validate.m is launched, the user will be prompted to indicate the last printed values for readCursor and printCursor. These values enable the user to continue classification from the previous session. readCursor and printCursor values continually increase as the user validates data until the end of the file is reached. When this occurs, the program closes the GUI and notifies the user that the data has been validated.

#### 2.4.2.4 The Output

Each time the user presses ENTER after validating a record displayed in the GUI, Validate.m writes data in a new row of the output file. The output file contains all data from the original per vehicle data file, plus additional information. The first four columns in the output file contain file paths and links to images obtained from videos during validation. A column titled "Used?" contains a 1 and/or 2 to denote whether the vehicle appeared in the primary or secondary video. "Array" contains the correct lane number for each vehicle, while "Original Array" contains lane number recorded prior to validation. It can be assumed that when the numbers are identical, no change has been made by the user. The same principal applies to "Class" and "Original Class." "Error type" is a column containing a 1 for inaccurate classification, a 2 for inaccurate lane, or a 3 if both class and lane were inaccurate. Columns titled "Markers" and "Comments" contain marker numbers and comments added by the user. These cells are left empty if the user does not add information.

As mentioned previously, the value of printCursor enables the program to resume the validation process without overwriting the output file. The program uses printCursor to append additional data to the end of the file instead of creating new output file, meaning that for each input file under validation, one output file is created. Output file can be used to study classification errors.

## 2.5 Video Tools Summary

The second video-processing tool was unlike the first in both purpose and method. The first tool was designed to automate the process of vehicle classification in a video to provide ground-truth data for studying classification accuracy of an AVC equipment. The second tool was designed to identify specific errors made by the AVC device and to allow manual validation for each vehicle classification. This tool takes advantage of additional individual vehicle data gathered for quickly sorting through videos and requiring only a yes or no answer to a question about each classification.

One drawback of the validation tool is that vehicles not counted by the AVC device are typically hidden from the user. In this case, the user will only be shown frames containing vehicles counted by the AVC device; other frame will be skipped. Since the purpose of the tool is identifying classification errors (as opposed to manually classifying each vehicle) this oversight is not a problem. If the validation tool is used to manually classify all vehicles appearing in a video, some vehicles would be missed if the AVC device failed to count them.

The validation tool was used to identify common classification errors and to improve the algorithm used by the AVC device. Since the program is not intended to sort through and process each frame of the video, the time required to validate AVC devise per-vehicle data is significantly reduced when compared with previous methods.

Although the developed video-processing tool was efficient and time saving, its accuracy was limited to 94-98% in best cases. Therefore, the PI has decided to manually process the video recordings for determining vehicle classification. This process was time consuming but its accuracy was guaranteed. The accuracy study and its results presented in Chapter 3 and 4 were obtained by manually processing the video recordings.

# 3 Chapter III: The study of Classification Accuracy

To investigate classification accuracy of ODOT AVC/WIM sites, several on-site deployments were made to record videos capturing traffic flow as vehicles traveled over site sensors. This chapter presents the analysis and results of vehicle classification accuracy based on one-minute time binned ADR data. This chapter also presents analyses performed in project Phase I (year one) during which time the research team did not have the tools or ability to record per vehicle (PVR) data. In Phase II, PEEK Traffic provided the research team the mechanism to collect PVR data. These analyses and results are presented in Chapter 4, which also provides an accuracy study of the ODOT classification algorithm developed and provided by Mr. Daryl Johnson. This scheme is named "ODOT Scheme F".

## 3.1 Classification Errors using 1 minute bins:

After ground-truth data was obtained, a comparison with the classification device output was completed. The following factors were investigated.

1) General distribution of vehicle classes during field-test periods is obtained by both the classification device and VVT for each lane of the site under inspection, and then for distribution of vehicles traveling in the same direction on all lanes combined. Distribution comparison allows visual site-specific observations.

2) Error per class is calculated using equation (1). The error reported represents classification errors occurring at each site: a) Mis-detection when VVT records a vehicle and ADR does not; b) False-detection when ADR records a vehicle and VVT does not show the vehicle; or c) combination of both mis-detection and false-detection.

$$Er = \left(1 - \frac{\min(x, y)}{\max(x, y)}\right)\%, \tag{1}$$

where $x$ represents the ADR count, and y represents the VVT count.
A total of seven AVC field-test deployments were carried. Deployment information is shown in Table 3.

| *Date* | *Site Name* | *Start Time* | *Stop Time* | *Observation Time* | *Labels of Lanes Observed* |
|---|---|---|---|---|---|
| 6/10/2013 | AVC19 | 16:30:00 | 17:45:00 | 1:15:00 | 6 |
| 6/13/2013 | AVC10 | 13:17:00 | 14:48:00 | 1:31:00 | 4,5,6 |
| 6/21/2013 | AVC18 | 16:37:00 | 17:39:00 | 1:02:00 | 1,2,3 |
| 7/11/2013 | AVC24 | 17:18:00 | 18:22:00 | 1:04:00 | 5,6,7,8 |
| 7/11/2013 | AVC47 | 12:59:00 | 14:23:00 | 1:24:00 | 1,2 |
| 8/16/2013 | AVC19 | 8:26:00 | 9:27:00 | 1:01:00 | 6 |
| 8/16/2013 | AVC19 | 11:19:00 | 13:16:00 | 1:57:00 | 6 |

**Table 3 -** Deployments Summary

Test site selection was not random; instead they were carefully chosen to provide a wide spectrum of vehicle traffic and flow characteristics at various locations. Some sites are located on rural 2-lane highways; others are located on major highways near Oklahoma City or Tulsa.

## 3.2 Deployments and Data Collection:

The following sections provide an extensive analysis of each deployment.

### 3.2.1 AVC19 Deployment

AVC19 is located on highway I-44 in Tulsa. ADR 2000 device is used for automatic vehicle classification using loop-axle-loop configuration. This site was visited twice: one visit was on 6-10-2013; another on 8-16-2013. Vehicle traffic on lane 6 was observed during both visits. Deployment on 6-10-2013 commenced at 16:30:00 and ended at 17:45:00. A total of 1:15:00 video recording data were captured and processed. Results are presented in Table 4. Figure 21 shows a comparison of vehicle classification distribution during the deployment period.

A repeat deployment on AVC19 occurred on 8-16-2013 and aimed at capturing morning congestion and noon-to-afternoon traffic flow. Two separate periods were recorded and studied: period 1 from 8:26:00 to 9:27:00 and period 2 from 11:19:00 to 13:16:00.

| Class | ADR Count | Video Count | Class Error |
|---|---|---|---|
| 1 | 2 | 8 | **75%** |
| 2 | 256 | 332 | **23%** |
| 3 | 90 | 150 | **40%** |
| 4 | 1 | 0 | **100%** |
| 5 | 15 | 10 | **33%** |
| 6 | 4 | 8 | **50%** |
| 7 | 0 | 3 | **100%** |
| 8 | 14 | 0 | **100%** |
| 9 | 43 | 57 | **25%** |
| 10 | 1 | 1 | **0%** |
| 11 | 0 | 0 | **-** |
| 12 | 0 | 0 | **-** |
| 13 | 0 | 0 | **-** |
| 14 | 0 | 0 | **-** |
| 15 | 0 | 0 | **-** |
| Sum | 426 | 569 | |

**Table 4 -** AVC19 / 6-10-2013 deployment

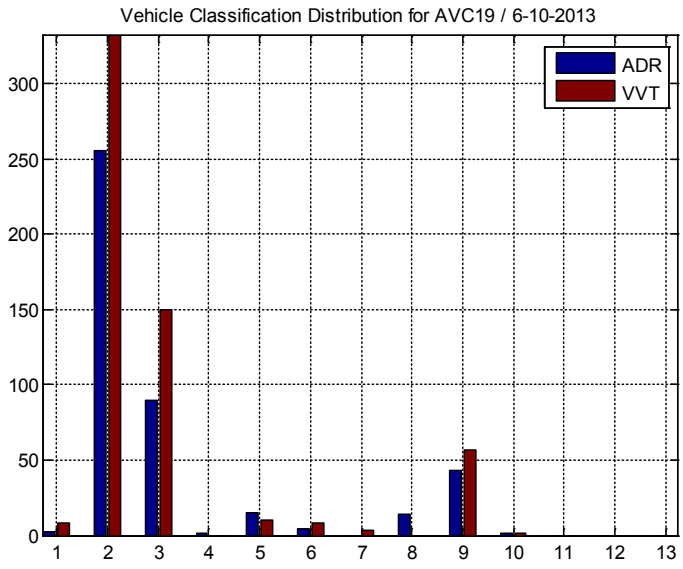


**Figure 21** - Classes Distribution for AVC19 / 6-10-2013

Table 5 provides results for observation period 1. An increased number of class 5 vehicles was recorded by ADR. The sum of class 2 and class 3 vehicles was less than that recorded by video data, suggesting that class 2 and class 3 vehicles are wrongly classified as class 5 by the ADR device. The sum of all detected vehicles for the ADR device is larger than that of the video-based system, which suggests that the ADR device is segmenting several vehicles and then counting them as separate vehicles. Figure 22 shows a comparison of vehicle classification distribution for test observation period 1.

| Class | ADR Count | Video Count | Class Error |
|---|---|---|---|
| 1 | 1 | 0 | **100%** |
| 2 | 104 | 175 | **41%** |
| 3 | 134 | 112 | **16%** |
| 4 | 6 | 2 | **67%** |
| 5 | 76 | 20 | **74%** |
| 6 | 12 | 11 | **8%** |
| 7 | 0 | 0 | - |
| 8 | 15 | 4 | **73%** |
| 9 | 34 | 36 | **6%** |
| 10 | 0 | 0 | - |
| 11 | 0 | 0 | - |
| 12 | 0 | 0 | - |
| 13 | 0 | 0 | - |
| 14 | 0 | 0 | - |
| 15 | 0 | 0 | - |
| Sum | 382 | 360 | |

**Table 5** - AVC19 / 8-16-2013 deployment / Period 1

Table 5 shows classification errors occurred for classes 1, 2, 3 and 4. Moreover, a larger percentage of errors was recorded for classes 5 and 8 in particular.

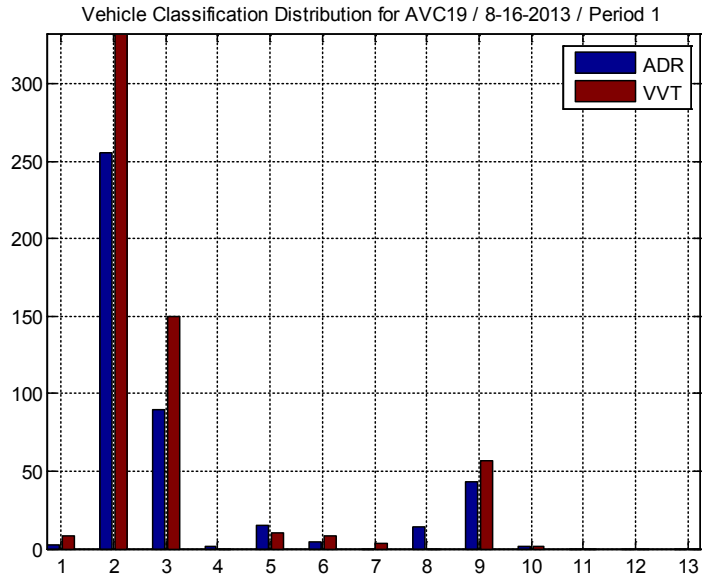


**Figure 22 -** Vehicle Classification Distribution for AVC19 / 8-16-2013 / Period 1

Observation period 2 included more misclassifications when compared to those in period 1, as shown in Table 6. ADR device generated larger counts for almost all vehicle classes. Figure 23 shows a comparison of vehicle classification distribution for this test period.

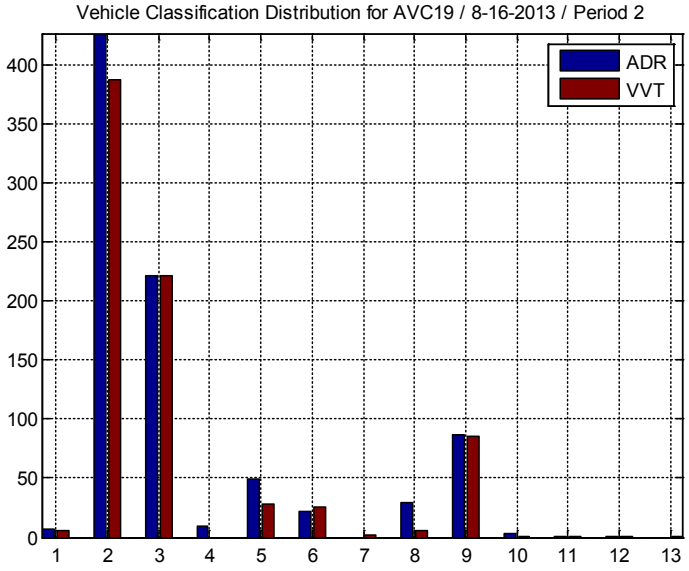


**Figure 23 -** Vehicle Classification Distribution for AVC19 / 8-16-2013 / Period 2

| Class | ADR Count | Video Count | Error |
|---|---|---|---|
| 1 | 7 | 5 | **29%** |
| 2 | 427 | 388 | **9%** |
| 3 | 221 | 222 | **0%** |
| 4 | 9 | 0 | **100%** |
| 5 | 49 | 28 | **43%** |
| 6 | 22 | 25 | **12%** |
| 7 | 0 | 2 | **100%** |
| 8 | 29 | 5 | **83%** |
| 9 | 87 | 85 | **2%** |
| 10 | 3 | 1 | **67%** |
| 11 | 1 | 1 | **0%** |
| 12 | 1 | 1 | **0%** |
| 13 | 0 | 1 | **100%** |
| 14 | 0 | 0 | **-** |
| 15 | 0 | 0 | **-** |
| Sum | 856 | 764 | |

**Table 6** - AVC19 / 8-16-2013 deployment / Period 2

### 3.2.2 AVC10 Deployment

AVC10 is located on highway 169 in Tulsa. ADR device is used for automatic vehicle classification implementing the same loop-axle-loop configuration. The site was visited on 6-13-2013. Vehicle traffic flow on lanes 4, 5, and 6 were observed. Deployment commenced at 13:17:00 and ended at 14:48:00. A total of 1:31:00 video data recording was captured and processed. The results are shown in Tables 7, 8 and 9. The ADR device was set to collect classification data in one-minute bins that were later accumulated.

As previously observed, the ADR device wrong classified class 2 and 3 vehicles as class 5. When comparing one-minute bins collected by the ADR device to video records, a high percentage of errors was observed for nearly all vehicle classes. Similar to AVC19, AVC 10 exhibited high error rates in classes 4, 5 and 8. In addition, class 7 had two mis-detections that amplified the error reported for this class substantially when compared to the previous site.

Figures 24, 25, and 26 show a comparison of vehicle classification distribution during the test period.

| Class | ADR Count | Video Count | Class Error |
|---|---|---|---|
| 1 | 13 | 13 | **0%** |
| 2 | 773 | 753 | **3%** |
| 3 | 264 | 269 | **2%** |
| 4 | 1 | 0 | **100%** |
| 5 | 28 | 6 | **79%** |
| 6 | 6 | 8 | **25%** |
| 7 | 0 | 1 | **100%** |
| 8 | 2 | 0 | **100%** |
| 9 | 12 | 10 | **17%** |
| 10 | 1 | 0 | **100%** |
| 11 | 1 | 1 | **0%** |
| 12 | 0 | 0 | **-** |
| 13 | 0 | 0 | **-** |
| 14 | 0 | 0 | **-** |
| 15 | 0 | 0 | **-** |
| Sum | 1101 | 1061 | |

**Table 7 -** AVC10 / 6-13-2013 deployment – Lane 4

| Class | ADR Count | Video Count | Error |
|---|---|---|---|
| 1 | 16 | 10 | **38%** |
| 2 | 799 | 871 | **8%** |
| 3 | 436 | 398 | **9%** |
| 4 | 14 | 3 | **79%** |
| 5 | 76 | 15 | **80%** |
| 6 | 22 | 32 | **31%** |
| 7 | 2 | 4 | **50%** |
| 8 | 13 | 2 | **85%** |
| 9 | 66 | 70 | **6%** |
| 10 | 2 | 2 | **0%** |
| 11 | 1 | 1 | **0%** |
| 12 | 0 | 0 | **-** |
| 13 | 0 | 0 | **-** |
| 14 | 0 | 0 | **-** |
| 15 | 0 | 0 | **-** |
| Sum | 1447 | 1408 | |

**Table 8 -** AVC10 / 6-13-2013 deployment – Lane 5

| Class | ADR Count | Video Count | Error |
|---|---|---|---|
| 1 | 13 | 12 | **8%** |
| 2 | 317 | 304 | **4%** |
| 3 | 195 | 218 | **11%** |
| 4 | 37 | 1 | **97%** |
| 5 | 37 | 20 | **46%** |
| 6 | 82 | 117 | **30%** |
| 7 | 3 | 3 | **0%** |
| 8 | 15 | 6 | **60%** |
| 9 | 104 | 104 | **0%** |
| 10 | 3 | 2 | **33%** |
| 11 | 0 | 0 | **-** |
| 12 | 0 | 0 | **-** |
| 13 | 0 | 0 | **-** |
| 14 | 0 | 0 | **-** |
| 15 | 0 | 1 | **100%** |
| Sum | 806 | 788 | |

**Table 9 -** AVC10 / 6-13-2013 deployment – Lane 6

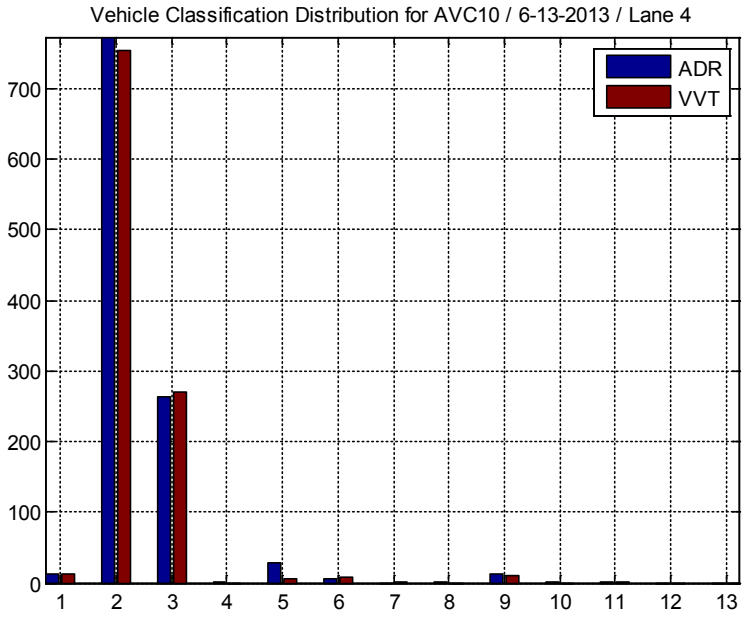


**Figure 24 -** Vehicle Classification Distribution for AVC10 / 6-13-2013 / Lane 4

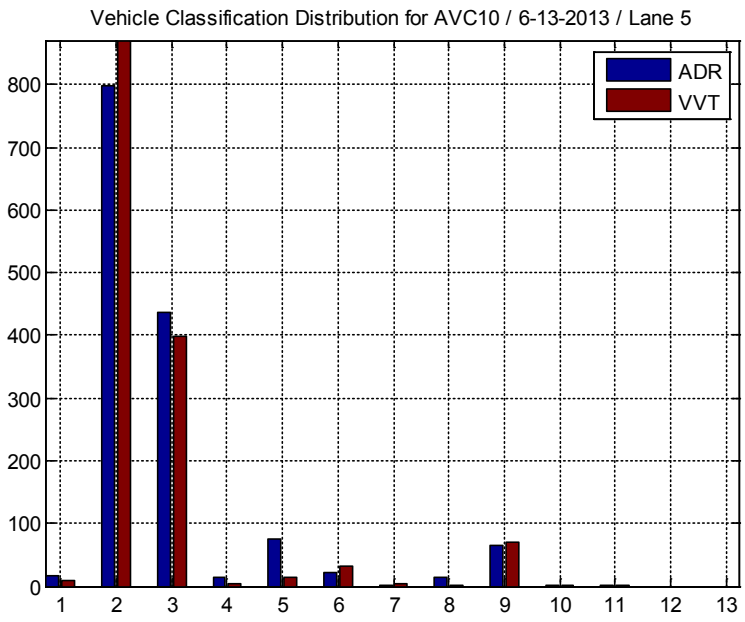


**Figure 25 -** Vehicle Classification Distribution for AVC10 / 6-13-2013 / Lane 5

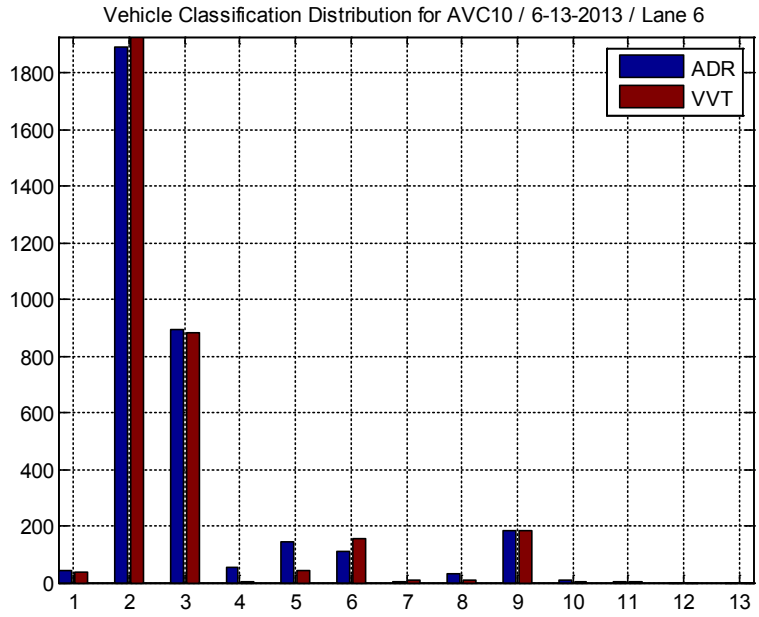


**Figure 26 -** Vehicle Classification Distribution for AVC10 / 6-13-2013 / Lane 6

### 3.2.3 AVC18 Deployment

AVC18 is located on highway 64 west of Tulsa. The ADR device was used for automatic vehicle classification. This site was visited on 6-21-2013. Traffic flows on lanes 1, 2, and 3 were observed. Deployment commenced at 16:37:00 and ended at 17:39:00. A total of 1:02:00 video data recording was captured and processed to obtain results presented in Tables 10, 11, and 12. ADR device was set to gather classification data in one-minute bins that were later accumulated.

| Class | ADR Count | Video Count | Error |
|---|---|---|---|
| 1 | 1 | 5 | **80%** |
| 2 | 564 | 553 | **2%** |
| 3 | 183 | 193 | **5%** |
| 4 | 1 | 0 | **100%** |
| 5 | 17 | 5 | **71%** |
| 6 | 2 | 3 | **33%** |
| 7 | 0 | 0 | **-** |
| 8 | 5 | 1 | **80%** |
| 9 | 12 | 12 | **0%** |
| 10 | 1 | 0 | **100%** |
| 11 | 0 | 0 | **-** |
| 12 | 0 | 0 | **-** |
| 13 | 0 | 0 | **-** |
| 14 | 0 | 0 | **-** |
| 15 | 0 | 0 | **-** |
| Sum | 786 | 772 | |

**Table 10 -** AVC18 / 6-21-2013 deployment – Lane 1

Once more, errors were observed in classes 4, 5, 8, and 10, in particular. In the case of class 10, a single false-detection amplified the error percentage substantially when compared with the error rate reported in previous site field-testing.

| Class | ADR Count | Video Count | Error |
|---|---|---|---|
| 1 | 3 | 10 | **70%** |
| 2 | 848 | 825 | **3%** |
| 3 | 259 | 285 | **9%** |
| 4 | 1 | 1 | **0%** |
| 5 | 27 | 4 | **85%** |
| 6 | 3 | 4 | **25%** |
| 7 | 0 | 0 | **-** |
| 8 | 5 | 1 | **80%** |
| 9 | 26 | 28 | **7%** |
| 10 | 2 | 1 | **50%** |
| 11 | 0 | 0 | **-** |
| 12 | 0 | 0 | **-** |
| 13 | 0 | 0 | **-** |
| 14 | 0 | 0 | **-** |
| 15 | 0 | 1 | **100%** |
| Sum | 1174 | 1160 | |

**Table 11 -** AVC18 / 6-21-2013 deployment – Lane 2

| Class | ADR Count | Video Count | Error |
|---|---|---|---|
| 1 | 1 | 18 | **94%** |
| 2 | 747 | 697 | **7%** |
| 3 | 239 | 259 | **8%** |
| 4 | 1 | 0 | **100%** |
| 5 | 22 | 1 | **95%** |
| 6 | 0 | 1 | **100%** |
| 7 | 1 | 1 | **0%** |
| 8 | 4 | 0 | **100%** |
| 9 | 5 | 6 | **17%** |
| 10 | 0 | 0 | **-** |
| 11 | 0 | 0 | **-** |
| 12 | 0 | 0 | **-** |
| 13 | 0 | 0 | **-** |
| 14 | 0 | 0 | **-** |
| 15 | 0 | 0 | **-** |
| Sum | 1020 | 983 | |

**Table 12 -** AVC18 / 6-21-2013 deployment – Lane 3

Figure 27, Figure 28, and Figure 29 show a comparison of vehicle classification distribution for this test period.

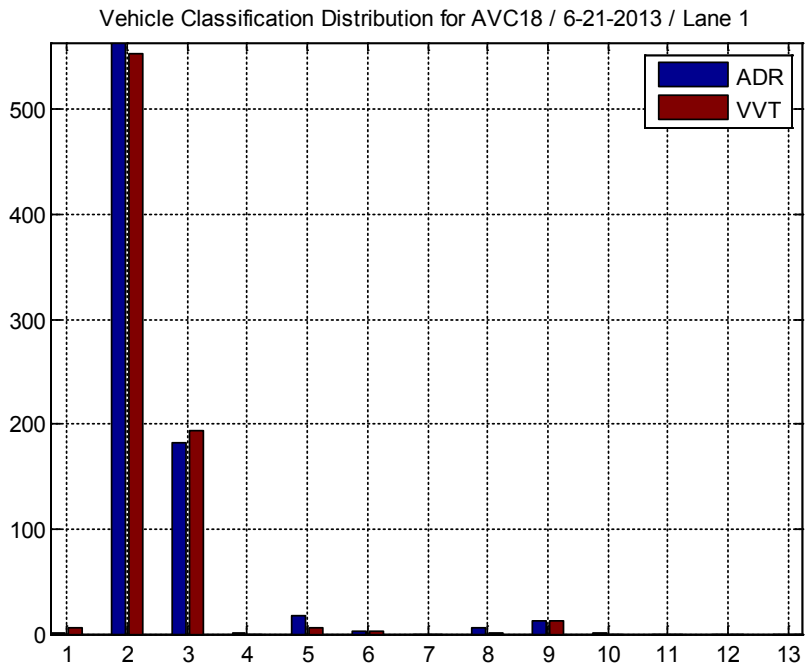


**Figure 27** - Vehicle Classification Distribution for AVC18 / 6-21-2013 / Lane 1

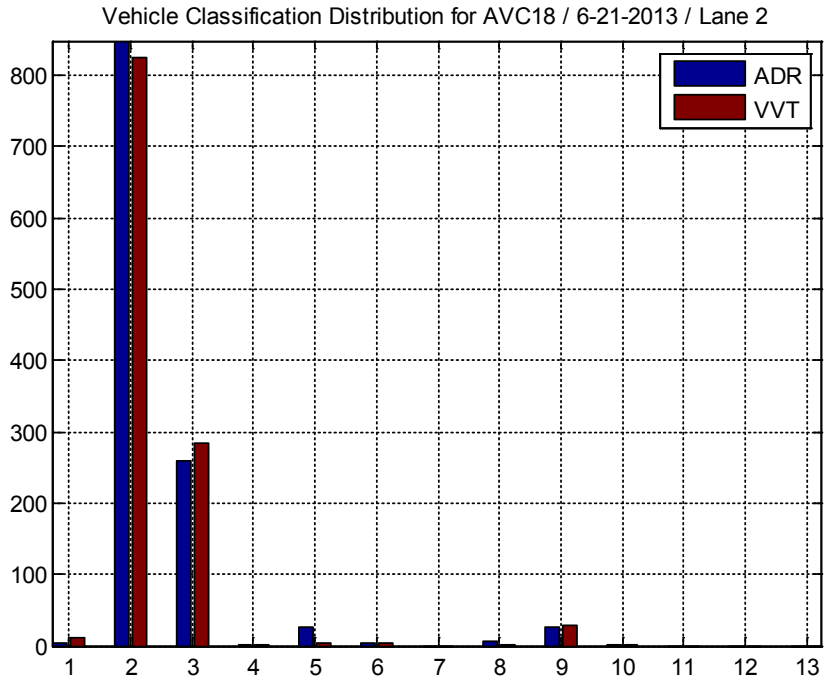


**Figure 28** - Vehicle Classification Distribution for AVC18 / 6-21-2013 / Lane 2

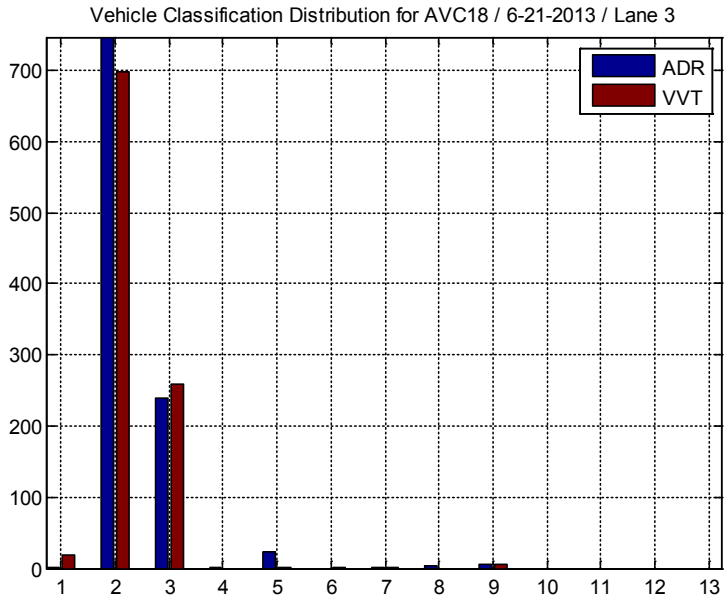


**Figure 29 -** Vehicle Classification Distribution for AVC18 / 6-21-2013 / Lane 3

### 3.2.4 AVC24 Deployment

AVC24 is located on highway 77 in Oklahoma City. This site was visited on 7-11-2013. Traffic flow on lanes 5, 6, 7, and 8 were observed. Deployment commenced at 17:18:00 and ended at 18:22:00. A total of 1:04:00 video data recording was captured and processed. Results are shown in Tables 13, 14, 15, and 16.

| Class | ADR Count | Video Count | Class Error |
|---|---|---|---|
| 1 | 3 | 4 | **25%** |
| 2 | 1056 | 1049 | **1%** |
| 3 | 258 | 249 | **3%** |
| 4 | 1 | 1 | **0%** |
| 5 | 25 | 1 | **96%** |
| 6 | 0 | 0 | - |
| 7 | 0 | 0 | - |
| 8 | 2 | 1 | **50%** |
| 9 | 1 | 1 | **0%** |
| 10 | 0 | 0 | - |
| 11 | 0 | 0 | - |
| 12 | 0 | 0 | - |
| 13 | 0 | 0 | - |
| 14 | 0 | 0 | - |
| 15 | 0 | 0 | - |
| Sum | 1346 | 1306 | |

**Table 13 -** AVC24 / 7-11-2013 deployment – Lane 5

| Class | ADR Count | Video Count | Class Error |
|---|---|---|---|
| 1 | 1 | 0 | **100%** |
| 2 | 1282 | 1272 | **1%** |
| 3 | 276 | 272 | **1%** |
| 4 | 0 | 1 | **100%** |
| 5 | 17 | 3 | **82%** |
| 6 | 3 | 3 | **0%** |
| 7 | 0 | 0 | **-** |
| 8 | 3 | 1 | **67%** |
| 9 | 3 | 3 | **0%** |
| 10 | 0 | 0 | **-** |
| 11 | 0 | 0 | **-** |
| 12 | 0 | 0 | **-** |
| 13 | 0 | 0 | **-** |
| 14 | 0 | 0 | **-** |
| 15 | 0 | 0 | **-** |
| Sum | 1585 | 1555 | |

**Table 14 -** AVC24 / 7-11-2013 deployment – Lane 6

| Class | ADR Count | Video Count | Class Error |
|---|---|---|---|
| 1 | 0 | 4 | **100%** |
| 2 | 1285 | 1263 | **2%** |
| 3 | 257 | 272 | **6%** |
| 4 | 2 | 0 | **100%** |
| 5 | 18 | 7 | **61%** |
| 6 | 0 | 0 | **-** |
| 7 | 0 | 0 | **-** |
| 8 | 9 | 4 | **56%** |
| 9 | 8 | 8 | **0%** |
| 10 | 0 | 0 | **-** |
| 11 | 0 | 0 | **-** |
| 12 | 0 | 0 | **-** |
| 13 | 0 | 1 | **100%** |
| 14 | 0 | 0 | **-** |
| 15 | 1 | 0 | **100%** |
| Sum | 1580 | 1559 | |

**Table 15 -** AVC24 / 7-11-2013 deployment – Lane 7

| Class | ADR Count | Video Count | Class Error |
|---|---|---|---|
| 1 | 1 | 1 | **0%** |
| 2 | 676 | 660 | **2%** |
| 3 | 136 | 139 | **2%** |
| 4 | 1 | 0 | **100%** |
| 5 | 13 | 5 | **62%** |
| 6 | 0 | 0 | **-** |
| 7 | 0 | 0 | **-** |
| 8 | 0 | 0 | **-** |
| 9 | 2 | 2 | **0%** |
| 10 | 0 | 0 | **-** |
| 11 | 0 | 0 | **-** |
| 12 | 0 | 0 | **-** |
| 13 | 0 | 0 | **-** |
| 14 | 0 | 0 | **-** |
| 15 | 0 | 0 | **-** |
| Sum | 829 | 807 | |

**Table 16 -** AVC24 / 7-11-2013 deployment – Lane 8

The same misclassification observations made during past field-testing sites occurred during this deployment, as well. Class 5 vehicles were detected as class 2 and 3. Classes 4 and 8 also had high classification errors. Figures 30, 31, 32, and 33 show a comparison of vehicle classification distribution for this test deployment.

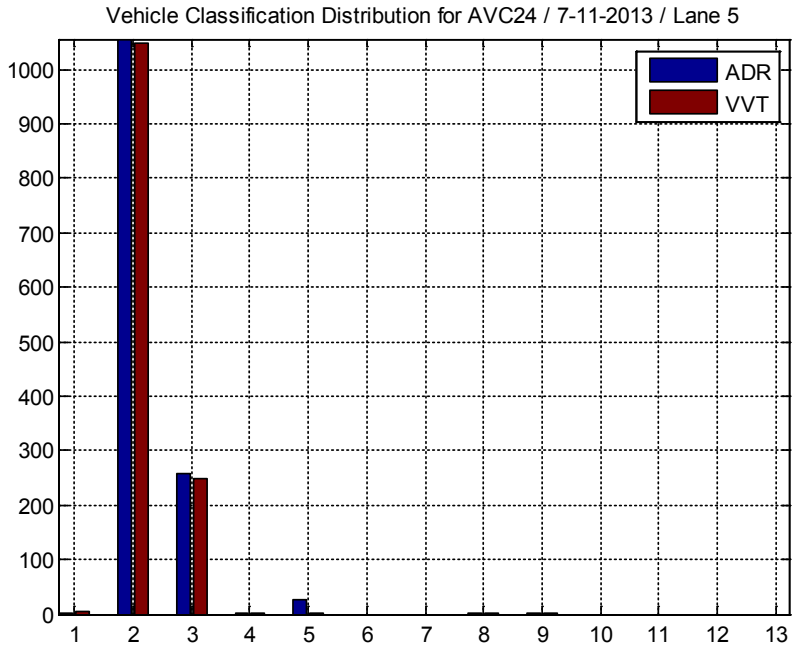


**Figure 30** - Vehicle Classification Distribution for AVC24 / 7-11-2013 / Lane 5

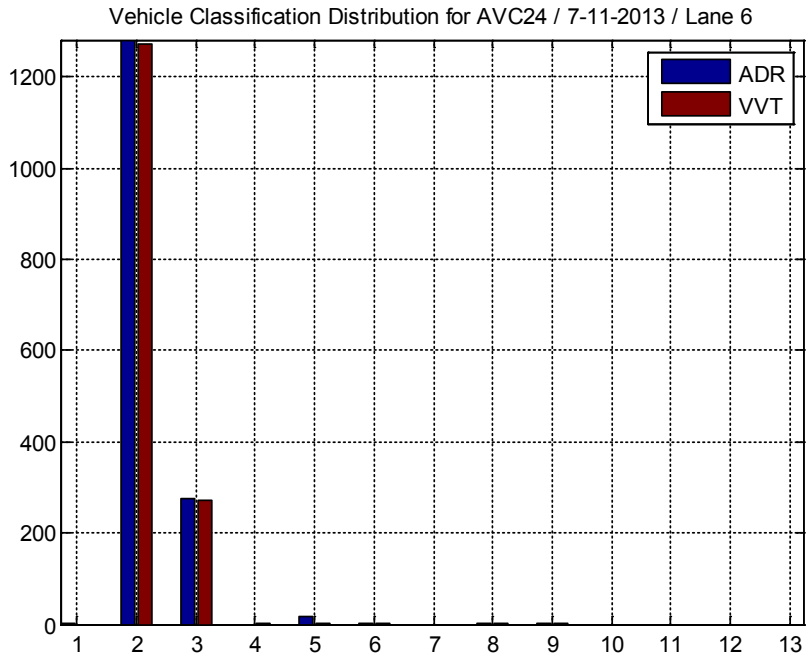


**Figure 31** - Vehicle Classification Distribution for AVC24 / 7-11-2013 / Lane 6

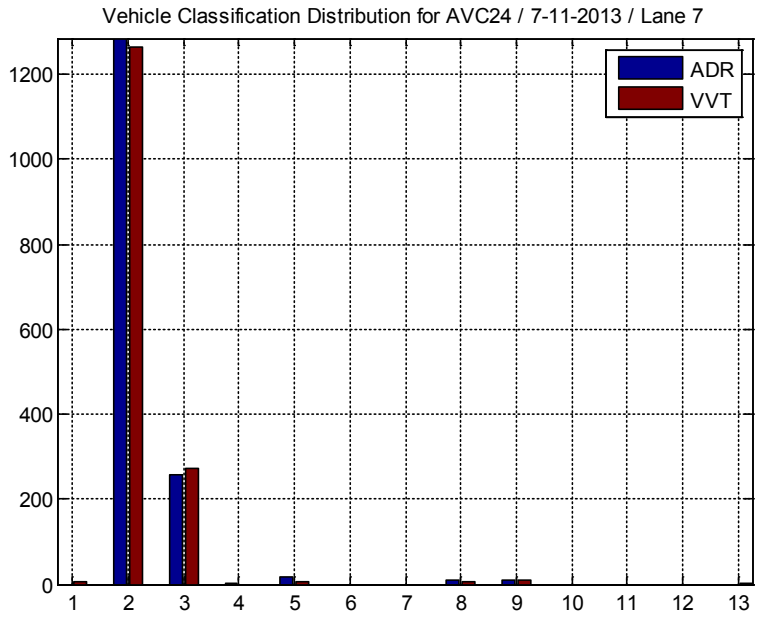


**Figure 32** - Vehicle Classification Distribution for AVC24 / 7-11-2013 / Lane 7

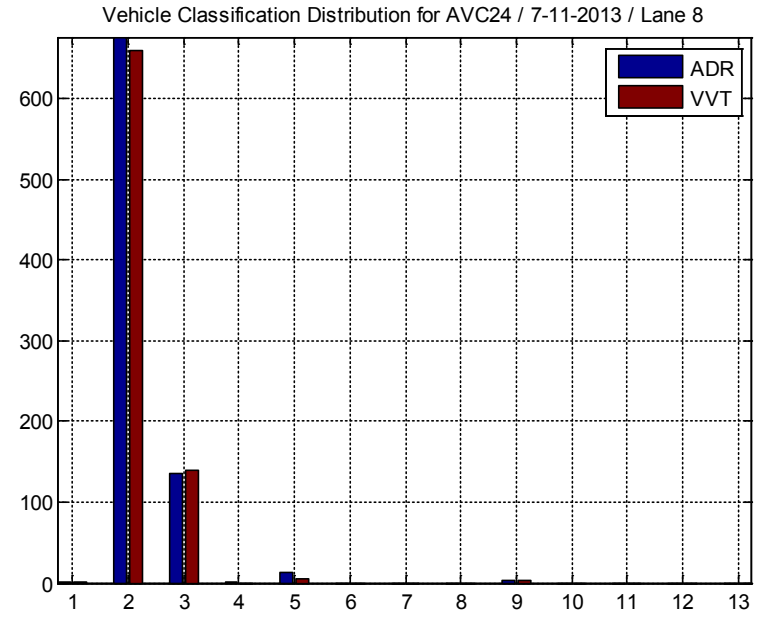


**Figure 33** - Vehicle Classification Distribution for AVC24 / 7-11-2013 / Lane 8

### 3.2.5 AVC47 Deployment

AVC47 is located on Route 66 outside Chandler. This site was visited on 7-11-2013. Traffic flows on lanes 1 and 2 were observed. Deployment commenced at 12:59:00 and ended at 14:23:00. A total of 1:24:00 video data recording was captured and processed to generate results shown in Tables 17 and 18.

| Class | ADR | Video | Class |
|---|---|---|---|
| 1 | 5 | 3 | **40%** |
| 2 | 111 | 116 | **4%** |
| 3 | 67 | 91 | **26%** |
| 4 | 4 | 0 | **100%** |
| 5 | 28 | 3 | **89%** |
| 6 | 3 | 5 | **40%** |
| 7 | 1 | 1 | **0%** |
| 8 | 6 | 1 | **83%** |
| 9 | 11 | 14 | **21%** |
| 10 | 0 | 0 | - |
| 11 | 0 | 0 | - |
| 12 | 0 | 0 | - |
| 13 | 0 | 0 | - |
| 14 | 0 | 0 | - |
| 15 | 0 | 0 | - |
| Sum | 236 | 234 | |

**Table 17** - AVC47 / 7-11-2013 deployment - Lane 1

| Class | ADR | Video | Class |
|---|---|---|---|
| 1 | 2 | 2 | **0%** |
| 2 | 120 | 113 | **6%** |
| 3 | 65 | 90 | **28%** |
| 4 | 0 | 0 | - |
| 5 | 17 | 3 | **82%** |
| 6 | 6 | 6 | **0%** |
| 7 | 1 | 1 | **0%** |
| 8 | 1 | 0 | **100%** |
| 9 | 4 | 4 | **0%** |
| 10 | 0 | 0 | - |
| 11 | 0 | 0 | - |
| 12 | 0 | 0 | - |
| 13 | 0 | 0 | - |
| 14 | 0 | 0 | - |
| 15 | 0 | 1 | **100%** |
| Sum | 216 | 220 | |

**Table 18** - AVC47 / 7-11-2013 deployment - Lane 2

Figures 34 and 35 show a comparison of vehicle classification distribution for this test period.

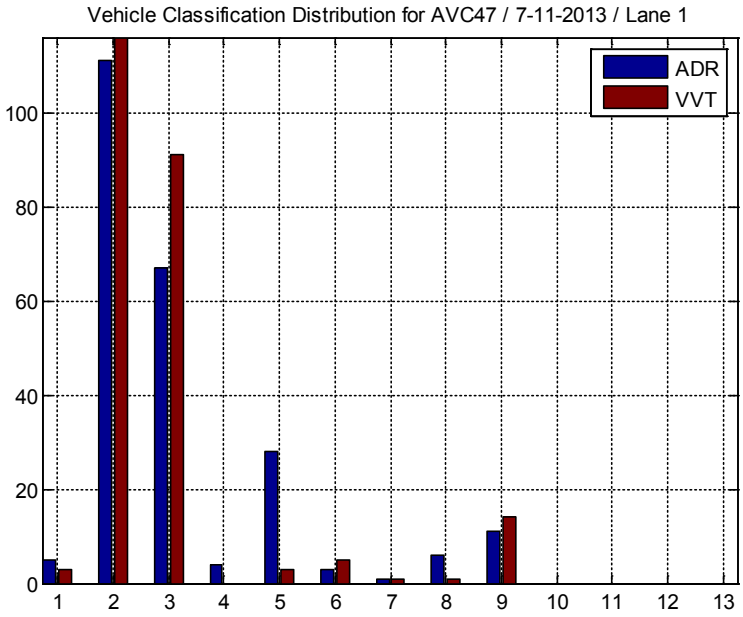


**Figure 34 -** Vehicle Classification Distribution for AVC47 / 7-11-2013 / Lane 1

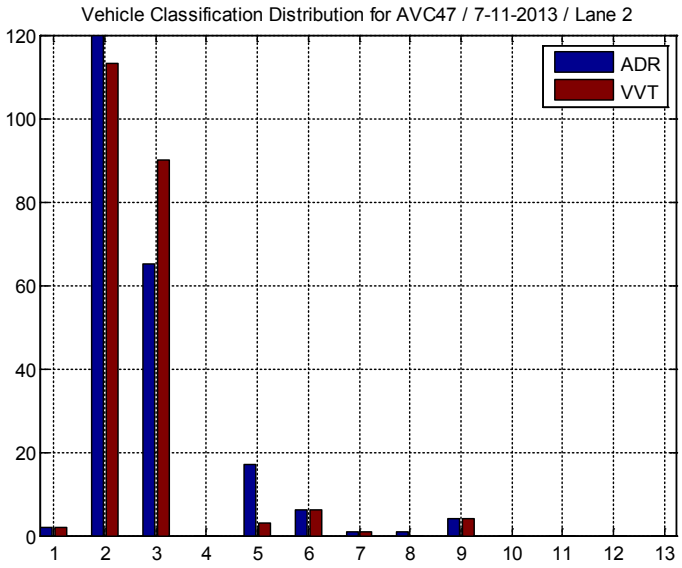


**Figure 35 -** Vehicle Classification Distribution for AVC47 / 7-11-2013 / Lane 2

## 3.3 ODOT Scheme F Algorithm Evaluation

A final step in Phase I of the classification accuracy study was implementing and testing a modified algorithm provided to us by Mr. Daryl Johnson at ODOT. Table 19 depicts the modified algorithm. Testing was conducted at AVC18 site. Traffic and ground-truth data was recorded between 14:43:00 to 15:14:00 using the FHWA-USA classification scheme; recording between 15:45:00 to 16:16:00 was performed after implementing ODOT scheme F. Data processing was performed on the one-minute binned data.

The ODOT modified scheme added a missing class 5 entry to the original FHWA-USA scheme. The addition describing a single truck and one axle trailer resulted in a clear improvement in class 5 vehicle accuracy.

| # AXLE | CLASS | VECHICLE DESCRIPTION | SPACING | SPACING | SPACING | SPACING | SPACING | SPACING | SPACING | SPACING |
|---|---|---|---|---|---|---|---|---|---|---|
| 2 | 1 | MOTORCYCLE | 0.0 - 6.0 | | | | | | | |
| 2 | 2 | AUTO | 6.0 - 10.2 | | | | | | | |
| 2 | 3 | PICKUP / VAN | 10.2 - 13.0 | | | | | | | |
| 2 | 5 | 2 D | 13.0 - 16.0 | | | | | | | |
| 2 | 4 | BUS | 16.0 - 40.0 | | | | | | | |
| 2 | 2 | AUTO | DEFAULT | | | | | | | |
| 3 | 2 | AUTO W/ 1 AXLE TRLR | 6.0 - 10.2 | 6.0 - 23.0 | | | | | | |
| 3 | 3 | PICKUP W/ 1 AXLE TRLR | 10.2 - 13.0 | 6.0 - 23.0 | | | | | | |
| 3 | 5 | 2 D W/ 1 AXLE TRLR | 13.0 - 16.0 | 6.0 - 23.0 | | | | | | |
| 3 | 6 | 3 AXLES SU | 6.0 - 22.0 | 0.0 - 6.0 | | | | | | |
| 3 | 4 | BUS W/ 3 AXLES | 22.0 - 40.0 | 0.0 - 6.0 | | | | | | |
| 3 | 8 | ≤ 4 AXLES ST | 12.0 - 17.0 | 14.0 - 40.0 | | | | | | |
| 3 | 6 | 3 AXLES SU | DEFAULT | | | | | | | |
| 4 | 2 | AUTO W/ 2 AXLES TRLR | 6.0 - 10.2 | 6.0 - 40.0 | 0.0 - 6.0 | | | | | |
| 4 | 3 | PICKUP W/ 2 AXLES TRLR | 10.2 - 13.0 | 6.0 - 35.0 | 0.0 - 6.0 | | | | | |
| 4 | 5 | 2 D W/ 2 AXLES TRLR | 13.0 - 16.0 | 6.0 - 40.0 | 0.0 - 6.0 | | | | | |
| 4 | 7 | ≥ 4 AXLES SU | 6.0 - 23.0 | 0.0 - 9.0 | 0.0 - 9.0 | | | | | |
| 4 | 8 | ≤ 4 AXLES ST | 6.0 - 20.0 | 0.0 - 6.0 | 6.0 - 40.0 | | | | | |
| 4 | 8 | ≤ 4 AXLES ST | 6.0 - 17.0 | 14.0 - 40.0 | 3.2 - 6.0 | | | | | |
| 4 | 8 | ≤ 4 AXLES ST | DEFAULT | | | | | | | |
| 5 | 9 | 5 AXLES ST | 6.0 - 22.0 | 0.0 - 6.0 | 6.0 - 40.0 | 0.0 - 23.0 | | | | |
| 5 | 11 | ≤ 5 AXLES MT | 6.0 - 17.0 | 11.0 - 25.0 | 6.0 - 18.0 | 11.0 - 25.0 | | | | |
| 5 | 9 | 5 AXLES ST | DEFAULT | | | | | | | |
| 6 | 10 | ≥ 6 AXLES ST | 6.0 - 22.0 | 0.0 - 6.0 | 0.0 - 40.0 | 0.0 - 11.0 | 0.0 - 11.0 | | | |
| 6 | 12 | 6 AXLES MT | 6.0 - 22.0 | 0.0 - 6.0 | 0.0 - 25.0 | 6.0 - 18.0 | 11.0 - 25.0 | | | |
| 6 | 10 | ≥ 6 AXLES ST | DEFAULT | | | | | | | |
| 7 | 10 | ≥ 6 AXLES ST | 6.0 - 22.0 | 0.0 - 6.0 | 0.0 - 40.0 | 0.0 - 13.0 | 0.0 - 12.0 | 0.0 - 12.0 | | |
| 7 | 13 | ≥ 7 AXLES MT | DEFAULT | | | | | | | |
| 8 | 13 | ≥ 7 AXLES MT | | | | | | | | |
| 9 | 13 | ≥ 7 AXLES MT | | | | | | | | |
| 10 | 15 | | | | | | | | | |
| 11 | 15 | | | | | | | | | |
| 12 | 15 | | | | | | | | | |
| 13 | 15 | | | | | | | | | |
| 14 | 15 | | | | | | | | | |
| | | | one - two | two - three | three - four | four - five | five - six | six - seven | seven - eight | eight - nine |

**Table 19** - Modified algorithm proposed by ODOT

A comparison of mis-detection and false-detection errors between both algorithms is presented in Figures 36 and 37. Clearly, the ODOT modified scheme improves classification accuracy of class 5 vehicles. Errors were mainly attributed to the missing entry in FHWA-USA. A slight

increase in false-detections in classes 6 and 4 was also reported. Minor increases and decreases for errors concerning the remaining classes indicate that this algorithm requires further improvement. Hence, researching an optimal algorithm that combines all missing entries and optimizes axle spacing thresholds between various classes is necessary to improve overall system accuracy.

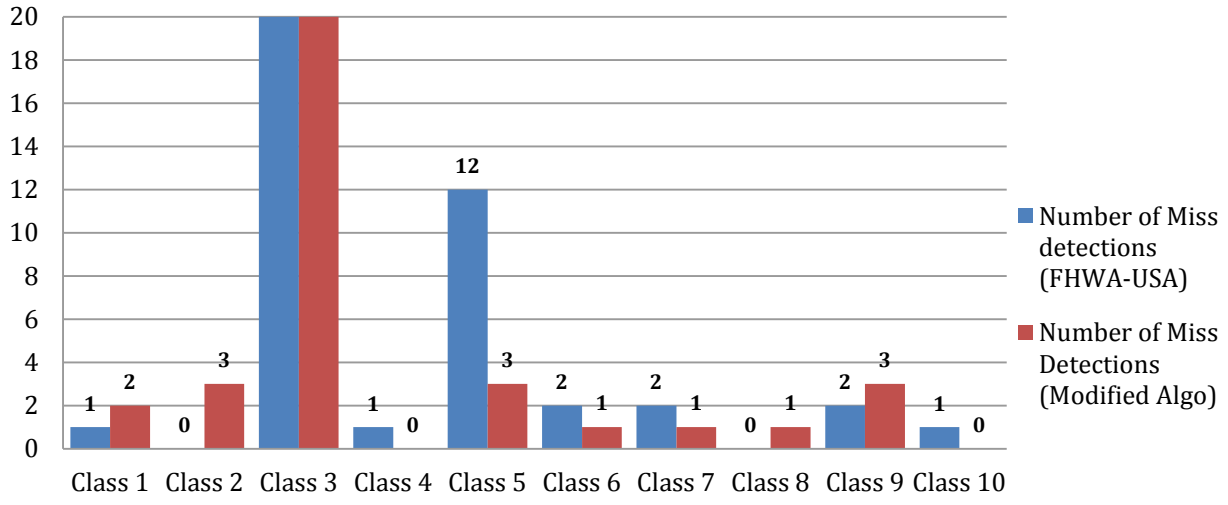


**Figure 36** - Miss detection error comparison between original scheme and modified algorithm

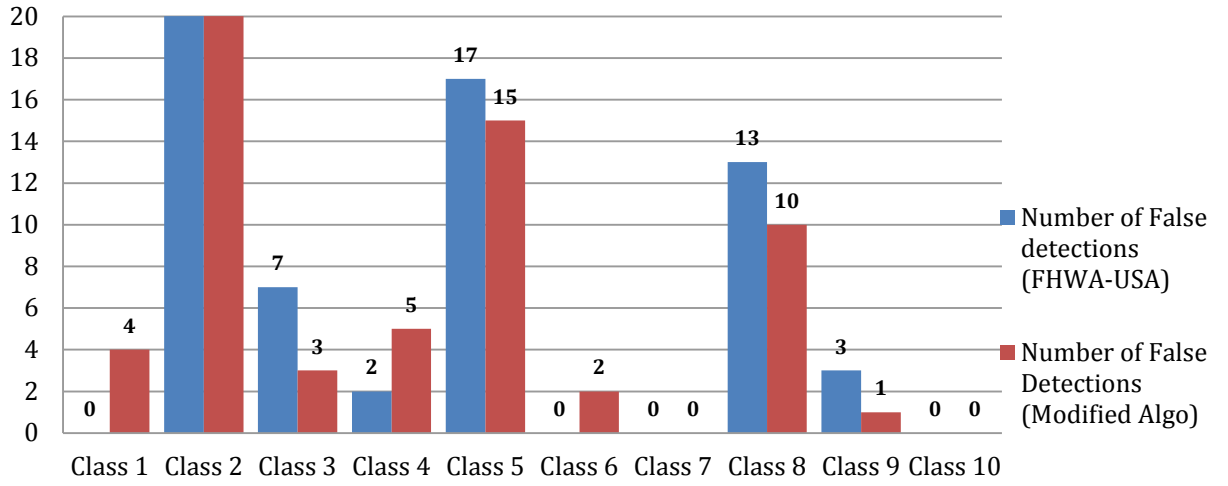


**Figure 37** - False-detection error comparison between original scheme and modified algorithm

# 4 Chapter IV: Development of an Improved Classification Scheme

Upon completion of classification accuracy testing at ODOT AVC sites with ADR units serving as a means for vehicle classification and data recording, a noteworthy amount of errors were detected in reported classification results, particularly for classes 2, 3, 5 and 8. It was surmised that axle spacing thresholds in the original Scheme F algorithm currently employed by ODOT was not accurately differentiating among classes and not reflecting wheelbase vehicles traveling Oklahoma state roadways and highways. It was clear that improving AVC site accuracy required new and revised classification algorithm thresholds. Furthermore, the new thresholds must be optimized to recognize current vehicle counts per class.

To determine optimal axle-spacing thresholds, the research team analyzed vehicle data collected during phase II (year two) of the project. With this information, the research team developed combinational patterns and statistical distributions of axle spacing per vehicle class (i.e., wheelbase distributions). Per vehicle data was required to build such distributions and was used to obtain more accurate estimates for adjusting and improving classification algorithm accuracy.

To obtain PVR axle-spacing data and vehicle count, a firmware modification to the ADR unit was performed prior to each deployment. Instead of recording data as time/speed binned files (customary for ODOT recording stations), the revised PVR method generated a file containing a record for each passing vehicle, including its class, axle spacing(s), and speed, among others. A PVR recording method was tested and validated by comparing wheelbase lengths reported by the vehicle manufacturing blueprints and those reported by the ADR unit of several vehicles. Margin of error was 1%; site wheelbase calibration was not performed prior to inserting data in the database.

## 4.1 Classification Errors using PVR data

Because statistical distribution of cars populating different FWHA class categories has changed over the years, original thresholds are no longer accurately representing current vehicle classes. This serves as the main explanation as to why the FHWA has continually recorded an increase in the number of errors since the original system was first conceived.

Large datasets of all class vehicle wheelbases were needed to obtain and build needed distributions. Data gathering was accomplished by recording PVR files from ADR units. In the first phase of data gathering for classification error analysis, data was obtained from ODOT AVC 18 and 19 sites, as shown in Table 20. Each site was monitored for approximately two hours on two separate visits. Video footage for three lanes per site was captured and processed. Obtained errors were categorized according to class.

Classification errors were primarily categorized as mis-detection and false-detection

1. Mis-detection errors occurred when a vehicle class was detected by the ground-truth system but not by the ADR classifier, resulting in a reduction of the total class vehicle count reported by the ADR unit.

2. False-detection errors occurred when a vehicle of a particular class was wrongfully classified in a different class, resulting in an increase of the total vehicle count of the wrong class reported by the ADR.

Mis-detection and false-detection are related—either a one-to-one or one-to-many relationship. One-to-one relationship describes vehicles that were mis-detected in one class but falsely assigned to a different class. One-to-many describes a vehicle of a particular class that was split into more than one vehicles belonging to different classes. Occasionally a class 9 vehicle are falsely detected by the ADR unit as a class 6 and a class 2 vehicle.

| Statistic | AVC18 | AVC19 |
|---|---|---|
| Date | 6/11/2014 | 6/19/2014 |
| Traffic | Free Flow | Free Flow |
| Time Begin | 11:51:05 | 14:24:43 |
| Time end | 14:00:44 | 16:26:19 |
| Time Duration | 2:09:39 | 2:01:36 |
| No. of Lanes | 3 | 3 |
| No. of vehicles | 3248 | 4188 |
| Total Number of Cars in Database | 7436 | |

**Table 20 -** Summary Statistics for the initial data acquisition ground-truth data sets

Data acquisition at these two locations was accomplished using the original algorithm, namely FHWA-USA that follows scheme F. Although the algorithm name includes “FHWA,” it was not developed by the federal agency nor was it promoted or required by the FHWA. Nonetheless, the FHWA-USA classification scheme is used in the current configuration of all of ODOT ADR units. Figure 36 illustrates the concept of error analysis and tree entry modification utilized while processing results reported in this chapter.

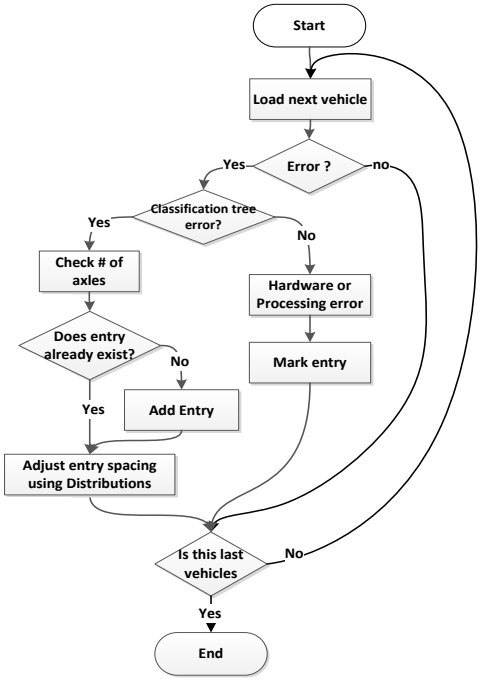


**Figure 36** - Error analysis and tree entry modification

To objectively quantify classification error in our study, the two aforementioned indicators were used. The mis-detecion error per class given in (2) is the percentage ratio of the difference between the ground-truth count and correctly classified vehicle count to the total number of ground-truth vehicle counts. The second indicator investigated was the false-detection error given in (3); it is the percentage ratio of the difference between the station reported total vehicle count and the correctly classified station vehicle count to the station reported total vehicle count.

$$Misdetection = \left( \frac{\text{Ground truth} - \text{Station Correct}}{\text{Ground truth}} \right)\% \tag{2}$$

$$False\,detection = \left( \frac{\text{Station reported} - \text{Station Correct}}{\text{Station reported}} \right)\% \tag{3}$$

## 4.2 Classification Error Summary based on Video Recordings

This section discusses classification errors per class that have been found while analyzing the PVR AVC data collected by the ADR units, excluding errors resulting from hardware malfunction or errors related to the behavior of vehicles passing over detection loops (e.g., lane changing over sensors that could result in false-detection or misreading).

- **CLASS 2**

Regarding class 2 errors, 98% of errors were the result of class 3 vehicles falsely classified as class 2, as depicted in Figure 37. This type of misclassification is the primary cause for class 2 detection error and the result of overlap in vehicle wheelbases that pertain to both classes. Additionally, a small number of class 2 errors resulted from detection of only one axle from a class 5 vehicle or a high speed class 1 motorcycle as it crossed the sensor. The default 1-axle entry is class 2, which is the reason fast traveling motorcycles are sometimes classified as class 2 vehicles.

**Figure** 37 - Class 2 major overlapping case

- **CLASS 3**

Figure 38 depicts the four primary contributing reasons for class 3 errors. First is the result of class 3 vehicles classified as class 2 (i.e., mis-detection). Second, large class 3 trucks with wheelbase lengths overlapping those of class 5 are sometimes classified as class 5 trucks (i.e., false-detection). Third, three-axle class 3 trucks overlap with class 8 trucks, which causes class 3 to be classified as class 8 upon sensor overpass (i.e., false-detection). Fourth, four-axle class 3 trucks overlap with class 8, once again causing misclassification as a class 8 truck (i.e., false-detection).

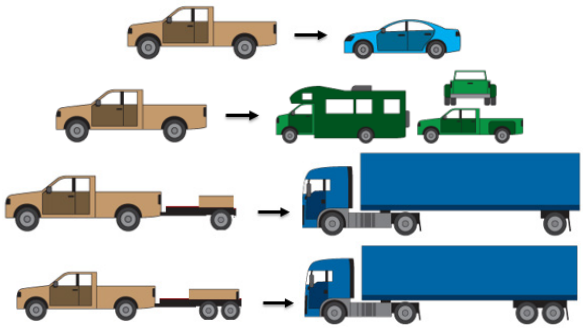

**Figure 38** - Class 3 major overlapping cases

- **CLASS 4**

The primary cause for class 4 errors was an overlap between small bus axle spacing and that of class 5 single unit trucks (SUTs), as depicted in Figure 39. In rare cases, the same was true for axel overlap with class 3 vehicles. Additionally, certain class 6 trucks overlapped with the axle space of class 4 trucks, again resulting in false-detection of a class 4 vehicle.

**Figure 39** - Class 4 major overlapping case

- **CLASS 5**

Figure 40 depicts reasons for class 5 detection errors. Four major causes include: 1) smaller 6-wheel trucks with wheelbase spacing overlapping with class 3; 2) three-axle class 5 vehicles overlapping with class 8; 3) four-axle class 5 vehicles overlapping with class 8; and 4) overlap with class 4 buses.

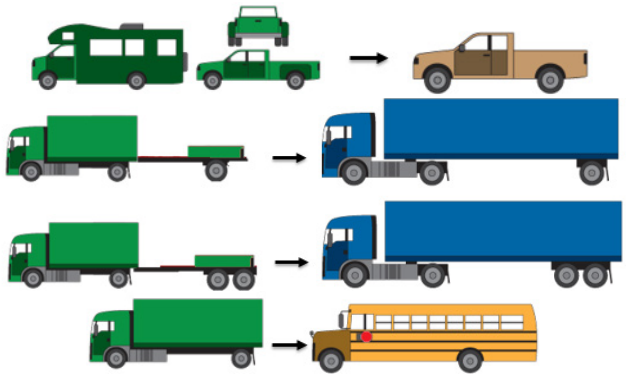

**Figure 40** - Class 5 major overlapping cases

- **CLASS 6**

Class 6 errors occurred because three-axle trucks sometimes overlapped with class 4 spacing of three-axle buses, as depicted in Figure 41. The result is a class 6 truck being classified as a class 4 bus. In essence, this leads to false-detection of class 4 buses and mis-detection of class 6 trucks.

**Figure 41** - Class 6 major overlapping case

- **CLASS 7**

Concerning class 7 trucks, a missing entry in the original tree resulted in class 7 SUTs with 5 axles being classified as class 9 according to the default 5-axle entry, as depicted in Figure 42.

**Figure 42** - Class 7 error case

- **CLASS 8**

Although Class 8 did not have a significant number of mis-detection errors, the class had a large percentage of false-detections mainly due to errors discussed above regarding class 3 and class 5. For these reasons, class 8 is considered one of the most problematic for vehicle classification.

- **CLASS 9**

Class 9 results were superior over other classes. Mis-detection was due to incorrect axle number detection. Class 9 vehicles were occasionally classified as class 6 and class 2 combinations, which is the default for a 0- or 1-axle entry, as depicted in Figure 43.

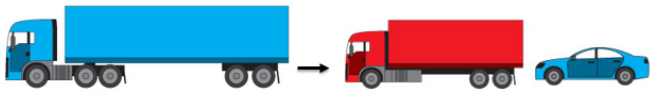

**Figure 43** - Class 9 error case

- **CLASS 10**

Specific entries depicted in Figure 44 were found to be missing from the original classification algorithm tree. Vehicles in class 10 were sometimes segmented into several smaller classes upon detection.

**Figure 44** - Class 10 missing entries

- **CLASS 11**

No errors were detected for class 11 in the initial phase of data collection and database construction.

- **CLASS 12**

Figure 45 depicts the missing entry, which caused class 12 vehicles to be misclassified as class 10—the default 6-axle entry.

**Figure 45** - Class 12 missing entry classified as class 10

## 4.3 Methodology

Statistical distribution of axle-spacing per class was performed to construct a new algorithm (axle spacing thresholds) that would predictably decrease the number of classification errors reported by the AVC classifier. PVR and video recordings were post processed. Axle spacing measured by the ADR unit was assigned to its correct vehicle classifications using the video recording. Distribution results statistically describe random variables (i.e., vehicle classes) corresponding to vehicles currently traveling on Oklahoma state roadways. Once distributions were developed and understood, the research team approximated them by Gaussian distribution models using least mean squared error for regression fitting and model error minimization. Finally, the research team implemented two different algorithms to find optimal thresholds axle-spacing thresholds differentiating various classifications. One optimal algorithm considers weights proportional to vehicle counts while the other algorithm uses equal weights.

Table 21 presents the combined results of the original FHWA-USA algorithm during all data acquisition deployments. Each row in the table shows the sum per class as recorded by the classification station (ADR unit), along with the correct classification for that sum distributed over all classes. The table serves as an instant indicator to aid in detecting classification errors for each particular class.

| Station sum | Class | Class 1 | Class 2 | Class 3 | Class 4 | Class 5 | Class 6 | Class 7 | Class 8 | Class 9 | Class 10 | Class 11 | Class 12 | Class 13 |
|---|---|---|---|---|---|---|---|---|---|---|---|---|---|---|
| 28 | Class 1 | 21 | 2 | 3 | 0 | 0 | 0 | 0 | 0 | 2 | 0 | 0 | 0 | 0 |
| 6011 | Class 2 | 17 | 3396 | 2579 | 0 | 3 | 1 | 2 | 0 | 13 | 0 | 0 | 0 | 0 |
| 2601 | Class 3 | 0 | 30 | 2492 | 4 | 70 | 0 | 1 | 2 | 2 | 0 | 0 | 0 | 0 |
| 102 | Class 4 | 0 | 0 | 0 | 9 | 65 | 23 | 1 | 0 | 4 | 0 | 0 | 0 | 0 |
| 536 | Class 5 | 0 | 0 | 241 | 2 | 292 | 0 | 0 | 0 | 1 | 0 | 0 | 0 | 0 |
| 157 | Class 6 | 0 | 0 | 1 | 0 | 0 | 137 | 1 | 0 | 17 | 1 | 0 | 0 | 0 |
| 17 | Class 7 | 0 | 0 | 0 | 0 | 0 | 0 | 17 | 0 | 0 | 0 | 0 | 0 | 0 |
| 218 | Class 8 | 0 | 0 | 84 | 0 | 81 | 1 | 1 | 50 | 1 | 0 | 0 | 0 | 0 |
| 798 | Class 9 | 0 | 0 | 0 | 0 | 1 | 1 | 3 | 0 | 792 | 1 | 0 | 0 | 0 |
| 26 | Class 10 | 0 | 0 | 0 | 0 | 0 | 0 | 0 | 0 | 0 | 26 | 0 | 0 | 0 |
| 4 | Class 11 | 0 | 0 | 0 | 0 | 0 | 0 | 0 | 0 | 0 | 0 | 4 | 0 | 0 |
| 12 | Class 12 | 0 | 0 | 0 | 0 | 0 | 0 | 0 | 0 | 0 | 0 | 0 | 12 | 0 |
| 3 | Class 13 | 0 | 0 | 0 | 0 | 0 | 0 | 0 | 0 | 0 | 1 | 0 | 0 | 2 |
| 4 | Class 15 | 0 | 0 | 0 | 0 | 0 | 0 | 0 | 0 | 0 | 2 | 0 | 0 | 2 |

Table 21 – Combined results of the original FHWA-USA algorithm during all data acquisition deployments

## 4.4 Axle Spacing Distribution Model

Data gathering was accomplished by recording PVR files during data acquisition. Histograms of vehicle axle spacing were constructed to reflect collected ground-truth data. An emerging distribution pattern of wheelbase spacing for each class was observed, based on the premise that vehicle axle spacing differences could be approximated by a probability density function (PDF). Figure 46 shows the resulting histogram plot for the first-axle spacing data collected using a database of 20,099 vehicles. Binning was performed per axle spacing sample value.

Some classes can be distinguished based on the number of axles regardless of overlap spacing, while others are affected by considerable overlap, which causes misclassification decisions. Similar histogram distribution derivations were conducted for consecutive axle spacing.

Based on the histogram plots and in accordance with the central limit theorem and law of large numbers, normal distribution was chosen as the approximation model for the study detailed in this report. Hence, normal distribution fitting was performed for all classes using least mean squared error criteria, as depicted in Figure 47, according to the model formula:

$$f(x,\mu,\sigma) = \frac{1}{\sigma\sqrt{2\pi}} e^{\frac{-(x-\mu)^2}{2\sigma^2}} \tag{5}$$

$$\mu = \frac{x_1 + x_2 + \ldots + x_n}{n} \tag{6}$$

$$\sigma = \sqrt{E\left[(X-\mu)^2\right]} \tag{7}$$

where $\mu$ is the mean and $\sigma$ is the standard deviation.

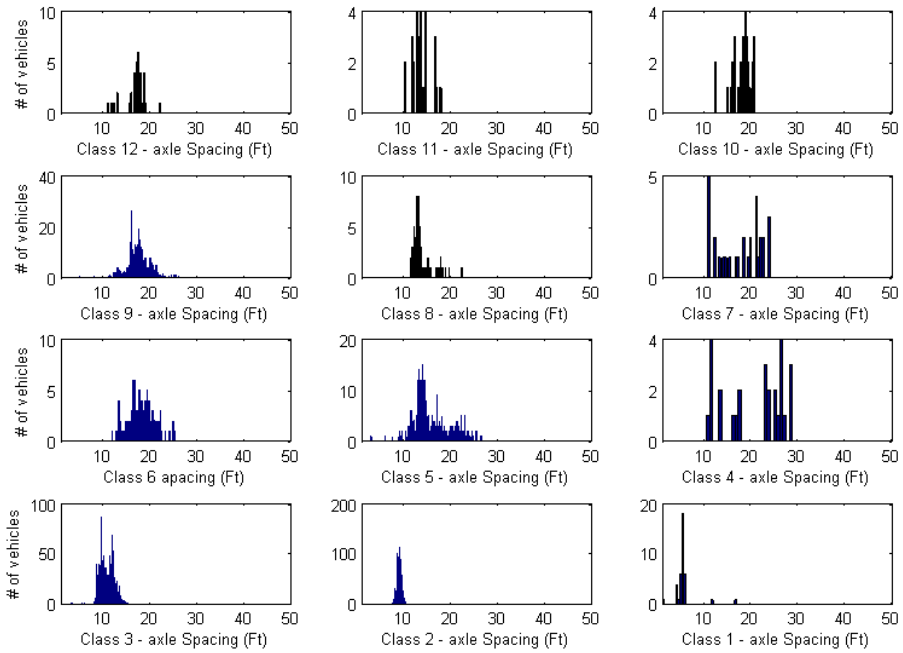


**Figure 46** - First axle spacing for classes 4 through 12 histogram plots

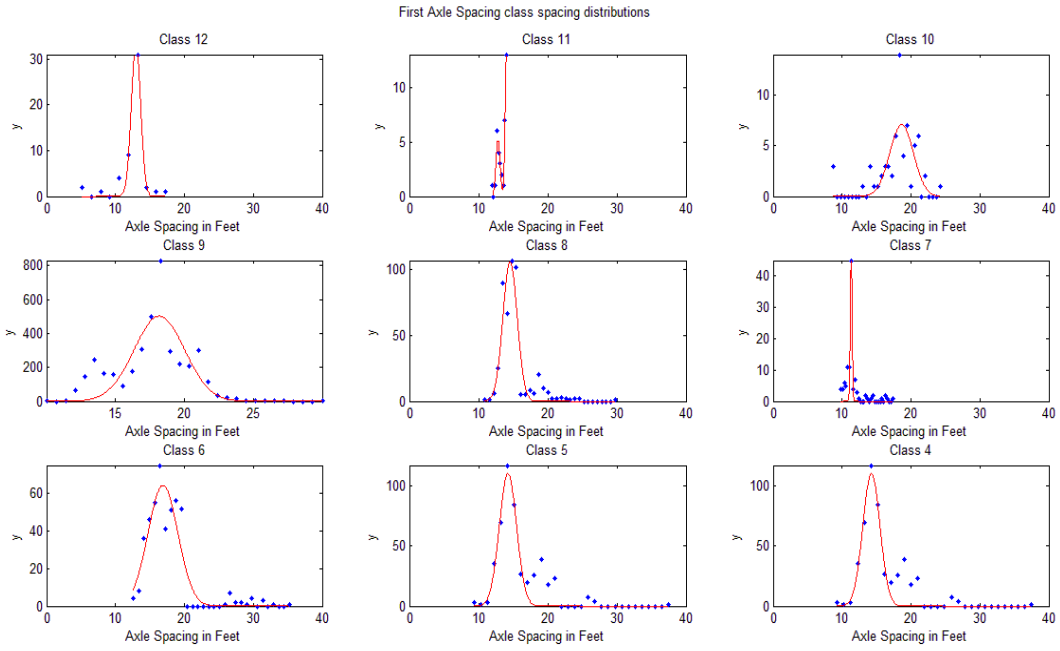


**Figure 47** - First axle spacing Gaussian PDF fitting

Prior to calculating optimal thresholds, error weights proportional to vehicle count were assigned per class to ensure overall system error would not increase after new threshold values were set—the reason being that not all classes had the same number of vehicle counts per unit of time.

Thus, equating weights amongst classes when calculating thresholds would result in decreased error for one particular class, but an overall increase in total system error. Weight assignment was based on vehicle count percentage attained from ground-truth data for each class. Classes were assigned one or more weights, each according to the number of distinguished, problematic, overlapping cases. Finally, an axle-spacing error minimization calculation was conducted to obtain optimal thresholds for separating classes with overlapping, thus problematic, spacing. Figure 48 shows PDFs plotted for all classes and all consecutive axle-spacing.

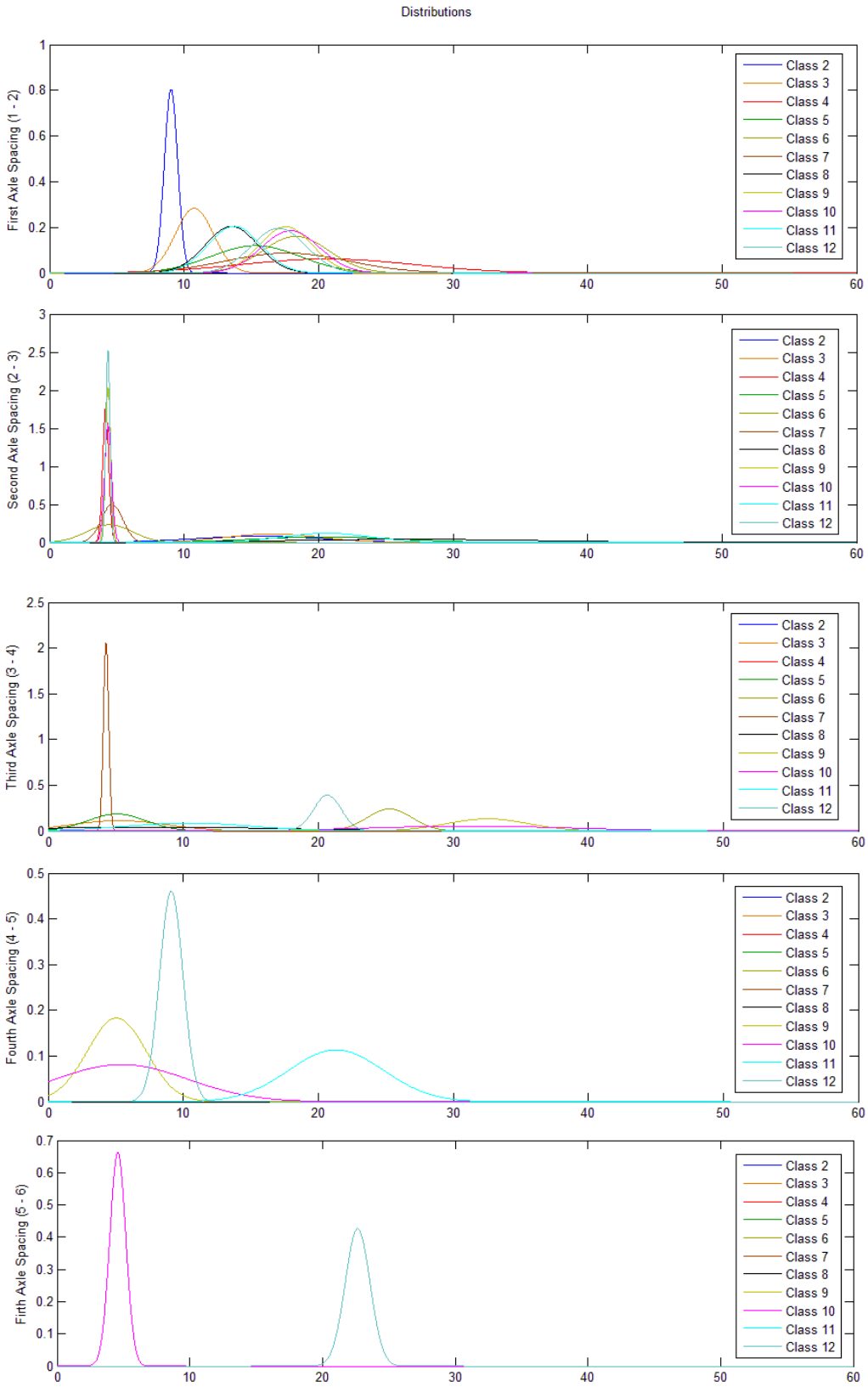


**Figure 48** - Distribution models overlapped for all classes, axle spacing's (1-2), (2-3), (3-4),(4-5) & (5-6).

## 4.5 Classification Algorithm Development

In constructing the newly proposed algorithm (we call it OU-FHWA13 scheme), each classification error detected during the PVR data was addressed. In addition, all missing entries from the original algorithm were added to the newly proposed one, and all problematic thresholds were calibrated using the distribution database and cumulative distribution functions (CDFs). The following presents a per class analysis of the aforementioned process.

CLASS 2

The chief error for class 2 (as indicated earlier) was due to first-axle spacing overlap with class 3. Figure 49 illustrates the intersection of both PDFs for classes 2 and 3. Forty four percent of class 2 vehicles, compared to 56% of class 3 vehicles, were counted in ground-truth video recorded data. In terms of weight calculation, 1.27 vehicles of class 2 equates to one vehicle of class 3. The *optimal weighted threshold that minimizes inaccuracies for class 2 vehicles was found to be 9.615 feet*. Since the ADR unit allows only one decimal digit in the algorithm, the actual threshold was set to 9.6 feet.

When no weights are used in the calculation, the optimal threshold becomes the one that equates the errors between class 2 and 3, regardless of vehicle class 2 or 3 counts. We call this threshold "equal error threshold." *Equal error threshold for class 2 vehicles 9.49 feet.* Figure 50 plots the weighted and equal error thresholds.

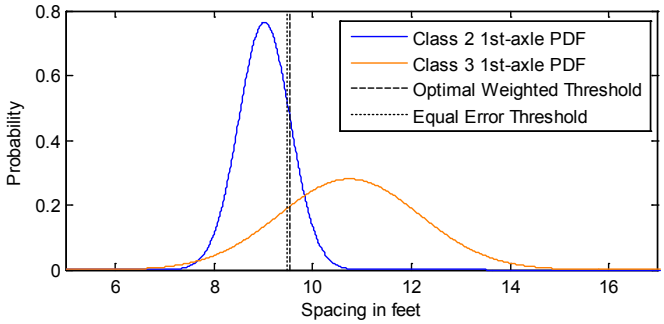


**Figure 49** - Class 2, Class 3—1st axle distribution

CLASS 3

Class 3 errors were segmented into four main types. The first was associated with class 2 vehicles, as explained above. The remaining class 3 errors were categorized as follows.

- 2-axle class 3 with class 5

Errors with class 5 were due to overlap in first-axle spacing. Figure 50 illustrates the intersection of both class 3 and 5 1st axle spacing PDFs. Ninety one percent of class 3 vehicles, compared to 9% of class 5 vehicles, were counted in the ground-truth video-recorded data. In terms of weight calculation, an error of 10.032 for class 5 equates to one of class 3. *The optimal threshold that*

*minimizes inaccuracies for this class 3 error type was found to be 13.456 feet*. (Threshold was set to 13.5 feet in the device, making 11 errors for class 5 equate to one for class 3 due to decimal point precision limitations of ADR equipment.) *The equal error threshold was found to be 12.1 feet.* Figure 50 plots the optimal weighted and equal error thresholds.

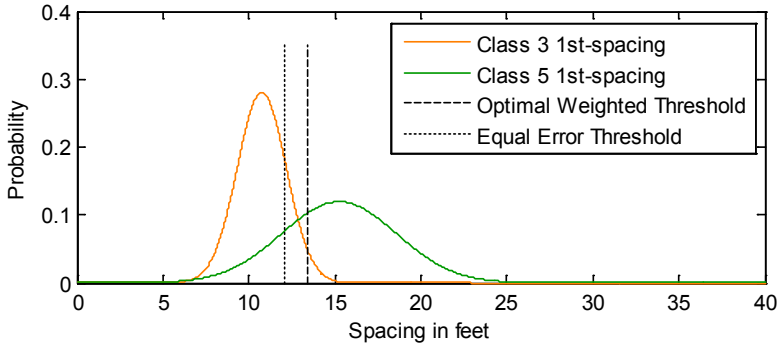


**Figure 49** - Class 3, Class 5 1st axle distribution

The weighted threshold used to differentiate between class 3 and class 5 vehicles was subsequently used to improve classification accuracy of class 8 vehicles. If 1st axle spacing of a vehicle is below the threshold value of 13.5 feet (separating class 3 and 5), the vehicle in question becomes a candidate of either class 3 or 8 but not class 5, even if the 2nd and 3rd vehicle axle spacings overlap with class 5 vehicles. On the other hand, if the vehicle's 1st axle spacing is above 13.5 feet, the vehicle becomes a candidate for class 5 or 8, but not 3, even if the 2nd and 3rd vehicle axle spacings overlap with class 3 vehicles. As a result, two 3-axle class 8 entries and three 4-axle class 8 entries were added to the algorithm to account for this argument and to enhance class 8 detection accuracy. This differed from the "one entry per number of axles" limitation in the original algorithm.

- 3-axle Class 3 with Class 8

Errors with class 8 were also caused by second-axle spacing overlap. Figure 51 shows the intersection of the 2nd axle spacing PDFs for both classes. Ninety five and three tenths percent of 3-axle class 3 vehicles compared to 4.7% of 3-axle class 8 vehicles were counted in ground-truth video recording data. In terms of weight calculation, an error of 20.27 of class 8 equates to one of class 3. *The weighted threshold that minimizes inaccuracies for this class 3 error type was set 23.2 feet*, making 20.8296 errors of class 5 equate to one of class 3. *The equal error threshold was found to be 19.4 feet.* Both thresholds are plotted in Figure 51.

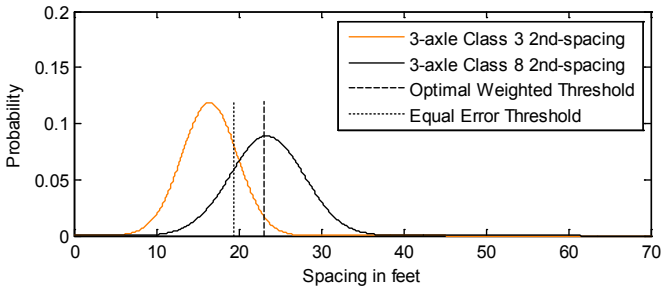


**Figure 50** - 3-axle Class 3, Class 8 2nd axle spacing distribution

- 4-axle Class 3 with Class 8

Four types of class 8 errors resulted from overlap in second-axle spacing. Figure 52 shows the intersection of class 3 and class 8 PDFs. Thirty five and four tenths percent of 4-axle class 3 vehicles compared to 64.6% of 4-axle class 8 were counted in the ground-truth video recorded data. In terms of error weight calculations, a 1.82 error for class 3 equates to 1.0 of class 8. *The weighted threshold was set to 29.4 feet, with class 3 error equaling 1.808 of class 8. Equal error threshold was determined to be 28.3 feet.*

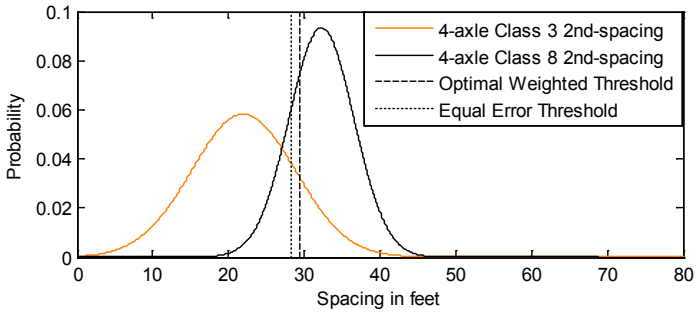


**Figure 51** - 4 axle Class 3, Class 8 2nd axle distribution

CLASS 4

Class 4 errors were one of the most problematic overlap errors of all classes. Figure 53 illustrates the 1st axle spacing between class 4, as well as the amount of overlap. The cause was the wide variety of large- and small-size buses. Notably, only a small sample of class 4 vehicles compared to other classes was obtained from ground-truth video dataset. Ninety seven and seven tenths percent of 2-axle class 5 compared to 2.3% of 2-axle class 4 vehicles were counted in the ground-truth data. In terms of error weigh calculations, an error of 42.12 for class 4 equated to one of class 5. *The weighted threshold was set to 22.5 feet, with class 4 error of 42.02 equates one of class 5.* Despite adjusting the threshold accordingly, it is clear that axle-spacing classification is not a viable solution for segregating class 4 and class 5.

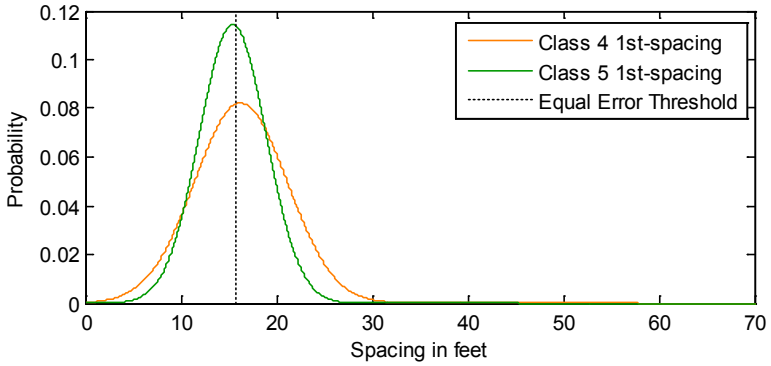


**Figure 52** - Class 4, Class 5 1st axle distribution

CLASS 5

Two types of class 5 errors were addressed while discussing class 3 and 4 errors above. The two remaining cases are errors that occur to class 8.

- 3-axle Class 5 with Class 8

Figure 54 shows the end axle spacing PDFs of 3-axle class 5 and 8. Ninety six and three tenths percent of 3-axle class 5 vehicles compared to 3.7% of 3-axle class 8 were counted in ground-truth video recorded data. In terms of error weigh calculations, an error of 26.20 for class 8 equates to one of class 5. *The weighted threshold was set at 28, with class 8 error of 26.287 to one of class 3. The equal error threshold was found to be 21.8 feet.*

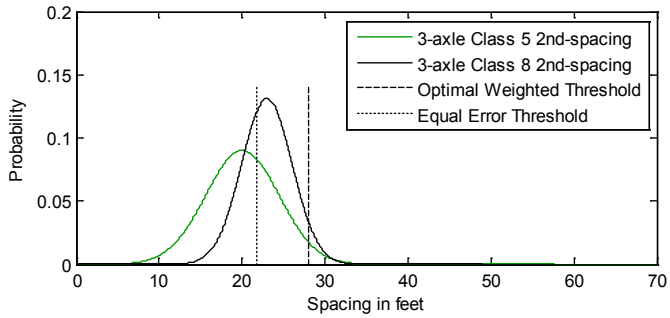


**Figure 53** - 3-axle Class 5, Class 8 2nd axle distribution

- 4-axle Class 5 to Class 8

Figure 55 shows the 2nd axle spacing PDFs of 4-axle class 5 and 8. Seventy three and seven tenths percent of 4-axle class 5 vehicles compared to 26.3% of 4-axle class 8 were counted in ground-truth data. In terms of error weight calculation, an error of 2.8 for class 8 equates to one of class 5. *The weighted threshold was set to 30.6, with a class 8 error of 2.8321 equates to one class 5. The equal error threshold was found to be 27.7 feet.*

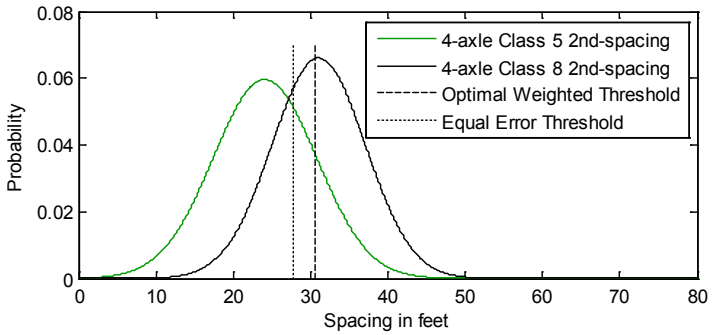


**Figure 54** - 4-axle Class 5, Class 8 2nd axle distribution

CLASS 6

Figure 56 shows the intersection of the 3-axle class 4 and 6 PDFs. Ninety five and nine tenths percent of class 4 vehicles compared to 4.1% of class 6 were counted in ground-truth video recorded data. In terms of error weight calculations, an error of 23.39 for class 4 equates to one of class 6. *The optimal weighted threshold is set to 25.5 feet with an error of 20.6 for class 4 to one of class 6. The equal error threshold was found to be 24.29 feet.*

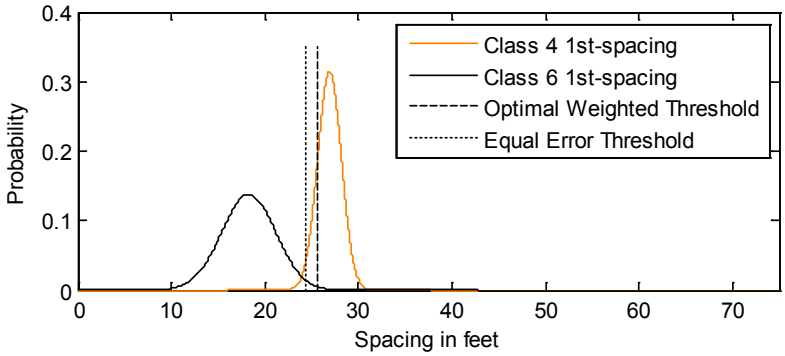


**Figure 55** - Class 4, Class 6 1st axle distribution

CLASS 7

A new missing entry was added for class 7; however, because there were no problematic overlapping cases, no distribution analysis was conducted.

CLASS 8

All problematic class 8 errors that were analyzed were relative to class 5 and class 3 vehicles. Errors appearing in relation to a class 9 truck being classified as a class 8 were caused by the miss detection of one axle from the class 9 truck. This case was found to occur in sparse cases at some sites and is not related to an error in the decision tree or algorithm. As such, this particular class 8 problem was neglected.

CLASS 9

Class 9 errors were related to incorrect axle reporting by the classification equipment. First-axle spacing range was short for no apparent reason. Hence, the range was extended to accommodate larger class 9 trucks.

CLASS 10, 11 AND 12.

Specific missing entries for class 10 were added. Class 11 experienced no problems, and thus no modifications were made to the algorithm. One missing entry for class 12 was also added.

## 4.6 Proposed Classification Algorithm and Scheme

Table 22 presents the OU-FHWA13—newly constructed classification tree. The spacing's set are in feet. Consecutive spacing's are labeled (SP) followed by a number indicating which spacing is being referred to e.g. (SP1 means first axle spacing). The change type column shows what type of change was done in regards to the original classification tree. "M" refers to modification of the original entry. "A "refers to the addition of an entry which was not present in the original classification tree. Table 23 presents the original FHWA-USA scheme used by ODOT for comparison with the one developed by the OU research team.

| Number of Axles | Class | Class Description | Axle Spacing | Change type |
|---|---|---|---|---|
| 0 | 2 | - | (Any) | - |
| 1 | 2 | - | (Any) | - |
| 2 | 1 | Motorcycle | (SP1 0 - 6.0) | - |
| 2 | 2 | Passenger Car | (SP1 6.0 - **9.6**) | **M** |
| 2 | 3 | Four tire single unit | (SP1 **9.6** -**13.5**) | **M** |
| 2 | 5 | Six tire single unit | (SP1 **13.5** - **22.5**) | **M** |
| 2 | 4 | Bus | (SP1 **22.5** - **40.0**) | **M** |
| 2 | 2 | 2 axle Default entry | (Any) | - |
| 3 | 2 | Class 2 with single axle trailer | (SP1 6.0 - **9.6**)(SP2 6.0 - **30.0**) | **M** |
| 3 | 3 | Class 3 with single axle trailer | (SP1 **9.6** - **13.5**)(SP2 6.0 - **23.2**) | **M** |
| 3 | 5 | Class 5 with single axle trailer | (SP1 **13.5** - **30**)(SP2 6.0 - **28** ) | **A** |
| 3 | 6 | Three axle single unit | (SP1 6.0 - **25.5**)(SP2 - 6.0) | **M** |
| 3 | 4 | three axle Bus | (SP1 **25.5** - 40.0)(SP2 - 6.0) | **M** |
| 3 | 8 | Three axle single Trailer | (SP1 **6.0** - **13.5**)(SP2 **23.2** - **50.0**) | **M** |
| 3 | 8 | Three axle single Trailer | (SP1 **13.5** - **15**)(SP2 **28** - **50.0**) | **A** |
| 3 | 3 | 3 axle Default entry | (Any)(Any) | **M** |
| 4 | 7 | Four axle single unit | (SP1 6.0 - **24.0**)(SP2 - 6.0)(SP3 - 6.0) | **M** |
| 4 | 8 | Four axle single trailer | (SP1 **6.0** - **18.0**)(SP2 - **6.0**)(SP3 **15.0** - **50.0**) | **A** |
| 4 | 8 | Four axle single trailer | (SP1 **6.0** - **13.5**)(SP2 **27.3** - **50.0**)(SP3 - **15.0**) | **A** |
| 4 | 8 | Four axle single trailer | (SP1 **13.5** - **18.0**)(SP2 **30.6** - **50.0**)(SP3 - **15.0**) | **A** |
| 4 | 2 | Class 2 with two axle tailer | (SP1 6.0 - **9.6**)(SP2 6.0 - **30.0**)(SP3 - **15.0**) | **M** |
| 4 | 3 | Class 3 with two axle tailer | (SP1 **9.6** - **13.5**)(SP2 6.0 - **29.4**)(SP3 - **15.0**) | **M** |
| 4 | 5 | Class 5 with two axle tailer | (SP1 **13.5** - **30**)(SP2 **6.0** - **30.6**)(SP3 0 - **15.0**) | **M** |
| 4 | 8 | 4 axle Default entry | (Any)(Any)(Any) | - |
| 5 | 3 | Class 3 with three axle trailer | (SP1 **9.6** - **13.5**)(SP2 **6.0** - **30.0**)(SP3 - **6.0**)(SP4 - **6.0**) | **A** |
| 5 | 5 | Class 5 with three axle trailer | (SP1 **13.5** - **30**)(SP2 **6.0** - **30.0**)(SP3 0 - **6.0**)(SP4 0 - **6.0**) | **A** |
| 5 | 7 | Five axle single unit | (SP1 **6.0** - **24.0**)(SP2 - **6.0**)(SP3 - **6.0**)(SP4 - **6.0**) | **A** |
| 5 | 9 | Five axle single trailer | (SP1 6.0 - **30.0**)(SP2 - 6.0)(SP3 6.0 - 50.0)(SP4 - 20.0) | **M** |
| 5 | 9 | Five axle single trailer | (SP1 **6.0** - **30.0**)(SP2 **30.0** - **50.0**)(SP3 - **6.0**)(SP4 - **6.0**) | **A** |
| 5 | 11 | Five axle multi trailer | (SP1 6.0 - 25.0)(SP2 15.0 - 50.0)(SP3 6.0 - 20.0)(SP4 6.0 - 50.0) | - |
| 5 | 9 | 5 axle Default entry | (Any)(Any)(Any)(Any) | - |
| 6 | 10 | Six single axle trailer | (SP1 6.0 - **25.0**)(SP2 - **6.0**) (SP2 - **6.0**)(SP3 **2.0** - **50.0**)(SP4 **2.0** - **6.0**) | **A** |
| 6 | 10 | Six single axle trailer | (SP1 6.0 - **25.0**)(SP2 - 6.0)(SP3 2.0 - 50.0)(SP4 2.0 - 6.0)(SP5 2.0 - 6.0) | **M** |
| 6 | 10 | Six single axle trailer | (SP1 6.0 - **25.0**)(SP2 **20.0** - **50.0**)(SP3 **2.0** - **6.0**)(SP4 **2.0** - **6.0**)(SP5 **2.0** - **6.0**) | **A** |
| 6 | 12 | Six axle multi trailer | (SP1 6.0 - **25.0**)(SP2 - 6.0)(SP3 15.0 - 50.0)(SP4 6.0 - 20.0)(SP5 6.0 - 50.0) | **M** |
| 6 | 12 | Six axle multi trailer | (SP1 **6.0** - **25.0**) (SP2 **6.0** - **40.0**)(SP3 **6.0** - **20.0**)(SP4 **15.0** - **50.0**)(SP5 - **6.0**) | **A** |
| 6 | 10 | Six single axle trailer | (Any)(Any)(Any)(Any)(Any) | - |
| 7 | 10 | Seven axle single trailer | (SP1 6.0 - 23.0)(SP2 - 6.0)(SP3 2.0 - 50.0)(SP4 2.0 - 6.0)(SP5 2.0 - 6.0)(SP6 2.0 - 6.0) | - |
| 7 | 10 | Seven axle single trailer | (SP1 **6.0** - **23.0**)(**SP2** - **6.0**)(SP3 **2.0** - **6.0**)(SP4 **2.0** - **50.0**)(SP5 **2.0** - **6.0**)(SP6 **2.0** - **6.0**) | **A** |
| 7 | 13 | Seven axle multi trailer | (Any)(Any)(Any)(Any)(Any)(Any) | - |
| 8 | 13 | Eight axle mutli trailer | (Any)(Any)(Any)(Any)(Any)(Any)(Any) | **M** |
| 9 | 13 | Nine axle multi trailer | (Any)(Any)(Any)(Any)(Any)(Any)(Any)(Any) | **M** |
| 10 | 13 | Ten axle multi trailer | (Any)(Any)(Any)(Any)(Any)(Any)(Any)(Any)(Any) | **M** |
| 11 | 15 | Eleven axle multi trailer | (Any)(Any)(Any)(Any)(Any)(Any)(Any)(Any)(Any)(Any)(Any) | - |
| 12 | 15 | Twelve axle multi trailer | (Any)(Any)(Any)(Any)(Any)(Any)(Any)(Any)(Any)(Any)(Any)(Any) | - |
| 13 | 15 | Thirteen axle multi trailer | (Any)(Any)(Any)(Any)(Any)(Any)(Any)(Any)(Any)(Any)(Any)(Any)(Any) | - |
| 14 | 15 | Fourteen axle multi trailer | (Any)(Any)(Any)(Any)(Any)(Any)(Any)(Any)(Any)(Any)(Any)(Any)(Any)(Any) | - |

**Table 22** - Newly Developed Classfication tree - OU-FHWA13

| Number of Axles | Class | Class Description | Axle Spacing |
|---|---|---|---|
| 0 | 2 | - | (Any) |
| 1 | 2 | - | (Any) |
| 2 | 1 | Motorcycle | (SP1 0 - 6.0) |
| 2 | 2 | Passenger Car | (SP1 6.0 - 10.2) |
| 2 | 3 | Four tire single unit | (SP1 10.2 - 13.0) |
| 2 | 5 | Six tire single unit | (SP1 13.0 - 20.0) |
| 2 | 4 | Bus | (SP1 20.0 - 40.0) |
| 2 | 2 | 2 axle Default entry | (Any) |
| 3 | 2 | Class 2 with single axle trailer | (SP1 6.0-10.2)(SP2 6.0-23.0) |
| 3 | 3 | Class 3 with single axle trailer | (SP1 10.2-13.0)(SP2 6.0-23.0) |
| 3 | 6 | Three axle single unit | (SP1 6.0-23.0)(SP2 -6.0) |
| 3 | 4 | three axle Bus | (SP1 20.0-40.0)(SP2 -6.0) |
| 3 | 8 | Three axle single Trailer | (SP1 6.0-17.0)(SP2 14.0-50.0) |
| 3 | 2 | 3 axle Default entry | (Any)(Any) |
| 4 | 7 | Four axle single unit | (SP1 6.0-23.0)(SP2 -9.0)(SP3 -9.0) |
| 4 | 8 | Four axle single trailer | (SP1 6.0-20.0)(SP2 -6.0)(SP3 6.0-50.0) |
| 4 | 8 | Four axle single trailer | (SP1 6.0-17.0)(SP2 14.0-50.0)(SP3 3.2-6.0) |
| 4 | 2 | Class 2 with two axle tailer | (SP1 6.0-10.2)(SP2 6.0-35.0)(SP3 -3.2) |
| 4 | 3 | Class 3 with two axle tailer | (SP1 10.2-13.0)(SP2 6.0-35.0)(SP3 -3.2) |
| 4 | 5 | Class 5 with two axle tailer | (SP1 13.0-20.0)(SP2 6.0-40.0)(SP3 -3.2) |
| 4 | 8 | 4 axle Default entry | (Any)(Any)(Any) |
| 5 | 5 | Class 5 with three axle trailer | (SP1 13.0-20.0)(SP2 6.0-40.0)(SP3 -3.2)(SP4 -3.2) |
| 5 | 9 | Five axle single trailer | (SP1 6.0-22.0)(SP2 -6.0)(SP3 6.0-50.0)(SP4 -23.0) |
| 5 | 11 | Five axle multi trailer | (SP1 6.0-17.0)(SP2 11.0-25.0)(SP3 6.0-18.0)(SP4 11.0-25.0) |
| 5 | 9 | 5 axle Default entry | (Any)(Any)(Any)(Any) |
| 6 | 10 | Six single axle trailer | (SP1 6.0-22.0)(SP2 -6.0)(SP3 -50.0)(SP4 -11.0)(SP5 -11.0) |
| 6 | 12 | Six axle multi trailer | (SP1 6.0-22.0)(SP2 -6.0)(SP3 -25.0)(SP4 6.0-18.0)(SP5 11.0-25.0) |
| 6 | 10 | Six single axle trailer | (Any)(Any)(Any)(Any)(Any) |
| 7 | 10 | Seven axle single trailer | (SP1 6.0-22.0)(SP2 -6.0)(SP3 -50.0)(SP4 -13.0)(SP5 -12.0)(SP6 -12.0) |
| 7 | 13 | Seven axle multi trailer | (Any)(Any)(Any)(Any)(Any)(Any) |
| 8 | 15 | Eight axle mutli trailer | (Any)(Any)(Any)(Any)(Any)(Any)(Any) |
| 9 | 15 | Nine axle multi trailer | (Any)(Any)(Any)(Any)(Any)(Any)(Any)(Any) |
| 10 | 15 | Ten axle multi trailer | (Any)(Any)(Any)(Any)(Any)(Any)(Any)(Any)(Any) |
| 11 | 15 | Eleven axle multi trailer | (Any)(Any)(Any)(Any)(Any)(Any)(Any)(Any)(Any)(Any) |
| 12 | 15 | Twelve axle multi trailer | (Any)(Any)(Any)(Any)(Any)(Any)(Any)(Any)(Any)(Any)(Any) |
| 13 | 15 | Thirteen axle multi trailer | (Any)(Any)(Any)(Any)(Any)(Any)(Any)(Any)(Any)(Any)(Any)(Any) |
| 14 | 15 | Fourteen axle multi trailer | (Any)(Any)(Any)(Any)(Any)(Any)(Any)(Any)(Any)(Any)(Any)(Any)(Any) |

**Table 23** - Original FHWA-USA classification tree

### 4.6.1 Entry Comparison between FHWA-USA and OU-FHWA13

This section presents a class-by-class entry comparison between the newly developed OU-FHWA13 and the original FHWA-USA algorithm being utilized by ODOT for classifying vehicles.

- CLASS 2:

Major error for class 2 was related to first-axle spacing overlap with class 3. A threshold separating class 2 from 3 was updated based on vehicle counts and the first axle-spacing PDF for both classes. This is shown in tables (24 - 27).

| Algorithm | Number of Axles | Class | Class Description | Axle Spacing |
|---|---|---|---|---|
| FHWA-USA | 2 | 2 | Passenger Car | (SP1 6.0 - 10.2) |
| OU_FHWA13 | 2 | 2 | Passenger Car | (SP1 6.0 - **9.6**) |

**Table 24 – Two axle class 2 entry comparison**

This first axle-spacing modification was subsequently updated in all instances of classes 2 and 3 for higher axle vehicle entries. The second-axle spacing for three-axle class 2 entries (passenger vehicle with a single-axle trailer) was extended to 30ft. The original scheme limits it to 23ft. The third axle-spacing for four-axle class 2 entries (passenger vehicle with a two-axle trailer) was extended to 15ft from 3.2ft with no errors. Both axle-spacing extensions resulted in no additional classification errors during evaluation.

| Algorithm | Number of Axles | Class | Class Description | Axle Spacing |
|---|---|---|---|---|
| FHWA-USA | 3 | 2 | Class 2 with single axle trailer | (SP1 6.0-10.2)(SP2 6.0-23.0) |
| OU_FHWA13 | 3 | 2 | Class 2 with single axle trailer | (SP1 6.0 - **9.6**)(SP2 6.0 - **30.0**) |

**Table 25 – Three-axle class 2 entry comparison**

| Algorithm | Number of Axles | Class | Class Description | Axle Spacing |
|---|---|---|---|---|
| FHWA-USA | 4 | 2 | Class 2 with two-axle tailer | (SP1 6.0-10.2)(SP2 6.0-35.0)(SP3 -3.2) |
| OU_FHWA13 | 4 | 2 | Class 2 with two-axle tailer | (SP1 6.0 - **9.6**)(SP2 6.0 - **30**.0)(SP3 - **15**.0) |

**Table 26 – Four-axle class 2 entry comparison**

One final modification was performed to remove the Three-axle default entry from class 2 to class 3. This default entry set in the original algorithm was a cause of much false-detection occurring in class 2 vehicles. The majority of three-axle entries were observed during data collection to be of class 3 vehicles and not class 2.

| Algorithm | Number of Axles | Class | Class Description | Axle Spacing |
|---|---|---|---|---|
| FHWA-USA | 3 | 2 | 3 axle Default entry | (Any)(Any) |
| OU_FHWA13 | 3 | 3 | 3 axle Default entry | (Any)(Any) |

**Table 27 – Default three axle entry comparison**

- CLASS 3:

As indicated earlier in section 4.2, class 3 errors were mainly of 4 types. The first error was related to the overlap with class 2 vehicles and has been corrected in the class 2 entry. The second error was in related to first-axle spacing overlap with class 5. A threshold calculated using the developed probability density distributions was updated and also maintained throughout all subsequent higher axle-count entries in class 3. The third and fourth errors were related to class 8—three and four axle trucks. One additional entry was added to OU-FHWA13 scheme to address a one instance of five-axle class 3 vehicle (a class 3 vehicle pulling three-axle trailers) was observed in the database. The updated entries are shown in tables (28– 32)

| Algorithm | Number of Axles | Class | Class Description | Axle Spacing |
|---|---|---|---|---|
| FHWA-USA | 2 | 3 | Four tire single unit | (SP1 10.2 - 13.0) |
| OU_FHWA13 | 2 | 3 | Four tire single unit | (**SP1 9.6** -**13.5**) |

**Table 28 – Two-axle class 3 entry comparison**

| Algorithm | Number of Axles | Class | Class Description | Axle Spacing |
|---|---|---|---|---|
| FHWA-USA | 3 | 3 | Class 3 with single axle trailer | (SP1 10.2-13.0)(SP2 6.0-23.0) |
| OU_FHWA13 | 3 | 3 | Class 3 with single axle trailer | (**SP1 9.6 - 13.5**)(SP2 6.0 - 23.2) |

**Table 29 – Three-axle class 3 entry comparison**

| Algorithm | Number of Axles | Class | Class Description | Axle Spacing |
|---|---|---|---|---|
| FHWA-USA | 4 | 3 | Class 3 with two axle tailer | (SP1 10.2-13.0)(SP2 6.0-35.0)(SP3 -3.2) |
| OU_FHWA13 | 4 | 3 | Class 3 with two axle tailer | (**SP1 9.6 - 13.5**)(SP2 6.0 - 29.4)(**SP3 - 15.0**) |

**Table 30 – Four-axle class 3 entry comparison**

| Algorithm | Number of Axles | Class | Class Description | Axle Spacing |
|---|---|---|---|---|
| FHWA-USA | - | - | - | - |
| OU_FHWA13 | 5 | 3 | Class 3 with three axle trailer | (**SP1 9.6 - 13.5**)(SP2 6.0 - 30.0)(SP3 - 6.0)(SP4 - 6.0) |

**Table 31 – Five-axle class 3 entry comparison**

| Algorithm | Number of Axles | Class | Class Description | Axle Spacing |
|---|---|---|---|---|
| FHWA-USA | 3 | 2 | 3 axle Default entry | (Any)(Any) |
| OU_FHWA13 | 3 | 3 | 3 axle Default entry | (Any)(Any) |

**Table 32 – Three-axle default entry comparison**

- CLASS 4:

Class 4 errors were occurring due to first-axle spacing overlap with class 5, due to today's short-wheelbase buses traveling the roadways. The threshold in the original scheme was causing a mis-detection for class 5 and false-detection for class 4—class 5 with wheelbase of minimum 20 is being wrong classify as class 4. As shown in table 21, the ADR classified 102 vehicles as class 4. The video recording actually shows that 9 vehicles were class 4; 65 vehicles were class 5; 23 vehicles were class 6; one vehicle was class 7; four vehicles were class 9. Furthermore, it was observed that the number of class 4 vehicles traveling the roadways is much less than those of class 5. Given that, the OU research team developed a new threshold—favoring class 5—to optimize classification accuracy while minimizing errors with class 5. Entries for FHWA_USA and OU-FHWA13 are shown in tables (33 – 34).

| Algorithm | Number of Axles | Class | Class Description | Axle Spacing |
|---|---|---|---|---|
| FHWA-USA | 2 | 4 | Bus | (SP1 20.0 - 40.0) |
| OU_FHWA13 | 2 | 4 | Bus | (**SP1 22.5 - 40.0**) |

**Table 33 – Two-axle class 4 entry comparison**

The same analysis and logic was applied to reduce class 4 errors with class 6.

| Algorithm | Number of Axles | Class | Class Description | Axle Spacing |
|---|---|---|---|---|
| FHWA-USA | 3 | 4 | three axle Bus | (SP1 20.0-40.0)(SP2 -6.0) |
| OU_FHWA13 | 3 | 4 | three axle Bus | **(SP1 25.5 - 40.0)**(SP2 - 6.0) |

**Table 34 – Three-axle class 4 entry comparison**

- CLASS 5:

Class 5 classification errors were mainly of four types. The first error type was related to the first-axle spacing overlap with class 3. This was addressed in class 3 error analysis section. The second error type was addressed in class 4 error analysis section. The third and fourth error types were related to three- and four-axle class 8 trucks. The research team divided class 8 vehicles into two groups based on first-axle spacing of class 8 vehicles. This division resulted in one group whose axle-spacing's overlap with class 3 vehicles; and a second group whose axle spacing's overlap with class 5 trucks. This class 8 vehicle segregation obtains far greater accuracy for these two types of class 5 errors. Effectively, the thresholds were set as previously described using the PDFs of both classes. The updated entries are shown in tables (35 - 38).

| Algorithm | Number of Axles | Class | Class Description | Axle Spacing |
|---|---|---|---|---|
| FHWA-USA | 2 | 5 | Six tire single unit | (SP1 13.0 - 20.0) |
| OU_FHWA13 | 2 | 5 | Six tire single unit | **(SP1 13.5 - 22.5)** |

**Table 35 – Two-axle class 5 entry comparison**

| Algorithm | Number of Axles | Class | Class Description | Axle Spacing |
|---|---|---|---|---|
| FHWA-USA | 4 | 5 | Class 5 with two axle trailer | (SP1 13.0-20.0)(SP2 6.0-40.0)(SP3 -3.2) |
| OU_FHWA13 | 4 | 5 | Class 5 with two axle trailer | (**SP1 13.5 - 30)(SP2 6.0 - 30.6)(SP3 - 15.0)** |

**Table 36 – Four-axle class 5 entry comparison**

| Algorithm | Number of Axles | Class | Class Description | Axle Spacing |
|---|---|---|---|---|
| FHWA-USA | 5 | 5 | Class 5 with three axle trailer | (SP1 13.0-20.0)(SP2 6.0-40.0)(SP3 -3.2)(SP4 -3.2) |
| OU_FHWA13 | 5 | 5 | Class 5 with three axle trailer | **(SP1 13.5 - 30)(SP2 6.0 - 30.0)(SP3 0 - 6.0)(SP4 0 - 6.0)** |

**Table 37 - Five-axle class 5 entry comparison**

Finally, a missing entry in the original scheme was responsible for roughly 14% of class 5 errors. These are three-axle class 5 vehicles. This entry was added in our developed OU-FHWA13 scheme as follows.

| Algorithm | Number of Axles | Class | Class Description | Axle Spacing |
|---|---|---|---|---|
| FHWA-USA | - | - | - | - |
| OU_FHWA13 | 3 | 5 | Class 5 with single axle trailer | **(SP1 13.5 - 30)(SP2 6.0 - 28 )** |

**Table 38 - Three axle class 5 entry comparison**

- CLASS 6:

Class 6 classification error was mainly related to axle-spacing overlap with class. It was addressed earlier. The scheme was updated as shown in Table 39.

| Algorithm | Number of Axles | Class | Class Description | Axle Spacing |
|---|---|---|---|---|
| FHWA-USA | 3 | 6 | Three axle single unit | (SP1 6.0-23.0)(SP2 -6.0) |
| OU_FHWA13 | 3 | 6 | Three axle single unit | **(SP1 6.0 - 25.5)(SP2 - 6.0)** |

**Table 39 – Three axle class 6 entry comparison**

- CLASS 7:

Class 7 classification error was due to missing an entry for five-axle class 7 vehicles. The upper limit of first-axle spacing was extended to 24 from 23 to reflect axle-spacing distributions developed during data collection. The updated entries are shown in tables (40 -41)

| Algorithm | Number of Axles | Class | Class Description | Axle Spacing |
|---|---|---|---|---|
| FHWA-USA | 4 | 7 | Four axle single | (SP1 6.0-23.0)(SP2 -9.0)(SP3 - |
| OU_FHWA13 | 4 | 7 | Four axle single unit | (**SP1 6.0 - 24.0**)(**SP2 - 6.0**)(**SP3 - 6.0**) |

**Table 40 – Four-axle class 7 entry comparison**

| Algorithm | Number of Axles | Class | Class Description | Axle Spacing |
|---|---|---|---|---|
| FHWA-USA | Missing | Missin | Missing | Missing |
| OU_FHWA13 | 5 | 7 | Five axle single unit | **(SP1 6.0 - 24.0)(SP2 - 6.0)(SP3 - 6.0)(SP4 - 6.0)** |

**Table 41 – Five-axle class 7 entry comparison**

- CLASS 8:

Class 8 classification errors was related to axle spacing overlap with class 3 and class 5, as indicated early in this section in addition to entries that are deemed missing by the research team. The following presents all new entries and modification updates implemented in the OU-FHWA13. The updated entries are shown in tables (42-47).

| Algorithm | Number of Axles | Class | Class Description | Axle Spacing |
|---|---|---|---|---|
| FHWA-USA | 3 | 8 | Three axle single Trailer | (SP1 6.0-17.0)(SP2 14.0-50.0) |
| OU_FHWA13 | 3 | 8 | Three axle single Trailer | **(SP1 6.0 - 13.5)(SP2 23.2 - 50.0)** |

**Table 42 – Three-axle class 8 entry comparison**

| Algorithm | Number of Axles | Class | Class Description | Axle Spacing |
|---|---|---|---|---|
| FHWA-USA | - | - | - | - |
| OU_FHWA13 | 3 | 8 | Three axle single Trailer | **(SP1 13.5 - 15)(SP2 28 - 50.0)** |

**Table 43 – Three-axle class 8 new entry**

| Algorithm | Number of Axles | Class | Class Description | Axle Spacing |
|---|---|---|---|---|
| FHWA-USA | 4 | 8 | Four axle single trailer | (SP1 6.0-17.0)(SP2 14.0-50.0)(SP3 3.2-6.0) |
| OU_FHWA13 | 4 | 8 | Four axle single trailer | **(SP1 6.0 - 13.5)(SP2 27.3 - 50.0)(SP3 - 15.0)** |

**Table 44 – Four-axle class 8 entry comparison**

| Algorithm | Number of Axles | Class | Class Description | Axle Spacing |
|---|---|---|---|---|
| FHWA-USA | - | - | - | - |
| OU_FHWA13 | 4 | 8 | Four axle single trailer | (**SP1 13.5 - 18.0)(SP2 30.6 - 50.0)(SP3 - 15.0)** |

**Table 45 – Four-axle class 8 new entry**

| Algorithm | Number of Axles | Class | Class Description | Axle Spacing |
|---|---|---|---|---|
| FHWA-USA | 4 | 8 | Four axle single trailer | (SP1 6.0-20.0)(SP2 -6.0)(SP3 6.0-50.0) |
| OU_FHWA13 | 4 | 8 | Four axle single trailer | (SP1 6.0 - 18.0)(SP2 - 6.0)(SP3 15.0 - 50.0) |

**Table 46 – Four-axle class 8 entry comparison**

| Algorithm | Number of Axles | Class | Class Description | Axle Spacing |
|---|---|---|---|---|
| FHWA-USA | 4 | 8 | 4 axle Default entry | (Any)(Any)(Any) |
| OU_FHWA13 | 4 | 8 | 4 axle Default entry | (Any)(Any)(Any) |

**Table 47 – Four-axle class 8 default entry comparison**

- CLASS 9:

No class 9 classification errors were found related to the algorithm. First-axle spacing was extended to 30ft from 20ft based on the first-axel PDF distribution developed during data collection. An entry was added to the scheme for class 9 vehicles with specific and unique axle spacing's that were observed on the roadways. Note, the original default five-axle class 9 entry was able to successfully classify this truck. The updated scheme is shown in tables 48 and 50.

| Algorithm | Number of Axles | Class | Class Description | Axle Spacing |
|---|---|---|---|---|
| FHWA-USA | 5 | 9 | Five axle single trailer | (SP1 6.0-22.0)(SP2 -6.0)(SP3 6.0-50.0)(SP4 -23.0) |
| OU_FHWA13 | 5 | 9 | Five axle single trailer | (**SP1 6.0 - 30.0**)(SP2 - 6.0)(SP3 6.0 - 50.0)(**SP4 - 20.0**) |

**Table 48 – Five-axle class 9 entry comparison**

| Algorithm | Number of Axles | Class | Class Description | Axle Spacing |
|---|---|---|---|---|
| FHWA-USA | - | - | - | - |
| OU_FHWA13 | 5 | 9 | Five axle single trailer | (**SP1 6.0 - 30.0**)(**SP2 30.0 - 50.0**)(**SP3 - 6.0**)(**SP4 - 6.0**) |

**Table 49 - Class 9 new entry**

| Algorithm | Number of Axles | Class | Class Description | Axle Spacing |
|---|---|---|---|---|
| FHWA-USA | 5 | 9 | 4 axle Default entry | (Any)(Any)(Any) |
| OU_FHWA13 | 5 | 9 | 4 axle Default entry | (Any)(Any)(Any) |

**Table 50 – Five-axle class 9 default entry comparison**

- CLASS 10:

Two new entries for class 10 were added for 6-axle and 7-axle class 10 trucks. It was observed that class 10 trucks were sometimes split into multiple smaller vehicles, despite the default six axle class entry that existed in the original scheme. The research team believes this might be the cause of similarity in axle spacing with smaller classes. The updated entries are shown in tables (51-52).

| Algorithm | Number of Axles | Class | Class Description | Axle Spacing |
|---|---|---|---|---|
| FHWA-USA | - | - | - | - |
| OU_FHWA13 | 6 | 10 | Six single axle trailer | (**SP1 6.0 - 25.0**)(**SP2 - 6.0**) (**SP2 - 6.0**)(**SP3 2.0 - 50.0**)(**SP4 2.0 - 6.0**) |

**Table 51 – Six-axle class 10 new entry**

| Algorithm | Number of Axles | Class | Class Description | Axle Spacing |
|---|---|---|---|---|
| FHWA-USA | - | - | - | - |
| OU_FHWA13 | 7 | 10 | Seven axle single trailer | (**SP1 6.0 - 23.0**)(**SP2 - 6.0**)(**SP3 2.0 - 6.0**)(**SP4 2.0 - 50.0**)(**SP5 2.0 - 6.0**)(**SP6 2.0 - 6.0**) |

**Table 52 – Seven-axle class 10 new entry**

The first-axle spacing upper limit was extended to 25ft from 22ft to reflect class 10 PDF distribution developed during data collection, as shown in table 53.

| Algorithm | Number of Axles | Class | Class Description | Axle Spacing |
|---|---|---|---|---|
| FHWA-USA | 6 | 10 | Six single axle trailer | (SP1 6.0-22.0)(SP2.0 - 6.0)(SP3 0 - 50.0)(SP4 0 -11.0)(SP5 -11.0) |
| OU_FHWA13 | 6 | 10 | Six single axle trailer | (**SP1 6.0 - 25.0**)(SP2.0 - 6.0)(**SP3 2.0 - 50.0**)(**SP4 2.0 - 6.0**)(**SP5 2.0 - 6.0**) |

**Table 53 – Six-axle class 10 entry comparison**

One additional entry was added in the OU-FHWA13 to describe a particular class 10 axle-spacing of vehicle traveling on the roadways, although the vehicle was classified correctly using the FHWA-USA scheme. The entry is shown in table 54.

| Algorithm | Number of Axles | Class | Class Description | Axle Spacing |
|---|---|---|---|---|
| FHWA-USA | - | - | - | - |
| OU_FHWA13 | 6 | 10 | Six single axle trailer | (SP1 6.0 - 25.0)(SP2 20.0 - 50.0)(SP3 2.0 - 6.0)(SP4 2.0 - 6.0)(SP5 2.0 - 6.0) |

**Table 54 – Six-axle class 10 additional entry**

- CLASS 11:

No class 11 errors were recorded during the study. Threshold updates were performed to reflect the axle-spacing of the class 11 vehicles. The number of class 11 recorded during the study was 4 which is not enough to construct a good class distributions. However, the team decided to make some algorithm adjustments based on the limited collected data. ODOT may elect to keep the original class 11 entries. The updated entry is shown in table 55.

| Algorithm | Number of Axles | Class | Class Description | Axle Spacing |
|---|---|---|---|---|
| FHWA-USA | 5 | 11 | Five axle multi trailer | (SP1 6.0-17.0)(SP2 11.0-25.0)(SP3 6.0-18.0)(SP4 11.0-25.0) |
| OU_FHWA13 | 5 | 11 | Five axle multi trailer | (**SP1 6.0 - 25.0**)(**SP2 15.0 - 50.0**)(**SP3 6.0 - 20.0**)(**SP4 6.0 - 50.0**) |

**Table 55 – Five-axle class 11 entry comparison**

- CLASS 12:

A missing entry for class 12 was added and slight calibration to the original class 12 entry in FHWA-USA was done. Entries are shown in tables 56 and 57.

| Algorithm | Number of Axles | Class | Class Description | Axle Spacing |
|---|---|---|---|---|
| FHWA-USA | - | - | - | - |
| OU_FHWA13 | 6 | 12 | Six axle multi trailer | (**SP1 6.0 - 25.0**) (**SP2 6.0 - 40.0**)(**SP3 6.0 - 20.0**)(**SP4 15.0 - 50.0**)(**SP5 - 6.0**) |

**Table 56 - Class 12 missing entry**

| Algorithm | Number of Axles | Class | Class Description | Axle Spacing |
|---|---|---|---|---|
| FHWA-USA | 6 | 12 | Six axle multi trailer | (SP1 6.0-22.0)(SP2 -6.0)(SP3 - 25.0)(SP4 6.0-18.0)(SP5 11.0-25.0) |
| OU_FHWA13 | 6 | 12 | Six axle multi trailer | (**SP1 6.0 - 25.0**)(SP2 - 6.0)(**SP3 15.0 - 50.0**)(**SP4 6.0 - 20.0**)(**SP5 6.0 - 50.0**) |

**Table 57 - Class 12 entry comparison**

- CLASS 13:

Vehicles with eight to ten axles were classified as class 13 as supposed to only seven-axle vehicles as defined in the FHWA-USA.

# 5 Chapter V: Field-Testing of the Developed Classification Algorithm

Evaluation of the developed classification algorithm was performed after embedding the newly calculated optimal thresholds into the algorithm which will call it OU-FHWA13. Experimental field testing of the algorithm was conducted into three consecutive testing rounds, during which the algorithm was constantly refined according to the obtained results to improve its performance. Both mis-detection and false-detection indicators were used as measuring criteria for algorithm accuracy.

## 5.1 Algorithm Evaluation and Improvement: First Round

The field-testing was based on initial data acquisition in which PVR data was recorded and processed, leading to the construction of the initial distribution database. The algorithm, constructed according to the process presented earlier, was calibrated by adding missing entries and using distributions to optimize entry thresholds. Testing was performed on ODOT sites AVC07 and AVC31. Table 58 summarizes 1st round site testing statistics information. No analysis was performed on the data collected from AVC31 due to low count of site passing vehicles.

| Statistic | AVC07 | | AVC31 | |
|---|---|---|---|---|
| Date | 6/25/2014 | 6/25/2014 | 6/24/2014 | 6/24/2014 |
| Traffic | Free Flow | Free Flow | Free Flow | Free Flow |
| Time Begin | 11:44:02 | 10:40:48 | 16:05:15 | 17:06:11 |
| Time end | 12:45:14 | 11:43:26 | 17:03:35 | 18:07:19 |
| Time Duration | 1:01:12 | 1:02:38 | 0:58:20 | 1:01:08 |
| No. of Lanes | 3 | 3 | 3 | 3 |
| No. of vehicles | 3406 | 3179 | 443 | 385 |
| Total Number of Cars in Database | 14849 | | | |

**Table 58** - Summary Statistics for round one field test

The original FHWA-USA decision tree and our OU-FHWA13 were each run for one hour back-to-back on the same site. Tables 59 and 60 present the numerical counts and analysis results obtained by the original and developed algorithms. Figures 57 and 58 summarize these results obtained for this round of field-testing. A substantial improvement for classes 8, 2, 3, 5, and 6 were observed.

| Class | Video count (ground-truth) | ADR count | Correct ADR count | Mis-detection error | False-detection error |
|---|---|---|---|---|---|
| **Class 1** | 6 | 9 | 6 | 0% | 33% |
| **Class 2** | 952 | 1689 | 943 | 1% | 44% |
| **Class 3** | 1645 | 815 | 797 | 52% | 2% |
| **Class 4** | 7 | 37 | 2 | 71% | 95% |
| **Class 5** | 182 | 198 | 106 | 42% | 46% |
| **Class 6** | 37 | 42 | 35 | 5% | 17% |
| **Class 7** | 4 | 3 | 3 | 25% | 0% |
| **Class 8** | 16 | 85 | 16 | 0% | 81% |
| **Class 9** | 300 | 271 | 271 | 10% | 0% |
| **Class 10** | 5 | 5 | 5 | 0% | 0% |
| **Class 11** | 4 | 4 | 4 | 0% | 0% |
| **Class 12** | 6 | 6 | 6 | 0% | 0% |
| **Class 13** | 0 | 0 | 0 | 0% | 0% |

**Table 59 –** AVC07, original algorithm field test results for round one field test

| Class | Video count (ground-truth) | ADR count | Correct ADR count | Mis-detection error | False-detection error |
|---|---|---|---|---|---|
| **Class 1** | 19 | 15 | 13 | 32% | 13% |
| **Class 2** | 1552 | 1487 | 1412 | 9% | 5% |
| **Class 3** | 1360 | 1414 | 1250 | 8% | 12% |
| **Class 4** | 5 | 9 | 0 | 100% | 100% |
| **Class 5** | 169 | 177 | 118 | 30% | 33% |
| **Class 6** | 38 | 37 | 37 | 3% | 0% |
| **Class 7** | 1 | 1 | 1 | 0% | 0% |
| **Class 8** | 9 | 13 | 9 | 0% | 31% |
| **Class 9** | 255 | 255 | 255 | 0% | 0% |
| **Class 10** | 7 | 7 | 7 | 0% | 0% |
| **Class 11** | 4 | 4 | 4 | 0% | 0% |
| **Class 12** | 2 | 2 | 2 | 0% | 0% |
| **Class 13** | 0 | 0 | 0 | 0% | 0% |

**Table 60 –** AVC07, new algorithm field test results for round one field test

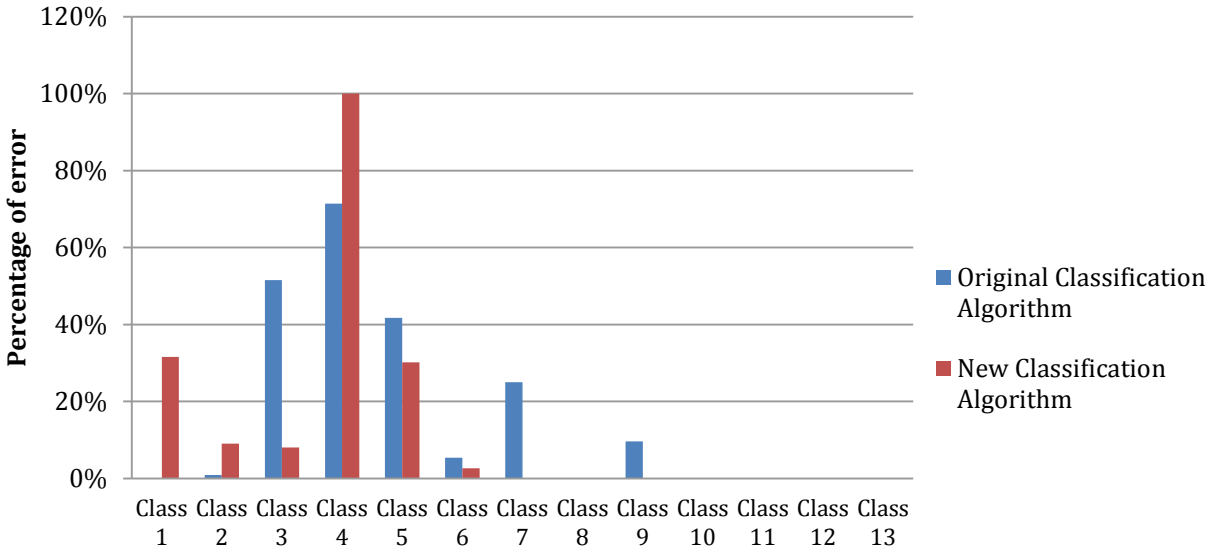


**Figure 56** - AVC 07: Mis-detection error comparison between the original and the developed algorithm

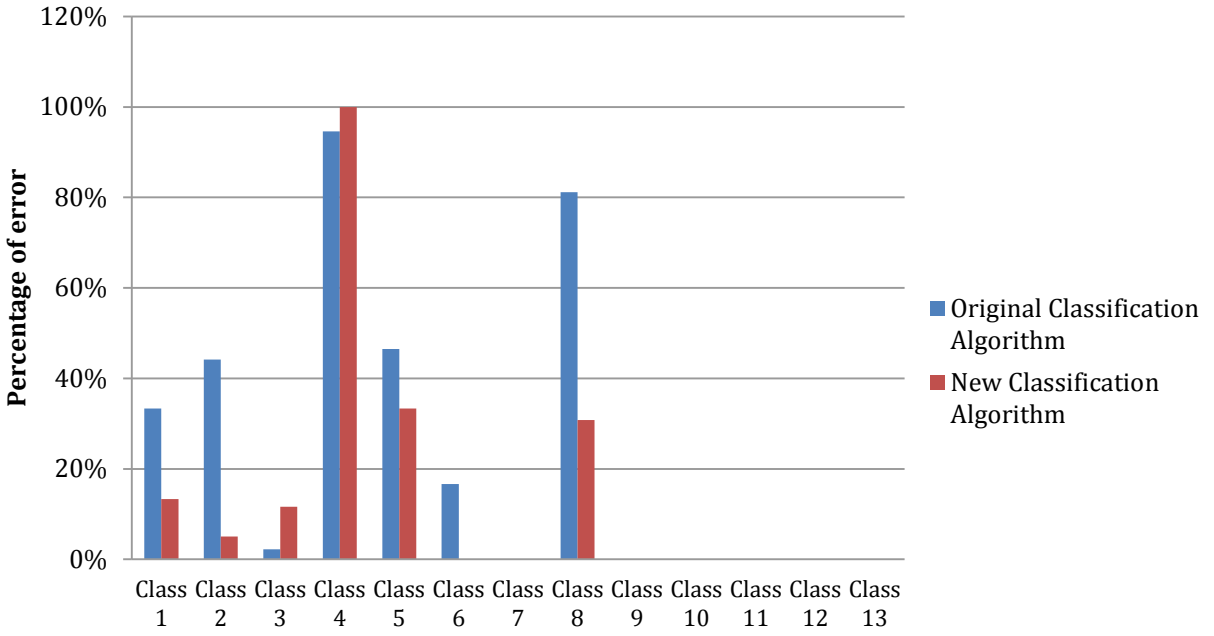


**Figure 57** - AVC 07: False-detection error comparison between the original and developed algorithm

## 5.2 Algorithm Evaluation and Improvement: Second Round

Data (axle spacing and video recordings) collected during first round of testing was added to the distribution database. At this stage of the project, the distribution database was populated with 14,849 vehicles. The developed algorithm was updated once again to improve its accuracy before a second round of testing commenced. Three site deployments and field-testing were conducted at ODOT AVC19. Table 61 shows related information for round 2 site deployment.

| Statistic | AVC19 | | |
|---|---|---|---|
| Date | 7/15/2014 | 7/16/2014 | 7/16/2014 |
| Traffic | Free Flow | Free Flow | Free Flow |
| Time Begin | 14:55:15 | 11:14:37 | 14:55:15 |
| Time end | 16:01:36 | 12:20:00 | 16:01:36 |
| Time Duration | 1:06:21 | 1:05:23 | 1:06:21 |
| No. of Lanes | 3 | 3 | 3 |
| No. of vehicles | 2087 | 1526 | 1637 |
| Total Number of Cars in Database | | 20099 | |

**Table 61** - Summary Statistics for round two field test

Tables 62 and 63 present the numerical vehicle counts and analysis results obtained from testing both algorithms (original and OU developed), while Figures 59 and 60 graphically illustrate errors results from the second round of field-testing. Similar to round 1 testing, further reduction in errors was confirmed for classes 5, 2, and 3. Although a minimal number of samples for class 8 (and higher) were available during round 2 testing, results depicted fewer errors. Nevertheless, a slight shift of thresholds in the calibrating process indicated that more data was required for the distribution database. Hence, a third round of testing was necessary.

| Class | Video count (ground-truth) | ADR count | Correct ADR count | Mis-detection error | False-detection error |
|---|---|---|---|---|---|
| **Class 1** | 3 | 2 | 2 | 33% | 0% |
| **Class 2** | 453 | 803 | 449 | 1% | 44% |
| **Class 3** | 709 | 333 | 315 | 56% | 5% |
| **Class 4** | 5 | 12 | 5 | 0% | 58% |
| **Class 5** | 78 | 67 | 39 | 50% | 42% |
| **Class 6** | 10 | 11 | 10 | 0% | 9% |
| **Class 7** | 0 | 0 | 0 | 0% | 0% |
| **Class 8** | 6 | 36 | 6 | 0% | 83% |
| **Class 9** | 172 | 172 | 172 | 0% | 0% |
| **Class 10** | 2 | 2 | 2 | 0% | 0% |
| **Class 11** | 0 | 0 | 0 | 0% | 0% |
| **Class 12** | 6 | 6 | 6 | 0% | 0% |
| **Class 13** | 1 | 1 | 1 | 0% | 0% |

**Table 62 -** AVC19, original algorithm field test results for round two field test.

| Class | Video count (ground-truth) | ADR count | Correct ADR count | Mis-detection error | False-detection error |
|---|---|---|---|---|---|
| **Class 1** | 15 | 8 | 6 | 60% | 25% |
| **Class 2** | 1035 | 986 | 919 | 11% | 7% |
| **Class 3** | 748 | 803 | 664 | 11% | 17% |
| **Class 4** | 2 | 6 | 1 | 50% | 83% |
| **Class 5** | 85 | 81 | 54 | 36% | 33% |
| **Class 6** | 18 | 17 | 17 | 6% | 0% |
| **Class 7** | 0 | 0 | 0 | 0% | 0% |
| **Class 8** | 9 | 13 | 8 | 11% | 38% |
| **Class 9** | 166 | 166 | 166 | 0% | 0% |
| **Class 10** | 0 | 0 | 0 | 0% | 0% |
| **Class 11** | 3 | 3 | 3 | 0% | 0% |
| **Class 12** | 1 | 1 | 1 | 0% | 0% |
| **Class 13** | 0 | 0 | 0 | 0% | 0% |

**Table 63 -** AVC19, new algorithm field test results for round two field test

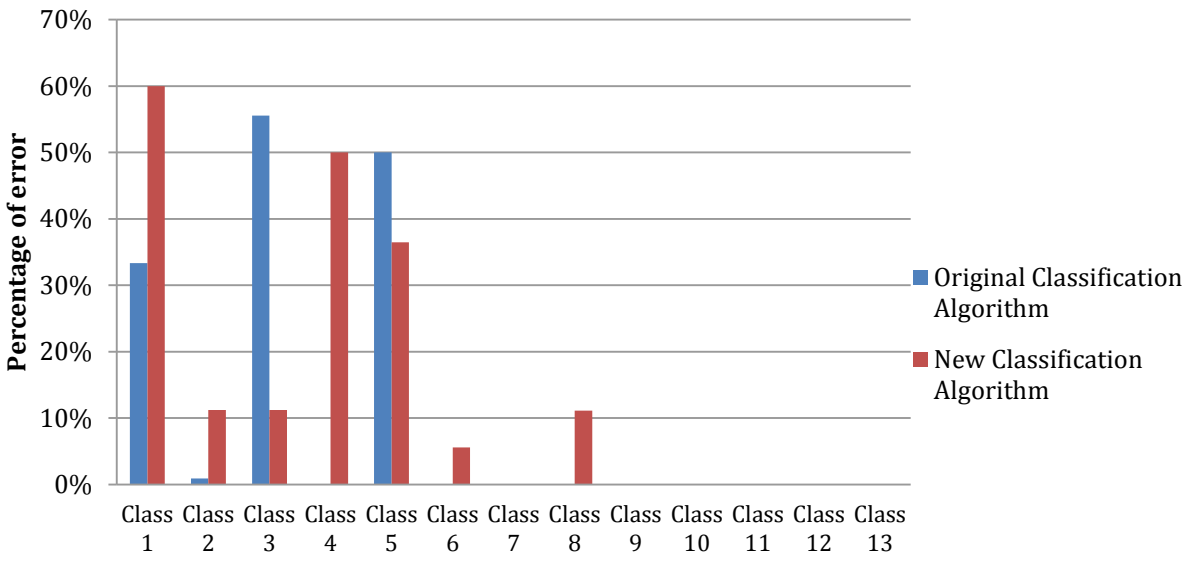


**Figure 59** - AVC19: Mis-detection error comparison between the original and the developed algorithm

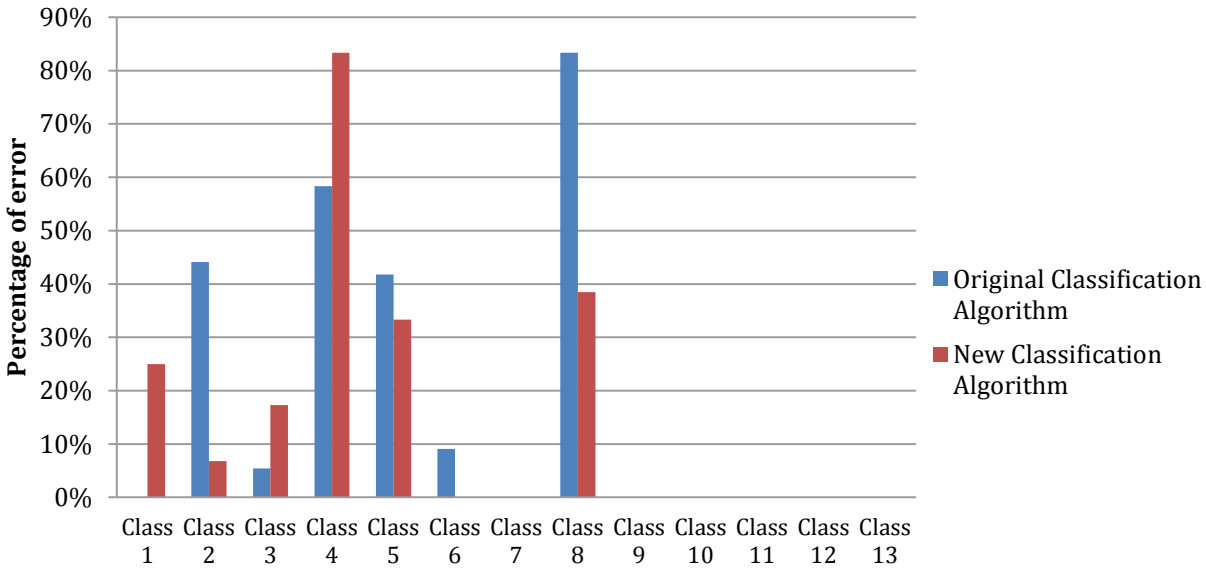


**Figure 58** - AVC19: False-detection error comparison between the original and developed algorithm

## 5.3 Algorithm Evaluation: Third and Final Round

Additional algorithm accuracy testing was performed during the third and final round of data collection. At this stage, the database was populated with 20,099 vehicles—the sum of all ground-truth data obtained thus far. Final threshold value adjustments were performed using all vehicle data in the same manner as previously presented. Testing was performed for two hours on all six lanes at ODOT AVC18. Table 64 summarizes the deployment information. Testing was performed on two separate visits to AVC18. During the first visit, classification data was collected via the original FHWA-USA scheme used by ODOT. During the second visit, classification data was collected via OU-FHWA13 scheme developed by the OU research team. .Surprisingly, the total vehicles count and vehicle count per class were almost a match. Figure 61 depicts class vehicle counts recorded for the algorithms during both deployments.

| Statistic | AVC18 | |
|---|---|---|
| Date | 8/11/2014 | 8/05/2014 |
| Traffic | Free Flow | Free Flow |
| Time Begin | 14:04:09 | 11:57:13 |
| Time end | 16:16:18 | 14:09:24 |
| Time Duration | 2:12:09 | 2:12:11 |
| No. of Lanes | 6 | 6 |
| No. of vehicles | 6169 | 5888 |
| Total Number of Cars in Database | 12057 | |

**Table 64** - Summary Statistics for phase three field test

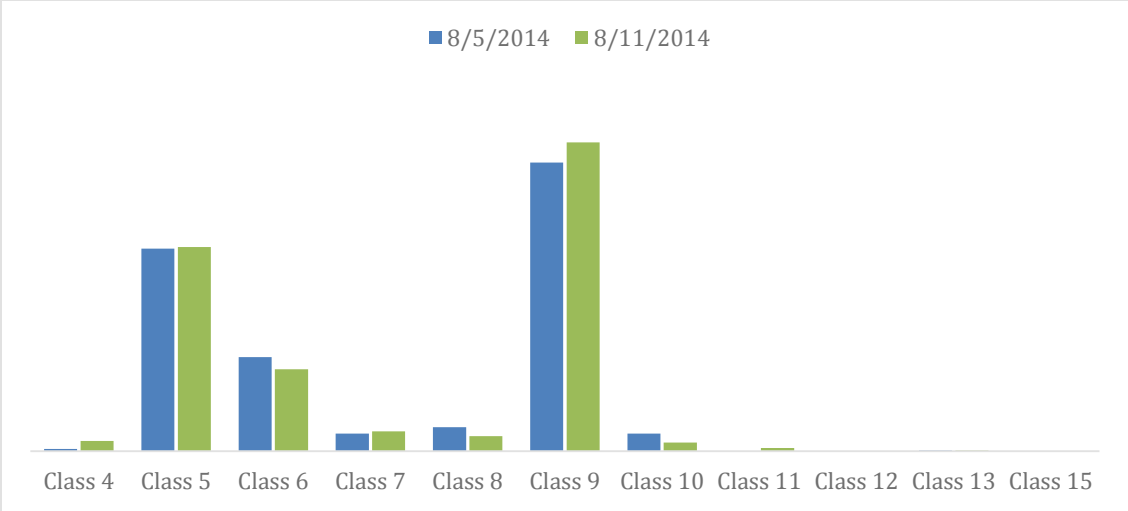


**Figure 59** - Vehicle count comparison between new algorithm testing date and original algorithm testing date.

Figure 61 shows ground-truth vehicle counts per class obtained during first (FHWA-USA testing) and second (OU-FHWA13 testing) deployment. Only class 4 through 15 counts are depicted in the figure. A matched number of vehicles per class in both deployments makes comparison easier. Tables 65 and 66 present results obtained during field-testing for both the original FHWA-USA algorithm and the developed OU-FHWA13 algorithm. The tables include ground-truth vehicle counts, ADR reported counts, ADR correctly classified counts, mis-detection error, and false-detection error percentages per class. Figures 62 and 63 graphically depict results listed in Tables 31 and 32.

Tables and figures demonstrate a sizable decrease of 45% was achieved for False-detection errors for class 8 vehicles. This improvement was primarily attributed to a reduction in the number of False-detections that occurred when class 3 or class 5 vehicles with trailers were traveling over the ADR sensors. Adding just a few entries to the decision tree and using optimal thresholds found via axle spacing distribution analyses resulted in significant improvement for class 8 error ratio.

A substantial improvement for class 2 and class 3 was also evident in the results. The threshold separating these classes reflects actual wheelbase spacing distribution of vehicles currently traveling on roadways. Some transportation agencies combine class 2 and 3 all together to eliminate errors among these classes. This approach significantly reduces the errors among both class 2 and 3.

Class 5 exhibited a noticeable reduction in errors mainly due to the reduction of false-detection errors occurring when large class 3 trucks were inadvertently classified as class 5 vehicles. Class 6 also experienced a decrease in mis-detection relative to class 4 buses. The OU-FHWA13 algorithm ignores short buses since it was found that very few travel Oklahoma state roadways and highways. Class 7 and class 10 vehicle classification improved as a result of inserting new entries that were missing in the original algorithm into the decision tree.

| Class | Video count (ground-truth) | ADR count | Correct ADR count | Mis-detection error | False-detection error |
|---|---|---|---|---|---|
| **Class 1** | 29 | 17 | 13 | 55% | 24% |
| **Class 2** | 2023 | 3519 | 2004 | 1% | 43% |
| **Class 3** | 3026 | 1433 | 1380 | 54% | 4% |
| **Class 4** | 3 | 53 | 2 | 33% | 96% |
| **Class 5** | 252 | 271 | 147 | 42% | 46% |
| **Class 6** | 116 | 104 | 92 | 21% | 12% |
| **Class 7** | 22 | 14 | 14 | 36% | 0% |
| **Class 8** | 30 | 97 | 28 | 7% | 71% |
| **Class 9** | 359 | 355 | 349 | 3% | 2% |
| **Class 10** | 22 | 19 | 19 | 14% | 0% |
| **Class 11** | 0 | 0 | 0 | 0% | 0% |
| **Class 12** | 0 | 0 | 0 | 0% | 0% |
| **Class 13** | 1 | 2 | 1 | 0% | 50% |
| **Class 15** | 0 | 4 | 2 | 0% | 50% |

**Table 65** - AVC18, original algorithm—FHWA-USA—final round field test results

| Class | Ground-truth video count | Total counted by the ADR | Correctly classified by the ADR | Mis-detection error | False-detection error |
|---|---|---|---|---|---|
| **Class 1** | 50 | 30 | 24 | 52% | 20% |
| **Class 2** | 3101 | 2994 | 2825 | 9% | 6% |
| **Class 3** | 2205 | 2349 | 2007 | 9% | 15% |
| **Class 4** | 13 | 6 | 3 | 77% | 50% |
| **Class 5** | 254 | 241 | 181 | 29% | 25% |
| **Class 6** | 102 | 110 | 102 | 0% | 7% |
| **Class 7** | 25 | 22 | 22 | 12% | 0% |
| **Class 8** | 19 | 25 | 18 | 5% | 28% |
| **Class 9** | 384 | 376 | 376 | 2% | 0% |
| **Class 10** | 11 | 11 | 11 | 0% | 0% |
| **Class 11** | 4 | 4 | 4 | 0% | 0% |
| **Class 12** | 0 | 0 | 0 | 0% | 0% |
| **Class 13** | 1 | 1 | 1 | 0% | 0% |
| **Class 15** | 0 | 0 | 0 | 0% | 0% |

**Table 66** - AVC18, new algorithm—OU-FHWA13—final round field test results

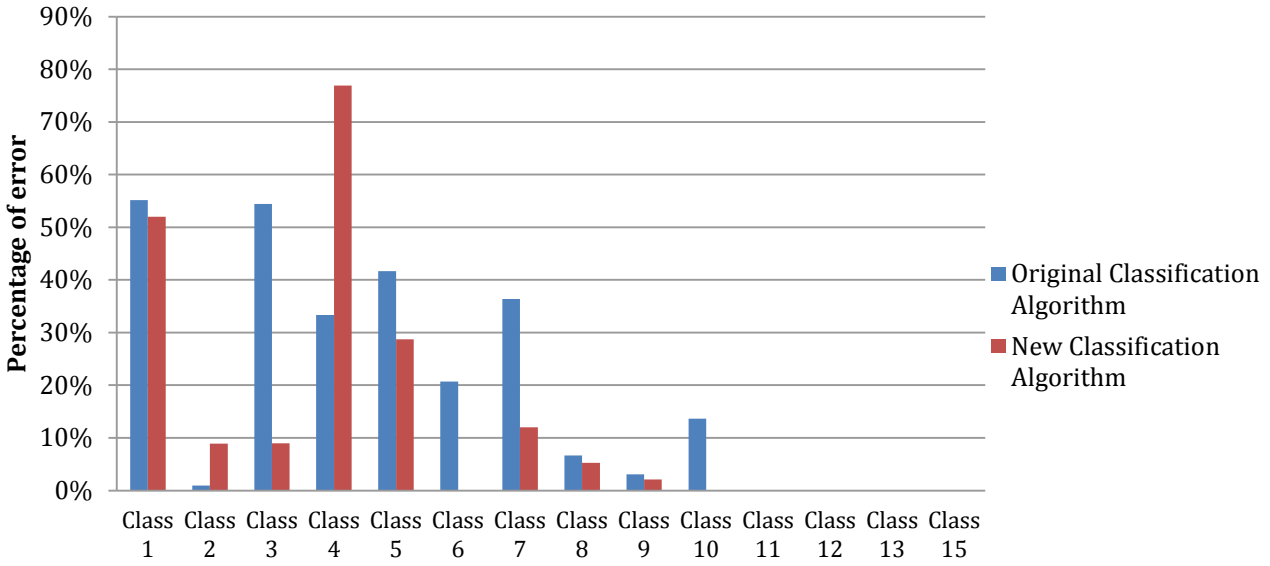


**Figure 60** - Mis-detection error comparison of field test results

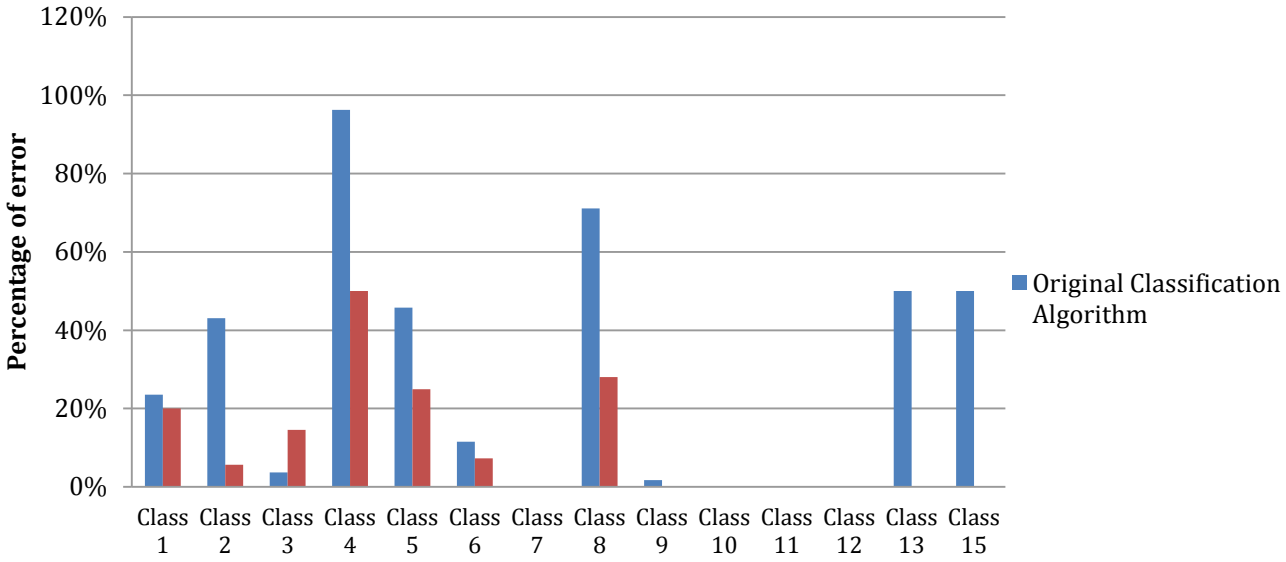


**Figure 61** - False-detection error comparison of field test results

We define a consolidated system error as the sum of the difference of actual vehicle number per class to the number of reported vehicles per class divided by the sum of the actual number of vehicles per class. This figure is considered an indicator of the number of system errors for a

particular vehicle type. Figure 64 indicates consolidated error results grouped by vehicle type. The new algorithm resulted in an error reduction of 15% for heavy trucks (MUTs classes 8 to 13), primarily due to improved classification for class 8 vehicles. A reduction of 4% was observed for light trucks (SUTs in classes 5 to 7), mainly due to class 5 error reduction and a decrease of class 6 errors with class 4. Finally, error for passenger vehicles (classes 1 to 4) were reduced by 57%, primarily due to overlap error reduction between classes 2 and 3.

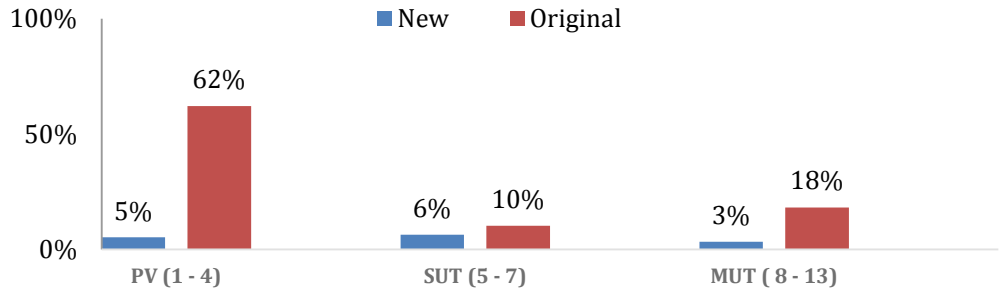


**Figure 62** - Consolidated system error by vehicle type

# 6 Chapter VII: Conclusion

In light of the integral role vehicle classification plays in highway and road design, the study conducted and completed for several ODOT sites was invaluable. Evaluating system classification accuracy required the development of new tools to acquire and process ground-truth data. Axle-based AVC classifiers reporting errors due to axle-spacing overlap between different classes were found to cause misclassification relative to spacing values programmed into the classification algorithm for each device. To alleviate this problem and decrease errors caused by overlap, a novel approach was proposed for constructing distribution databases that reflect actual ground-truth axle-spacing for vehicles currently traveling on Oklahoma roadways. The resulting database was used to build an improved algorithm that was tested adjacent to the one currently be deployed at ODOT sites. Results showed a 45% reduction in errors for class 8, which is the most problematic class of all 13 FHWA classes. In addition, the new approach resulted in substantial improvements in classes 5, 6, 2, and 3. Consolidated system error reported a 15% reduction in misclassified MUTs classes 8 to 13 (mainly due to classification improvements in class 8). Additionally, a 4% reduction was observed for SUTs in classes 5 to 7. A 50% error reduction was achieved for PVs, classes 1 to 4. Class 7 and class 10 errors were also reduced by adding entries not present in the original FWHA-USA algorithm that is currently utilized in ODOT systems.

# 7 References


[1] B. A. Harvey, G. Champion and R. Deaver, "Accuracy of traffic monitoring equipment field tests," in Vehicle Navigation and Information Systems Conference, 1993., 1993.

[2] B. A. Harvey, G. H. Champion, S. M. Richie and C. D. Ruby, "Accuracy of Traffic Monitoring Equipment," Georgia Department of Transportation, 1995.

[3] R. Schmoyer and P. S. Hu, "Analysis of Vehicle Classification and Truck Weight Data of the New England States: Is Data Sharing a Good Idea?," Center for Transportation Analysis, Oak Ridge National Laboratory, 1997.

[4] J. Stephens, J. Carson, D. Reagor and M. Harrington, "An Evaluation of Montana's State Truck Activities Reporting System," State of Montana, Department of Transportation, Motor Carrier Services and Planning Divisions, 2003.

[5] Carter and Burgess, Inc., "Best Practices Guidebook: Collecting Short Duration Manual Vehicle Classifications Counts On High Volume Urban Facilities," Division of Transportation Development, Colorado Department of Transportation, Denver, CO, 2005.

[6] Carter and Burgess, Inc., "Validation Of Urban Vehicle Classification Sampling Methdology," Denver, CO, 2005.

[7] S. Li, Y. Du and Y. Jiang, "Site Verification of Weigh-in-Motion Traffic and TIRTL Classification Data," J oint T ransportation Research Program, Indiana Department of T ransportation and Purdue University , W est Lafayette, Indiana, 2010.

[8] Minnesota Department of Transportation, "Update of Vehicle Classification for County Road Pavement Design," 2010.

[9] X. Yu, "Evaluation of Non-Intrusive Sensors for Vehicle Classification on Freeways," in Proceedings of 2nd International Symposium on Freeway and Tollway Operations, Honolulu, 2009.

[10] X. Yu and P. Prevedouros, "Performance and Challenges in Utilizing Non-Intrusive Sensors for Traffic Data Collection," Advances in Remote Sensing, vol. 2, no. 2, pp. 45-50, 2013.

[11] “Vehicle Classification Using FHWA 13-Category Scheme, Appendix A:." Traffic Recorder Instruction Manual: Vehicle Classification Using FHWA 13-Category Scheme. Texas DOT, n.d. Web. 10 Sept. 2013.

[12] Gonzalez, Rafael C., Richard E. Woods, and Steven L. Eddins. Digital Image Processing Using Matlab. Upper Saddle River, NJ: Pearson Prentice Hall, 2004. Print.

[13] Cobb, Wesley, Ming-Jung Seow, and Tao Yang. Foreground Object Detection in a Video Surveillance System. Behavioral Recognition Systems, Inc. (Houston, TX), assignee. Patent 8218819. 1 Sept. 2009. Print.

[14] Mithun, Niluthpol, Nafi Rashid, and S. M. Rahman. "Detection and Classification of Vehicles From Video Using Multiple Time-Spatial Images." IEEE Transactions on Intelligent Transportation Systems 13.3 (2012): 1215-225. IEEE Xplore Digital Library. IEEE, 28 Aug. 2012. Web. 9 Sept. 2013.

[15] Morris, B.T.; Trivedi, M.M., "Learning, Modeling, and Classification of Vehicle Track Patterns from Live Video," Intelligent Transportation Systems, IEEE Transactions on , vol.9, no.3, pp.425,437, Sept. 2008. Web. 12 Sept. 2013.

[16] Morris, B.; Trivedi, M., "Robust classification and tracking of vehicles in traffic video streams," Intelligent Transportation Systems Conference, 2006. ITSC '06. IEEE , vol., no., pp.1078,1083, 17-20 Sept. 2006. Web. 12 Sept. 2013.

[17] Belhumeur, P.N.; Hespanha, J.P.; Kriegman, D., "Eigenfaces vs. Fisherfaces: recognition using class specific linear projection," Pattern Analysis and Machine Intelligence, IEEE Transactions on, vol.19, no.7, pp.711,720, Jul 1997. 12 Sept. 2013.

[18] De Sousa Matos, F.M.; de Souza, R.M.C.R., "An image vehicle classification method based on edge and PCA applied to blocks," Systems, Man, and Cybernetics (SMC), 2012 IEEE International Conference on , vol., no., pp.1688,1693, 14-17 Oct. 2012. Web. 12 Sept. 2013.

[19] Lipton, A.J.; Fujiyoshi, H.; Patil, R.S., "Moving target classification and tracking from real-time video," Applications of Computer Vision, 1998. WACV '98. Proceedings., Fourth IEEE Workshop on , vol., no., pp.8,14, 19-21 Oct 1998. Web. 9 Sept 2013.

[20] Mikofski, Mark. “polyfitn,” Matlab File Exchange. Web. 28 March. 2014.

[21] Bosch, Anna, Zisserman, Andrew. “Pyramid Histogram of Oriented Gradients”. Oxford University, Visual Geometry Group. 28 March 2014.

[22] Petridis, Sergios. “Fischer’s Linear Dicriminant Analysis,” Matlab File Exchange. Web. 28 March. 2014.